EIGENVECTOR GEOMETRY OF THIRD ORDER LINEAR PHASE TRAJECTORIES

RICHARD C. DIETZ
and
DARREL E. WESTBROOK, JR.

EIGENVECTOR GEOMETRY OF THIRD ORDER LINEAR PHASE TRAJECTORIES

* * * * *

Richard C. Dietz

and

Darrel E. Westbrook, Jr.

EIGENVECTOR GEOMETRY OF THIRD ORDER LINEAR PHASE TRAJECTORIES

by

Richard C. Dietz II
Lieutenant Commander, United States Navy

and

Darrel E. Westbrook, Jr.
Lieutenant, United States Navy

Submitted in partial fulfillment of
the requirements for the degree of

MASTER OF SCIENCE
IN
ELECTRICAL ENGINEERING

United States Naval Postgraduate School
Monterey, California

1 9 6 2

EIGENVECTOR GEOMETRY OF THIRD ORDER LINEAR PHASE TRAJECTORIES

by

Richard C. Dietz

and

Darrel E. Westbrook, Jr

This work is accepted as fulfilling
the thesis requirements for the degree of

MASTER OF SCIENCE
IN
ELECTRICAL ENGINEERING

from the

United States Naval Postgraduate School

ACKNOWLEDGEMENTS

The authors wish to express their appreciation to the technicians of the U. S. Naval Postgraduate School Electrical Engineering and Photographic Laboratories for their assistance in constructing and photographing the models which form a vital part of this work.

A special word of thanks is extended to Professor George J. Thaler of the Department of Electrical Engineering for his assistance and encouragement in the completion of this investigation.

ABSTRACT

An investigation into the general nature and properties of phase trajectories of third order linear feedback control systems has been conducted.

The geometry of eigenvectors, eigenplanes, and the conic surface named the eigencone was investigated with respect to system root parameters. An analysis has been made of the orientation of eigenplanes of systems with three real roots, and of complex eigenplane geometry as the damping ratio ζ, and undamped natural frequency ω_n were varied. A method is introduced for determining system roots that will locate an eigenplane or complex eigenplane in a pre-determined location in third order error space.

Analog and digital computer programs used to obtain phase trajectories of third order linear systems are presented. The effect of root location in the s-plane on phase trajectories is discussed. A thorough analysis of the effect of initial conditions on real root and complex root phase trajectories is presented along with numerous photographs of three-dimensional phase trajectory models.

The inter-relation of phase trajectories, eigenvectors, and eigenplanes is analyzed. An analytical investigation of the response of a complex root system to a step input was made as a first step towards possible application of error space geometry to discontinuous control systems.

TABLE OF CONTENTS

Table of Contents

LIST OF ILLUSTRATIONS

List of Illustrations

List of Illustrations

Chapter I

INTRODUCTION

In recent years many papers have been written with regard to the analysis and design of discontinuous feedback control systems. In many of these papers, various schemes have been proposed for changing the system damping at some optimum time to produce a deadbeat response. However, the rigorous mathematical developments of the switching criteria in some of these proposals tend to obscure somewhat the overall picture. While this investigation does not concern itself with discontinuous systems, the phase trajectories of third order linear feedback control systems have a definite relationship to the eigenvector geometry of three-dimensional error space which lends itself to easy visualization of switching surfaces.

The general nature of the problem was to investigate the phase trajectories of third order linear feedback control systems in response to various initial conditions. It was intended originally to devote the major portion of the investigation to phase trajectories of systems characterized by one real root and a pair of complex conjugate roots and only to verify Han's work (Ref. 1) regarding the trajectories of systems with three real roots. However, during the course of the investigation, it was found that the phase trajectories of both these types of systems have a definite relationship to the eigenvectors associated with the system and to certain planes and surfaces defined by these eigenvectors. It was found possible to describe <u>any</u> phase trajectory of <u>any</u> third order linear system in response to <u>any</u> set of initial conditions in terms of their relationship to the eigenvectors associated with the system.

The use of eigenvectors to define surfaces and planes in phase space is not a new concept but this application has been largely confined to mathematical definitions and manipulations. The approach adopted during the course of this investigation was to construct various representative types of phase trajectories and eigenvectors in a three-dimensional coordinate system and observe them in relation to each other.

In the analysis and design of second order feedback control systems, in particular, those systems with non-linearities, the use of the phase plane has become wide-spread. It is conceivable that the use of phase space could also become a valuable tool in the analysis and design of third order and higher feedback control systems.

The basic concept of phase space is the choosing of a particular set of time variables of the control system as the coordinate axes of this space. In most feedback control systems, the system error automatically seeks zero, and the phase space coordinates are normally chosen as error, E, error rate or velocity, $\dot{E}$, and the (n-1) derivatives of error necessary for control system of order n. The behavior of the system is then described by the spatial coordinates E, $\dot{E}$, $\ddot{E}$, ... $E^{(n-1)}$. These coordinates are the previously mentioned time variables of the control system, and then the system may be described mathematically by,

$$a_n \frac{d^n E}{dt^n} + a_{n-1} \frac{d^{n-1} E}{dt^{n-1}} + a_{n-2} \frac{d^{n-2} E}{dt^{n-2}} + \cdots a_1 \frac{dE}{dt} + a_0 E = 0 \qquad \text{(I-1)}$$

For the third order systems which this paper is concerned with, Equation (I-1) becomes, in more familiar form,

$$\dddot{E} + a\ddot{E} + b\dot{E} + cE = 0 \qquad \text{(I-2)}$$

Thus at any time, t, there is a point in space, called the "state" point, which describes the behavior of the system, and as time varies from $t = 0$ to $t = \infty$, this state point traces a path in this three-dimensional space, called the phase trajectory. As time, t, approaches infinity, the system error seeks zero, and the phase trajectory approaches the origin of this phase space.

Since this three-dimensional space is based on system error and its derivatives, the phase space will hereafter be referred to as "error space".

In previous investigations using phase space, for example, Bogner's (Ref. 2), standard matrix techniques were used to manipulate phase space into principal coordinate space. This coordinate system uses the eigenvectors as coordinate axes. This transformation is particularly useful

in the analysis of higher order contactor servo systems. Since this investigation is based primarily on physical interpretation of phase trajectories, this transformation to principal coordinate axes was not made.

By limiting the order of the systems to be investigated to three, and by not transforming into principal coordinate space, physical representation of phase trajectories in three-dimensional error space was possible. To aid in this physical representation of phase trajectories, the coordinate planes and octants of third order error space are defined as in Fig. 1, and transparent lucite models of error space similar to Fig. 1 were constructed.

The various phase trajectories investigated were obtained from both digital and analog computers. Wire models of these trajectories were constructed in the coordinate system represented by the plastic models.

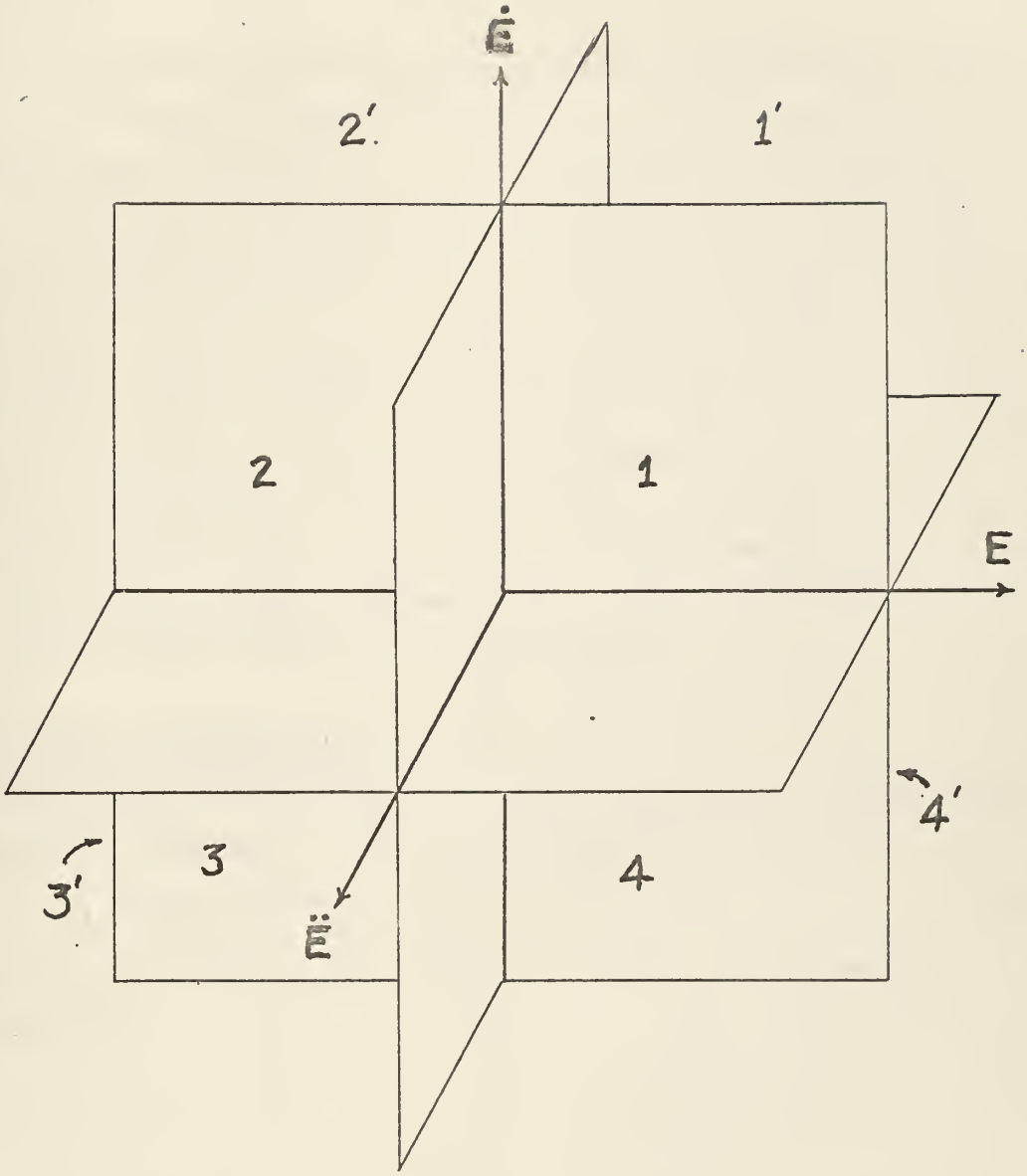

Fig. 1 Coordinate Planes of Third Order Error Space

Chapter II

EIGENVECTORS IN THIRD ORDER ERROR SPACE

General

It is well known that for each real root of a third order system there is an eigenvector which corresponds to a phase trajectory that is a straight line. (See Ref. 3.) For a system with three real and distinct roots, $r_1 < r_2 < r_3$, there are three eigenvectors. The eigenvector associated with the smallest root r_1 is referred to as the slow eigenvector since the time constant of r_1 is larger than those of the other two roots and produces a slower response. Similarly, since r_3 has the shortest time constant, its associated eigenvector is termed the fast eigenvector. Since the time constant of r_2 is some intermediate value between that of r_1 and r_3, the eigenvector associated with it is referred to as the intermediate eigenvector. In the case of a system defined by one real root and a pair of complex conjugate roots, due to the presence of only one real root, there will be only one eigenvector.

Determination of Eigenvectors

The differential equation of a linear third order feedback control system may be expressed in terms of the system error, E, as

$$\dddot{E} + a\ddot{E} + b\dot{E} + cE = 0 \qquad \text{(II-1)}$$

where, in terms of the system roots r_1, r_2 and r_3, all assumed real and distinct,

$$a = r_1 + r_2 + r_3$$

$$b = r_1r_2 + r_1r_3 + r_2r_3$$

$$c = r_1r_2r_3$$

This third order differential equation may be rewritten as three dependent first order differential equations by first setting $E = E_1$. Then,

$$\dot{E} = \dot{E}_1 = E_2 \qquad \text{(II-2a)}$$

$$\ddot{E} = \dot{E}_2 = E_3 \qquad \text{(II-2b)}$$

$$\dddot{E} = \dot{E}_3 = -cE_1 - bE_2 - aE_3 \qquad \text{(II-2c)}$$

The set of equations thus obtained can be written in matrix form as $\dot{E}_i = AE_i$, $i = 1,3$. Thus,

$$\begin{bmatrix} \dot{E}_1 \\ \dot{E}_2 \\ \dot{E}_3 \end{bmatrix} = \begin{bmatrix} 0 & 1 & 0 \\ 0 & 0 & 1 \\ -c & -b & -a \end{bmatrix} \times \begin{bmatrix} E_1 \\ E_2 \\ E_3 \end{bmatrix} \qquad \text{(II-3)}$$

The matrix of coefficients, A, has an eigenvalue λ if and only if there exists a vector $\vec{E}$ with components $\vec{E}_1$, $\vec{E}_2$ and $\vec{E}_3$ such that $A\vec{E} = \lambda\vec{E}$, where multiplication is matrix multiplication and $\vec{E}$ is considered to be a one column matrix. Such a vector $\vec{E}$ is called an eigenvector of the matrix. Eigenvectors exist satisfying $A\vec{E} = \lambda\vec{E}$ only when λ satisfies the determinant $(A - \lambda I) = 0$, where I is the identity matrix.

$$\det (A - \lambda I) = \begin{vmatrix} -\lambda & 1 & 0 \\ 0 & -\lambda & 1 \\ -c & -b & -(a+\lambda) \end{vmatrix} = 0 \qquad \text{(II-4)}$$

Expanding the determinant,

$$\lambda^3 + a\lambda^2 + b\lambda + c = 0 \qquad \text{(II-5)}$$

The expression obtained is the characteristic equation of the matrix, not to be confused with the characteristic equation of the feedback control system. Any root λ_i of this equation is an eigenvalue, and associated with each eigenvalue there is an eigenvector. The characteristic equation factors into the form

$$(\lambda_1 + r_1)(\lambda_2 + r_2)(\lambda_3 + r_3) = 0 \qquad \text{(II-6)}$$

Thus,

$$\lambda_1 = -r_1 \qquad \lambda_2 = -r_2 \qquad \lambda_3 = -r_3$$

To find the eigenvector associated with each root, each root is substituted in turn into the matrix equation $(A - \lambda_i I)\vec{E}_i = 0$.

$$\begin{bmatrix} -\lambda_i & 1 & 0 \\ 0 & -\lambda_i & 1 \\ -c & -b & -(a+\lambda_i) \end{bmatrix} \times \begin{bmatrix} \vec{E}_1 \\ \vec{E}_2 \\ \vec{E}_3 \end{bmatrix} = 0 \qquad \text{(II-7)}$$

$$-\lambda_i \vec{E}_1 + \vec{E}_2 = 0 \qquad \text{(II-8a)}$$

$$-\lambda_i \vec{E}_2 + \vec{E}_3 = 0 \qquad \text{(II-8b)}$$

$$-c\vec{E}_1 - b\vec{E}_2 - (a+\lambda_i)\vec{E}_3 = 0 \qquad \text{(II-8c)}$$

To obtain a solution, any two of the three equations may be solved in terms of one of the variables and an arbitrary constant K assumed for its value. The easiest choice here is to solve Equations (II-8a) and (II-8b) in terms of $\vec{E}_2$ and to assume $\vec{E}_2 = K$.

$$\vec{E}_1 = \frac{\vec{E}_2}{\lambda_i} = \frac{K}{\lambda_i} \qquad \text{(II-9a)}$$

$$\vec{E}_3 = \lambda_i \vec{E}_2 = \lambda_i K \qquad \text{(II-9b)}$$

The values obtained for $\vec{E}_1$, $\vec{E}_2$ and $\vec{E}_3$ may be checked by substitution into Equation II-8c.

The general expression for an eigenvector may then be written as

$$\vec{E} = \frac{K}{\lambda_i} \vec{E}_1 + K\vec{E}_2 + \lambda_i K\vec{E}_3 \qquad \text{(II-10)}$$

where $\vec{E}_1$, $\vec{E}_2$ and $\vec{E}_3$ may be considered as unit vectors along their respective axes. In terms of E, $\dot{E}$, $\ddot{E}$ and r_i, where r_i is any distinct real root of the system, this expression may be written as

$$\vec{E} = \frac{K}{-r_i} \vec{E} + K\dot{\vec{E}} - r_i K\ddot{\vec{E}} \qquad \text{(II-11)}$$

From this general expression of an eigenvector in three dimensional error space, it is seen that an eigenvector has a fixed orientation which is dependent only upon the location of the associated real root.

Throughout the course of the investigation when it was desired to determine the eigenvectors of a particular system, it was necessary to locate only one point on a particular eigenvector to orient it properly in space. From the general expression derived for an eigenvector, any arbitrary point on an eigenvector is given by the coordinates $(E, \dot{E}, \ddot{E}) = \left(\frac{K}{-r_i}, K, -r_i K\right)$.

For example, assume a system with real roots at $r_1 = .5$, $r_2 = 1.0$ and $r_3 = 3.0$. Here the roots are defined as positive when they are located in the left half of the complex s-plane. By assuming a value for K, the coordinates of a point on each of the eigenvectors may be determined. Let it be assumed that K=1. The resulting point on each of the eigenvectors are listed below.

Eigenvector	$(E, \dot{E}, \ddot{E})$
slow	(-2, 1, -.5)
intermediate	(-1, 1, -1)
fast	(-0.333, 1, -3)

Note that all three eigenvectors lie in octant 2'. (Refer to Fig. 1). However, suppose that K = -1. Then

Eigenvector	$(E, \dot{E}, \ddot{E})$
slow	(2, -1, .5)
intermediate	(1, -1, 1)
fast	(0.333, -1, 3)

These eigenvectors all lie in octant 4. A model of this example is shown in Fig. 2.

If the roots of the system had been chosen as negative, i.e., located in the right half of the complex s-plane, then the eigenvectors would be located in octants 1 and 3'. Thus, for a third order system, all possible eigenvectors of the system are restricted to octants 1, 2', 3' and 4.

The Eigencone

From observations of eigenvector location in three dimensional models, it was theorized that there is a conical surface in three dimensional error space which is the locus of all possible eigenvectors for a third order system. In order to prove this theory, the coordinates of any arbitrary point $(E, \dot{E}, \ddot{E})$ on an eigenvector are written in parametric form as

$$E = \frac{K}{-r_i} \qquad \dot{E} = K \qquad \ddot{E} = -r_i K \tag{II-12}$$

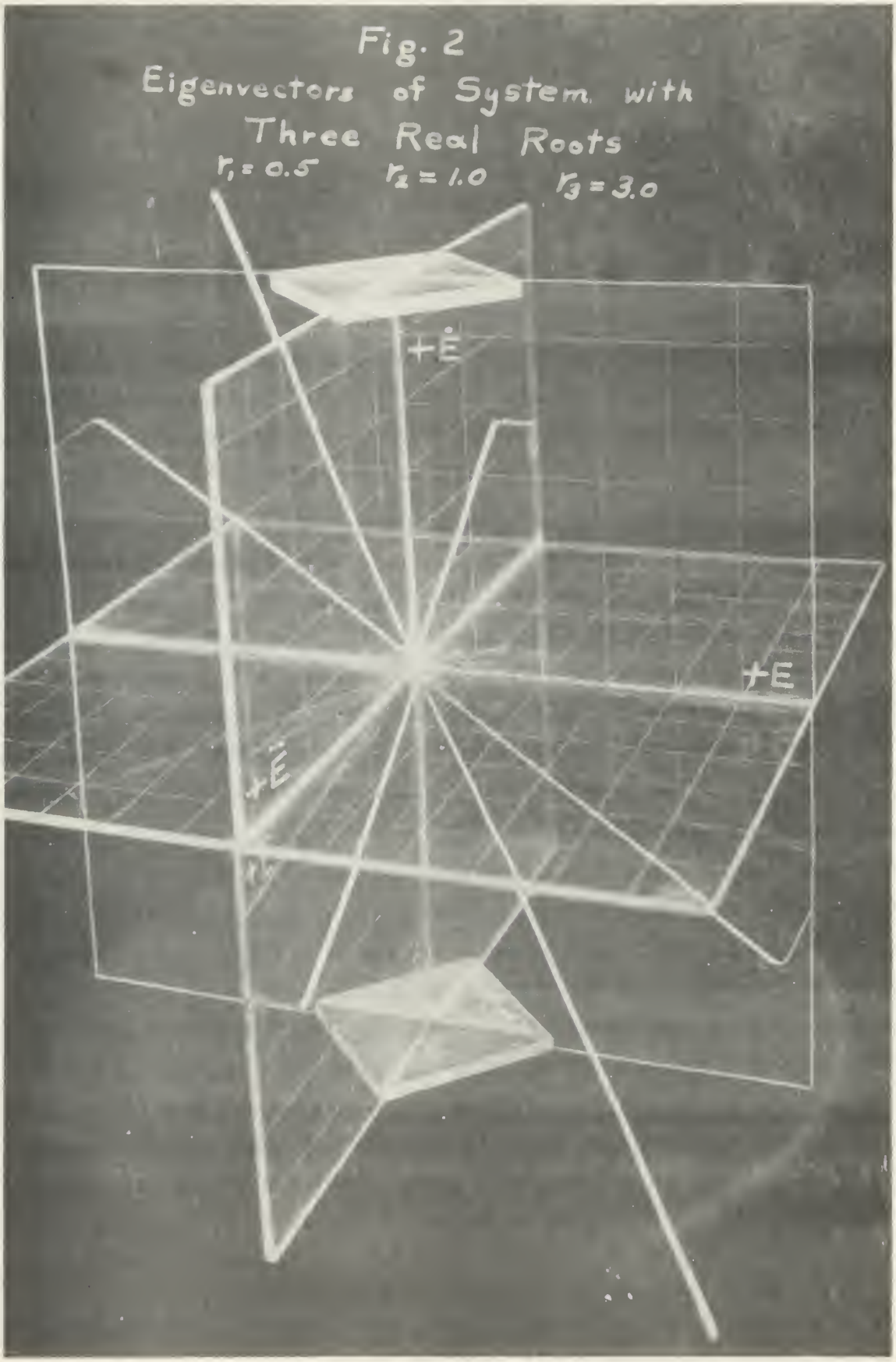
Fig. 2
Eigenvectors of System with
Three Real Roots
$r_1 = 0.5$ $r_2 = 1.0$ $r_3 = 3.0$
+Ė
+E
+Ë

Eliminating the parameter K and solving for r_i,

$$\dot{E} + r_i E \approx 0 \quad ; \quad r_i \approx -\frac{\dot{E}}{E} \tag{II-13a}$$

$$\dot{E} + \frac{\ddot{E}}{r_i} \approx 0 \quad ; \quad r_i \approx -\frac{\ddot{E}}{\dot{E}} \tag{II-13b}$$

Eliminating r_i from these equations leaves

$$\dot{E}^2 - E\ddot{E} \approx 0 \tag{II-14}$$

which is the equation of a right elliptical cone. Since direct substitution of the parametric equations for any arbitrary point on an eigenvector satisfies this equation of a right elliptical cone, the surface of the cone is the locus of all possible eigenvectors associated with the roots of a third order system.

This cone, which will be referred to as the eigencone, can be visualized as shown in Fig. 3 as the surface formed by an infinite number of eigenvectors emanating radially from the origin of the coordinate system. Figure 3 shows only that portion of the eigencone determined by the eigenvectors of roots located in the left half of the complex s-plane. An exploded view of the eigencone section located in octant 2' is shown in Fig. 4. Figure 5 shows this same section of the eigencone in its proper location as viewed looking into octant 4.

From these photographs it is apparent that the apex of the eigencone is located at the origin of error space and is tangent to both the E and $\ddot{E}$ axes. It is symmetrical about the line $E \approx \ddot{E}$ in the $E/\ddot{E}$ plane and is bisected by this plane. It will be noted in Fig. 5 that the surface of the eigencone nearest the E axis is labled SLOW while the surface nearest the $\ddot{E}$ axis is labled FAST. The eigenvectors in these regions correspond to phase trajectories which have response times characteristic of these labels. By referring again to the parametric equations of a point on an eigenvector Equation (II-12), it will be noted that for $r_i < 1.0$, the eigenvector will be located in the SLOW region while for $r_i > 1.0$, the eigenvector will be located in the FAST region. When $r_i \approx 1.0$ the eigenvector is equidistant from both the E and $\ddot{E}$ axes. It should be pointed out here that the classification of eigenvectors into slow,

intermediate and fast is not according to the labels on the eigencone, but is applied only to eigenvectors associated with the roots of a given system. It is incorrect to arbitrarily call all eigenvectors slow if they are associated with $r_i < 1.0$ or fast if $r_i > 1.0$. For different systems, the slow eigenvector of one may have a faster response than the fast eigenvector in the other. The labeling of the eigencone into slow and fast regions is intended to indicate the relative speed of response as related to the eigenvectors, and not to establish any sharp line of demarcation.

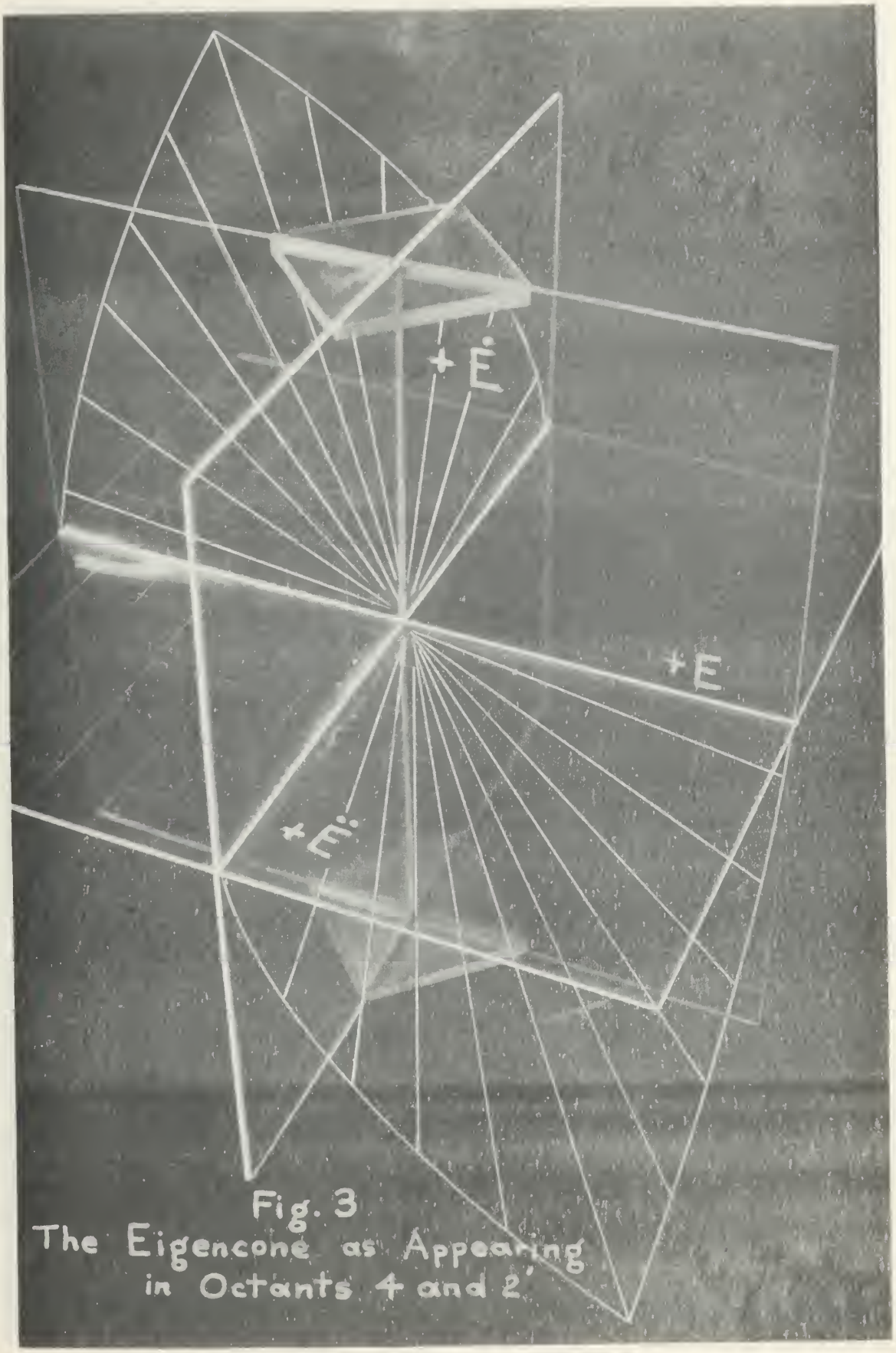

Fig. 3
The Eigencone as Appearing in Octants 4 and 2'

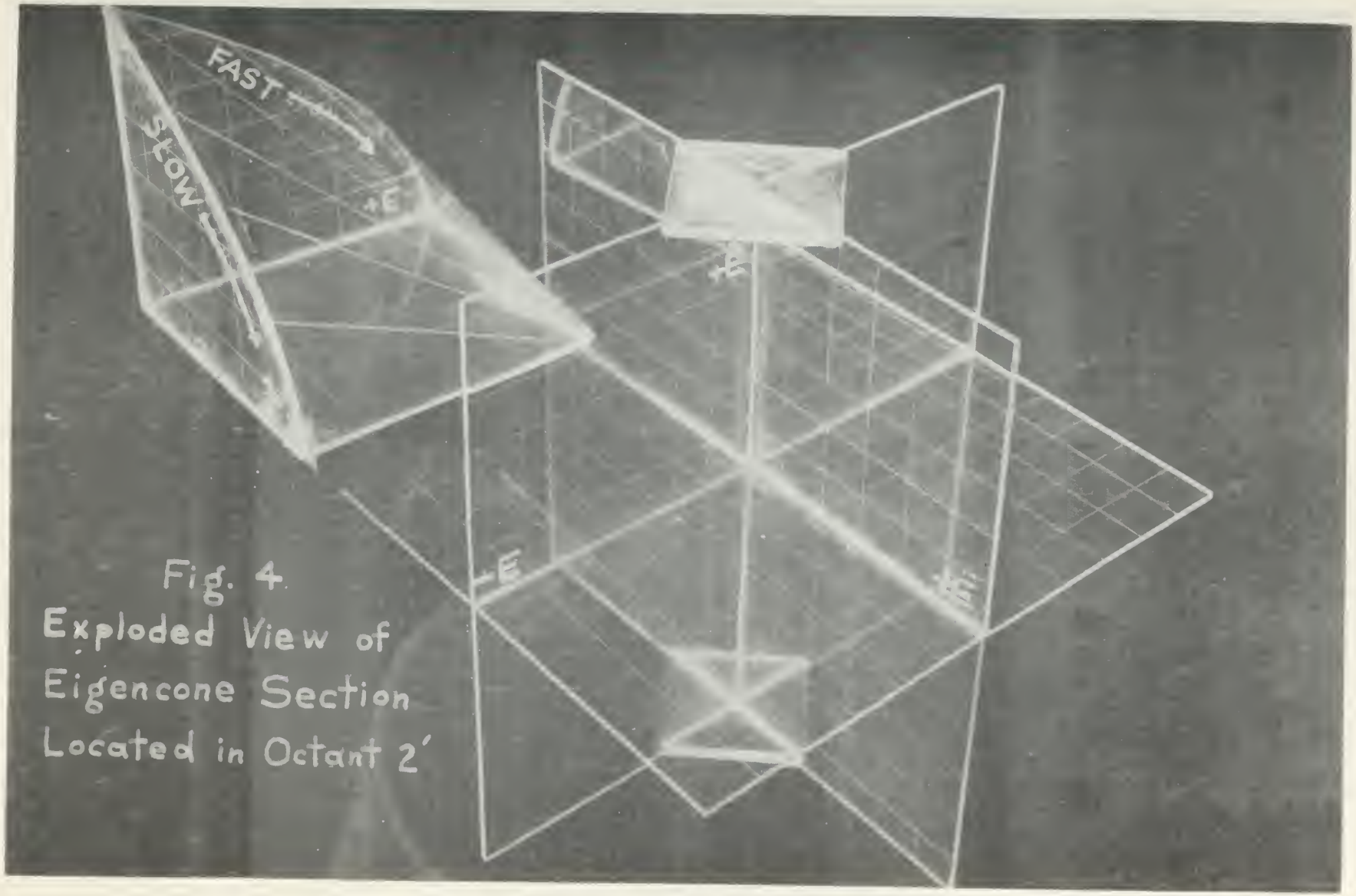

Fig. 4
Exploded View of
Eigencone Section
Located in Octant 2'

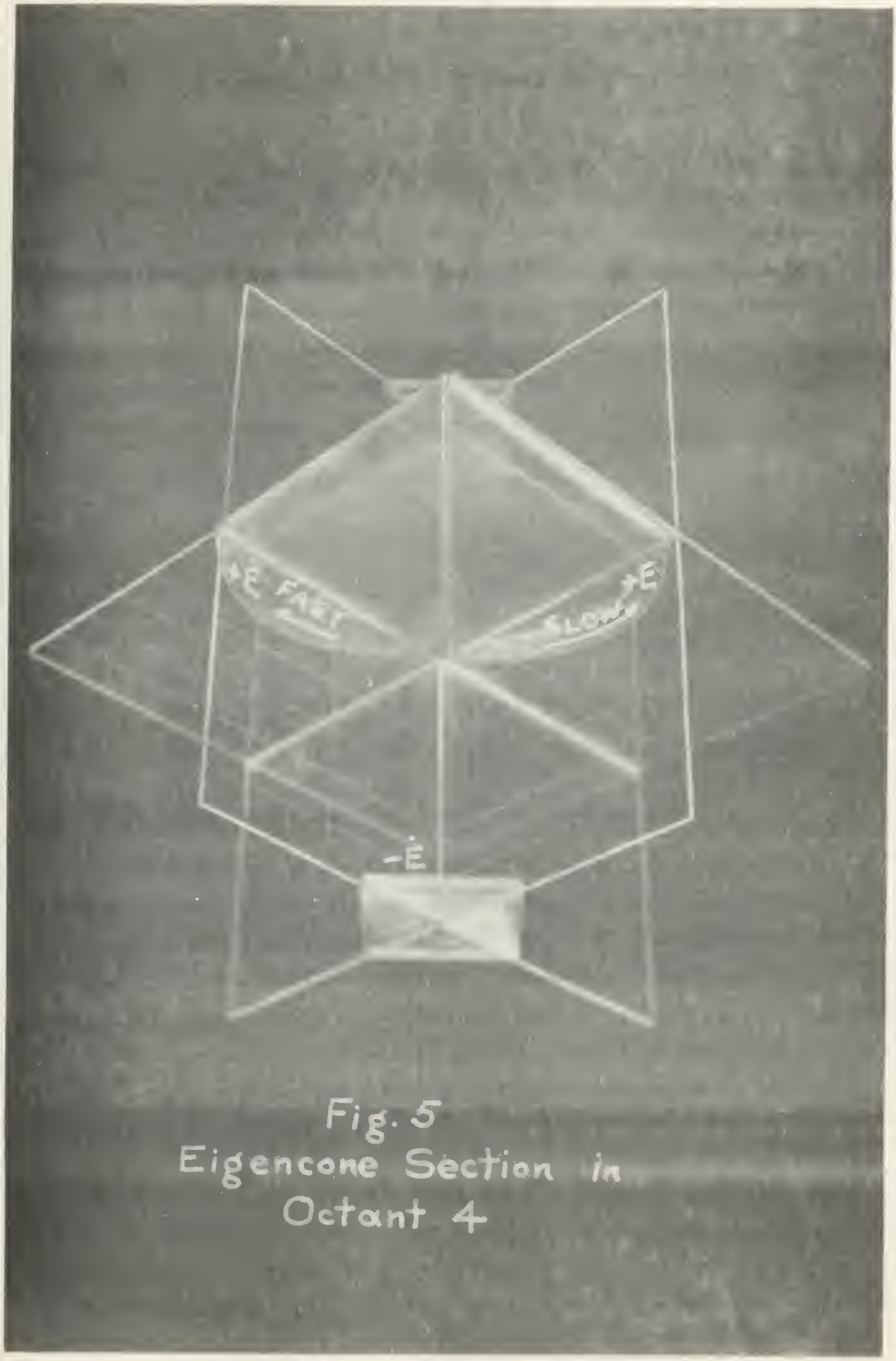

Fig. 5
Eigencone Section in
Octant 4

Chapter III

EIGENPLANES IN THIRD ORDER ERROR SPACE

General

It has been shown (Ref. 1, 4, 5) that any two eigenvectors in error space define a plane, passing through the origin of error space, called an eigenplane (or sometimes a "hyperplane"). The eigenplane has an equation one order lower than the order of the characteristic equation of the control system. The eigenplane equation is obtained by suppressing the root corresponding to the pertinent eigenvector in the differential equation of the system. Thus, in general,

$$\mu = \ddot{E}^{n-1} + \sum_{i=2}^{n} r_i \ddot{E}^{n-2} + \ldots + \prod_{i=2}^{n} r_i E = 0 \qquad \text{(III-1)}$$

For the third order case with real distinct roots, $r_1 < r_2 < r_3$,

$$\begin{aligned} \mu_1 &= \ddot{E} + (r_2+r_3)\dot{E} + r_2 r_3 E = 0 \quad (r_1 \text{ suppressed}) \\ \mu_2 &= \ddot{E} + (r_1+r_3)\dot{E} + r_1 r_3 E = 0 \quad (r_2 \text{ suppressed}) \\ \mu_3 &= \ddot{E} + (r_1+r_2)\dot{E} + r_1 r_2 E = 0 \quad (r_3 \text{ suppressed}) \end{aligned} \qquad \text{(III-2)}$$

are the defining equations for the three eigenplanes.

The eigenplanes in third order error space are also defined by two straight lines, the two eigenvectors corresponding to the two roots contained in the eigenplane equation. That is, the eigenplane defined by suppressing the smallest root, r_1, whose corresponding eigenvector is the slow eigenvector, contains, and can be defined by, the intermediate and fast eigenvectors. In a like manner, the other two eigenplanes are defined by the combination of slow and fast eigenvectors, and by the combination of slow and intermediate eigenvectors.

When referring to specific eigenplanes hereafter in this paper, the "First" eigenplane will mean that plane containing the intermediate and fast eigenvectors formed by suppressing the smallest root, r_1; the "Second" eigenplane will mean that plane containing the slow and fast

eigenvectors formed by suppressing the root, r_2; and the "Third" eigenplane will mean that plane containing the slow and intermediate eigenvectors formed by suppressing the largest root, r_3.

Eigenplanes of Systems With Three Real Distinct Roots

In a control system having three real distinct roots, there will, of course, exist three eigenplanes in error space. Since these eigenplanes are each defined by two eigenvectors, they should intersect the eigencone along lines corresponding to their two defining eigenvectors. This can be proved analytically by a simultaneous solution of the equations of the eigencone and of the eigenplane as shown below:

Equation of eigencone: $\dot{E}^2 - E\ddot{E} = 0$

Equation of eigenplane: $\mu = \dddot{E} + A\ddot{E} + B\dot{E} = 0$

where $A = r_1 + r_2$

$B = r_1 r_2$

Solving the equation of the eigencone for E yields:

$$E = \frac{\dot{E}^2}{\ddot{E}}$$

This expression for E, when substituted into the equation of the eigenplane, yields:

$$\dddot{E} + A\ddot{E} + B\left(\frac{\dot{E}^2}{\ddot{E}}\right) = 0$$

or

$$\ddot{E}^2 + A\dot{E}\ddot{E} + B\dot{E}^2 = 0$$

Now, assume $\dot{E}$ to have any arbitrary value, K. Hence, $\ddot{E}^2 + AK\ddot{E} + BK^2 = 0$, and this expression, when solved by the quadratic formula, yields for $\ddot{E}$,

$$\ddot{E} = \frac{-AK \pm \sqrt{(AK)^2 - 4BK^2}}{2}$$

or in terms of the roots, r_1 and r_2

$$\ddot{E} = \frac{-(r_1+r_2)K \pm \sqrt{r_1^2K^2 + 2r_1r_2K^2 + r_2^2K^2 - 4r_1r_2K^2}}{2}$$

$$= \frac{-r_1K - r_2K \pm \sqrt{r_1^2K^2 - 2r_1r_2K^2 + r_2^2K^2}}{2}$$

$$= \frac{-r_1K - r_2K \pm \sqrt{(r_1K - r_2K)^2}}{2}$$

$$= \frac{-r_1K - r_2K \pm (r_1K - r_2K)}{2}$$

Thus: $\ddot{E} = -r_2K, -r_1K$

$$E = \frac{\dot{E}^2}{\ddot{E}} = \frac{K^2}{-r_2K}, \frac{K^2}{-r_1K} = \frac{-K}{r_2}, \frac{-K}{r_1}$$

Hence: $(E, \dot{E}, \ddot{E}) = \left(\frac{-K}{r_1}, K, -Kr_1\right)$ and $\left(\frac{-K}{r_2}, K, -Kr_2\right)$

which are the coordinates of any point on the two eigenvectors defining the eigenplane, μ.

If one were to visualize all three eigenplanes in error space, a volume would be bounded by these three eigenplanes. This volume would be two pyramids, in octants 4 and 2' with their apexes at the origin of error space and their edges corresponding to the three eigenvectors of the system. Fig 6 is a pictorial representation of just the pyramid in octant 2' defined by the three eigenvectors and bounded by the three eigenplanes of a system with roots, $r_1 = 0.333$, $r_2 = 1.0$, and $r_3 = 3.0$.

The orientation of this pyramid is such that it will always lie within the eigencone and its size and shape will depend on the location

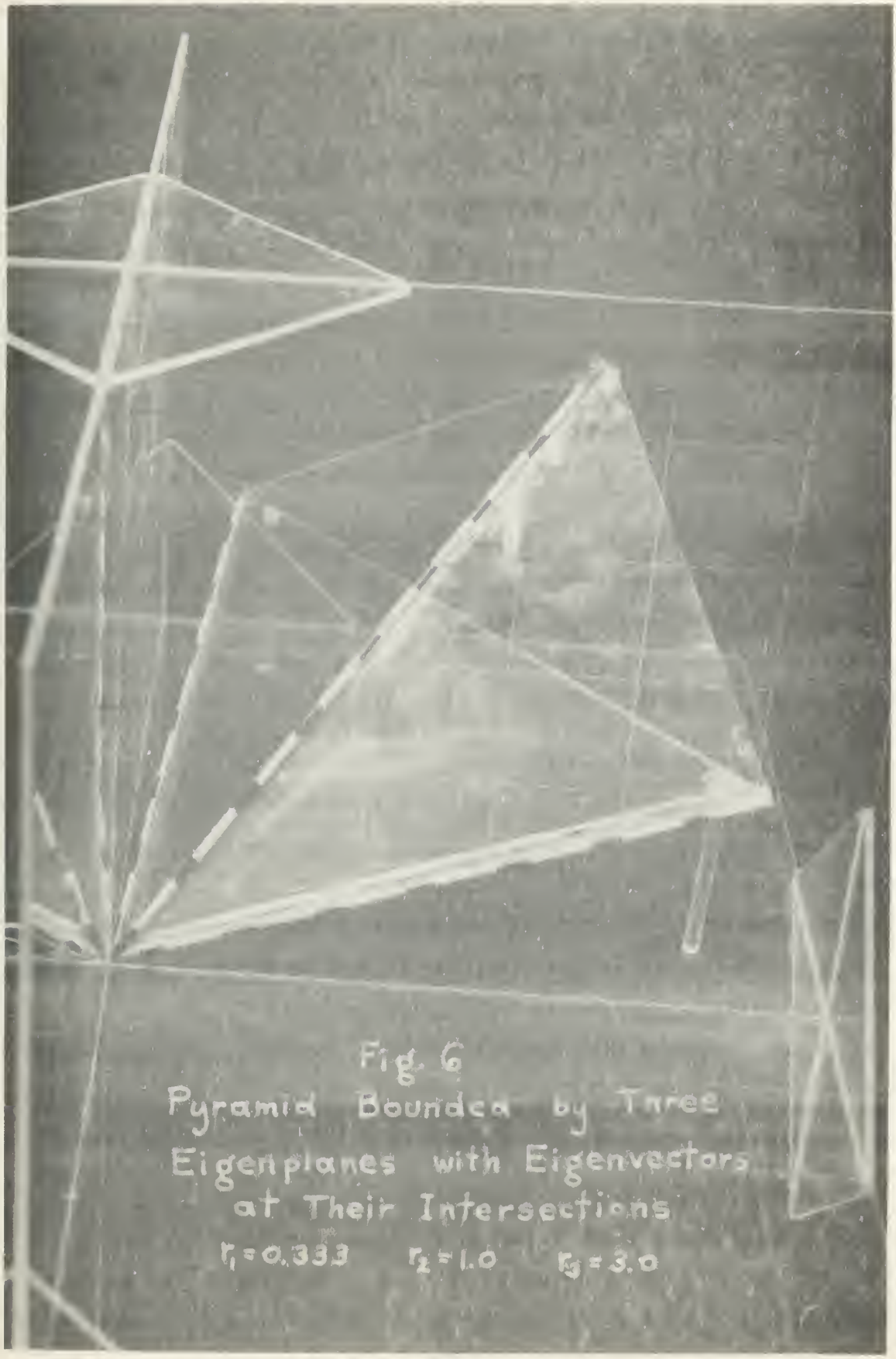

Fig. 6
Pyramid Bounded by Three
Eigenplanes with Eigenvectors
at Their Intersections
$r_1 = 0.333$ $r_2 = 1.0$ $r_3 = 3.0$

of the system roots on the axis of reals. If the system roots are all close together, the volume of the pyramid will be small as compared to the volume enclosed by the eigencone. Conversely, if r_1 is allowed to approach zero and r_3 is allowed to approach infinity, with $r_2 \cong 1.0$, the resulting pyramid will almost completely fill the eigencone.

If all three system roots are small, i.e., less than 1.0, the pyramid will be relatively small and oriented near the E axis; and, conversely, if all three roots are greater than 1.0, the pyramid will also be small, but oriented near the $\ddot{E}$ axis.

Eigenplanes of Systems Having One Real Root and a Complex Pair of Roots

For a control system having one real root and two conjugate complex roots, it can be readily seen from equations (III-2) which define the three general eigenplanes that only one eigenplane can exist for this system. If r_2 and r_3 are of the form $a \pm jb$, the eigenplanes μ_2 and μ_3 cannot exist because of the imaginary coefficients of E and $\dot{E}$ in Equation (III-1). Thus only one eigenplane, $\mu_1 = \ddot{E} + (r_2+r_3)\dot{E} + r_2 r_3 E = 0$, and, as was shown in the previous section, only one eigenvector with coordinates $\left(\mp \frac{k}{r_1}, \pm k, \mp k r_1\right)$ will exist in error space. This single eigenplane existing for this type system will subsequently be referred to as the "complex eigenplane".

Closer inspection of the equation of the complex eigenplane given above shows that since the real root, r_1, does not appear in the equation, the location of the complex eigenplane in error space is completely independent of the magnitude of the real root of the system.

An investigation of the effects of varying system parameters and complex root location was conducted to gain more knowledge about the orientation of the complex eigenplane in error space. In this phase of the investigation, the three-dimensional model was invaluable. By setting any one of the three coordinates of Equations (III-2) equal to zero, the traces in the three coordinate planes of the model were easily computed and drawn on the transparent coordinate frame. This permitted easy visualization of the eigenplanes and their orientation with respect to each other, to the eigenvectors, and to the eigencone.

The first investigation of the eigenplane location was made by keeping the damping ratio, ζ, of the system constant while varying the natural frequency of the system, w_n, keeping the real root of the system constant also. This is equivalent to the root movement shown to the right in Fig. 7.

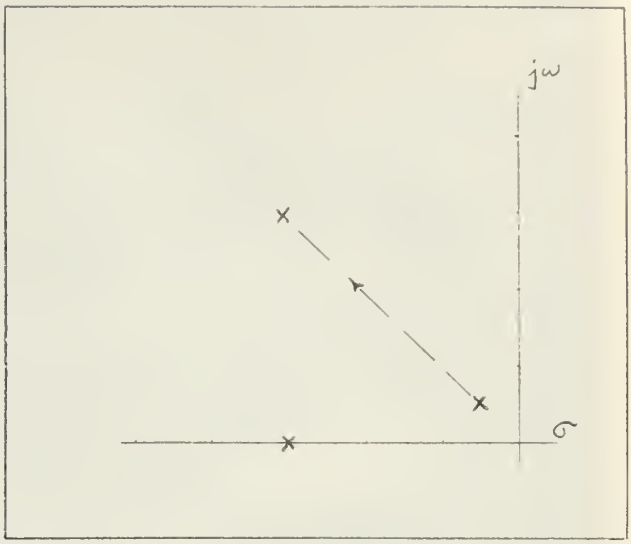

Fig. 7 Root Movement; w_n variable, ζ constant

The root locations investigated were:

$r_1 = 3.0 = \text{constant}$ $\qquad\qquad$ $\zeta = .707 = \text{constant}$

$r_{2,3} = .5 \pm j\ .5$	$w_n = .707$	(Case A)
$r_{2,3} = 1.0 \pm j\ 1.0$	$w_n = 1.414$	(Case B)
$r_{2,3} = 2.0 \pm j\ 2.0$	$w_n = 2.828$	(Case C)
$r_{2,3} = 3.0 \pm j\ 3.0$	$w_n = 4.242$	(Case D)

Models of the eigenplanes of these cases were built and from these it was seen that with ζ constant, varying w_n causes the eigenplane to "twist" around the eigencone. This twist can be easily seen in Fig. 8 which shows the eigenplanes for Cases A, B, C and D respectively.

As can also be seen from Fig. 9, views looking down the edges of the eigenplanes of Cases A, B, and C, the angle that the eigenplane makes with the eigencone appears to remain constant as w_n is varied. No attempt was made to analytically prove this angle to be constant, nor was an attempt made to derive a relationship of this angle to the value of ζ chosen in the investigation.

In the next phase of the investigation, the real root and the real part of the complex roots were kept constant while the imaginary part of the complex roots was varied.

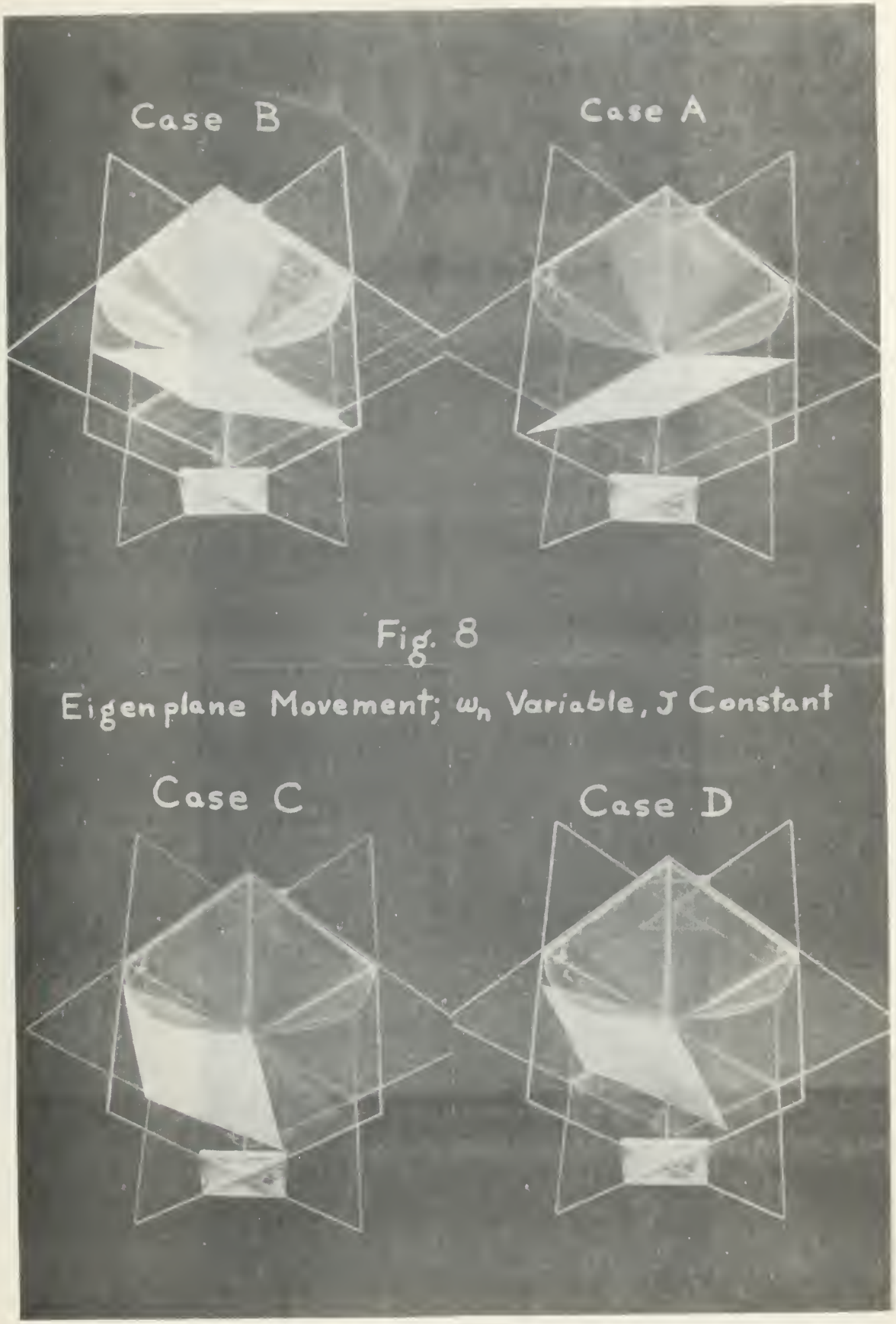

Fig. 8

Eigenplane Movement; ω_n Variable, J Constant

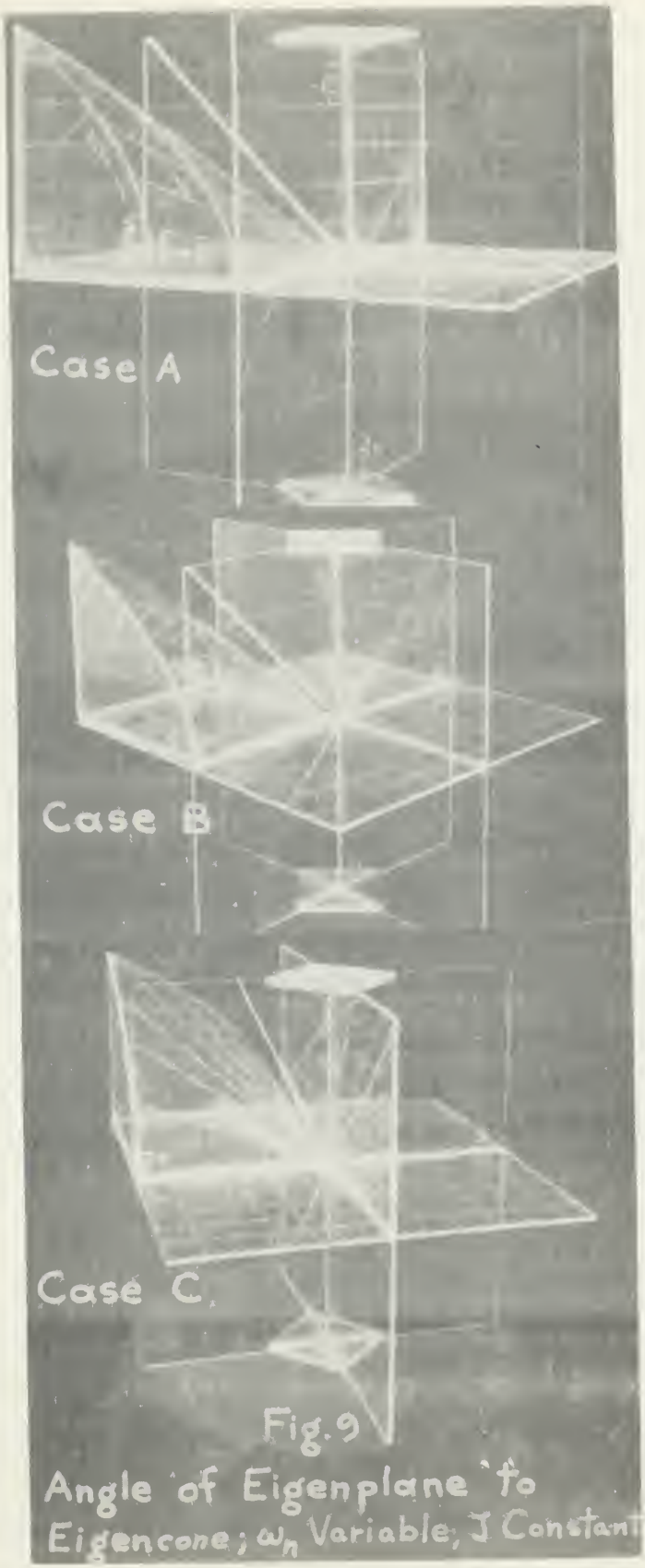

Fig. 9
Angle of Eigenplane to Eigencone; ω_n Variable, J Constant

This movement of the roots is shown at right in Fig. 10.

The root locations investigated were:

$r_1 = 3.0 = \text{constant}$

$r_{2,3} = 1.0 \pm j\ 1.0$ (Case B)

$r_{2,3} = 1.0 \pm j\ 2.0$ (Case F)

$r_{2,3} = 1.0 \pm j\ 3.0$ (Case G)

$r_{2,3} = 1.0 \pm j\ 4.0$ (Case H)

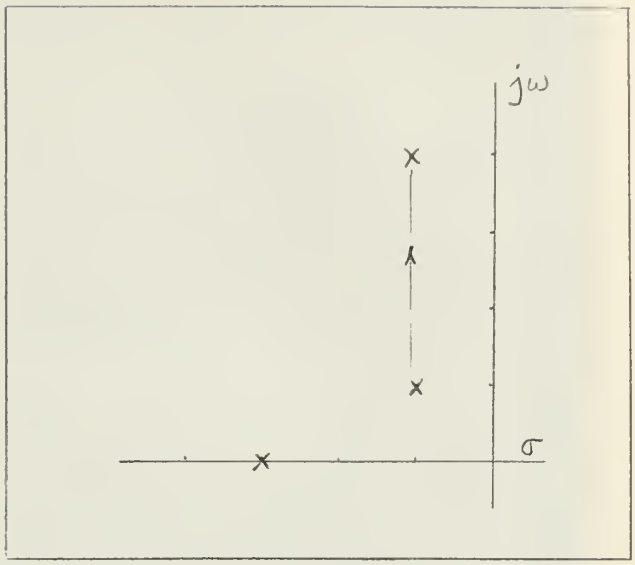

Fig. 10 Root Movement;
Im(x ± jy) variable,
Re(x ± jy) constant

In determining the equations of the traces of these complex eigenplanes in the coordinate planes, it was found that the trace of all complex eigenplanes, where they intersected the $\dot{E}/\ddot{E}$ plane, was constant. This is equivalent, in three dimensions, to a rotation of the complex eigenplane about a line in the $\dot{E}/\ddot{E}$ plane. This rotation of the complex eigenplane with the variation of the imaginary part of the complex roots is shown pictorially in Fig. 11 for Cases F, G and H.

Without the use of the three-dimensional models, it can be seen that the variation of only the imaginary part of the complex roots will have no effect on the trace of the eigenplane in the $\dot{E}/\ddot{E}$ plane. The equation of this trace is:

$$\ddot{E} + (r_2 + r_3)\ \dot{E} = 0$$

and, with r_2 and r_3 complex conjugates, the coefficient of the $\dot{E}$ term in the above expression depends only on the magnitude of the real part of the complex roots.

The final phase of this investigation of eigenplane geometry consisted of varying the system damping ratio, ζ, while holding the natural frequency of the system, w_n, constant.

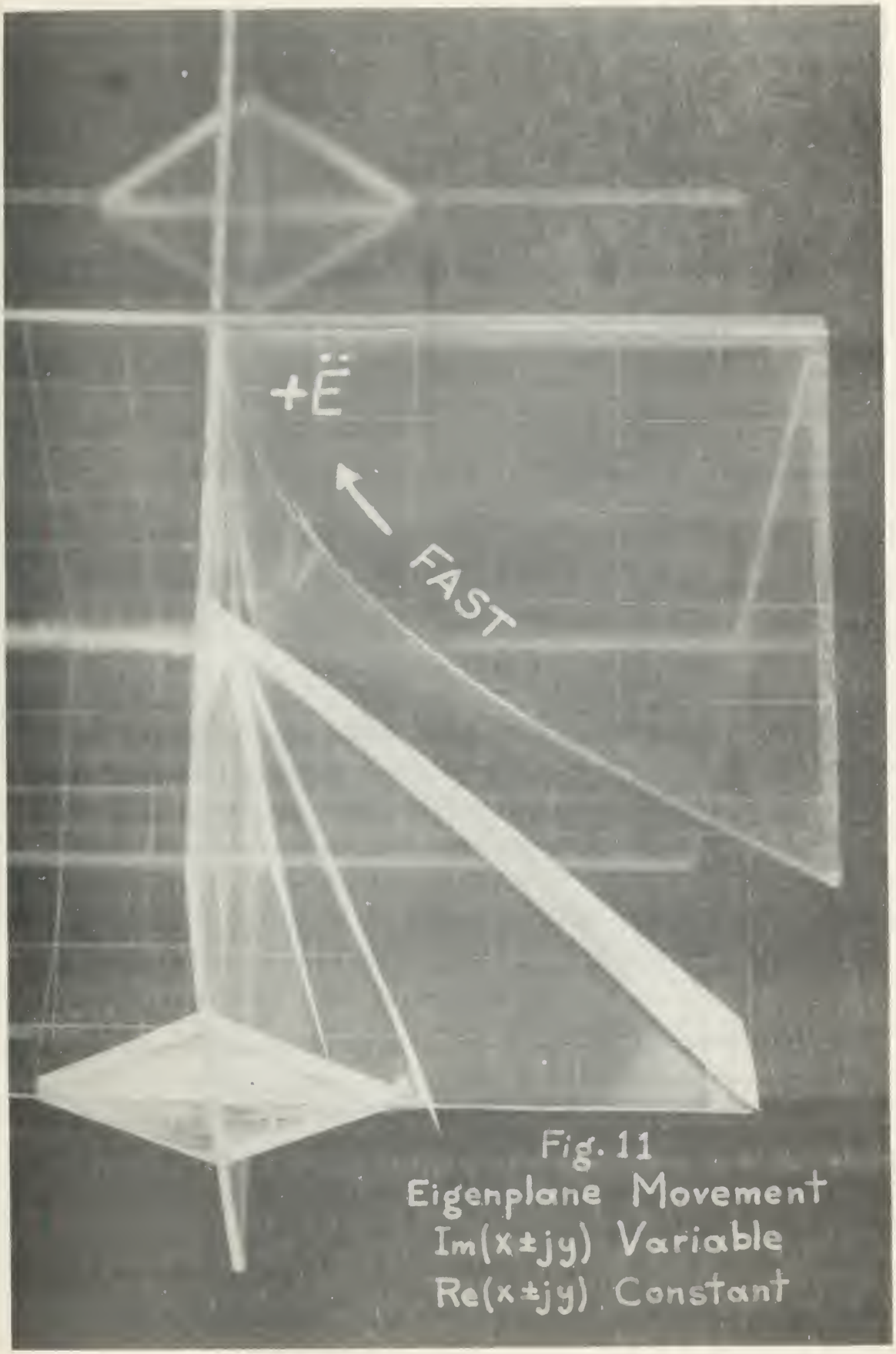

Fig. 11
Eigenplane Movement
Im(x±jy) Variable
Re(x±jy) Constant

This movement of the roots is shown at the right in Fig. 12. The root locations investigated were:

$r_1 = 3.0 = \text{constant}$

$w_n = 2.83 = \text{constant}$

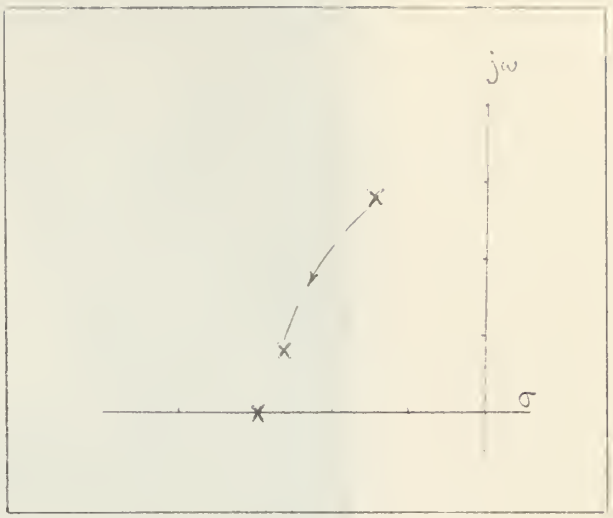

Fig. 12 Root Movement; ζ variable, w_n constant

$r_{2,3} = 1.414 \pm j2.45 \quad \zeta = .5 \quad$ (Case I)

$r_{2,3} = 2.0 \pm j2.0 \quad \zeta = .707 \quad$ (Case C)

$r_{2,3} = 2.45 \pm j1.414 \quad \zeta = .866 \quad$ (Case M)

$r_{2,3} = 2.735 \pm j .732 \quad \zeta = .966 \quad$ (Case J)

Here again, in determining the equations of the traces of these various complex eigenplanes, it was found that the trace of all complex eigenplanes, where they intersected one of the coordinate planes, was constant. In this instance, the constant trace was located in the $E/\ddot{E}$ plane. This, likewise, is the same as a rotation of the complex eigenplane about a line in the $E/\ddot{E}$ plane. This rotation of the complex eigenplane as the system ζ varies, with w_n held constant, is shown in Fig. 13, for Cases C, I, and J, respectively.

Further analysis of the last two phases of this investigation of the geometry of the eigenplane has led to a generalization regarding the orientation of the complex eigenplane as the location of the complex roots of a third order system is varied. That is, as the imaginary part of the complex roots is varied from large values to small values, (this is equivalent to increasing the system ζ) the complex eigenplane rotates toward the surface of the eigencone and as ζ reaches 1.0, the complex

Fig. 13
Eigenplane Movement
J Variable, ω_n Constant

eigenplane becomes tangent to the eigencone at the eigenvector corresponding to the magnitude of these two roots as they enter the axis of reals. At the moment of entry, the roots are real and repeated, and are associated with a common eigenvector. This may also be shown analytically by obtaining the equation of the eigenplane tangent to the eigencone.

The general form of a plane tangent to a conic surface at a point is:

$$\left(\frac{\partial \mathcal{F}}{\partial E}\right)_{\substack{E=E_o \\ \dot{E}=\dot{E}_o \\ \ddot{E}=\ddot{E}_o}} (E-E_o) + \left(\frac{\partial \mathcal{F}}{\partial \dot{E}}\right)_{\substack{E=E_o \\ \dot{E}=\dot{E}_o \\ \ddot{E}=\ddot{E}_o}} (\dot{E}-\dot{E}_o) + \left(\frac{\partial \mathcal{F}}{\partial \ddot{E}}\right)_{\substack{E=E_o \\ \dot{E}=\dot{E}_o \\ \ddot{E}=\ddot{E}_o}} (\ddot{E}-\ddot{E}_o) = 0$$

where $\mathcal{F}(E, \dot{E}, \ddot{E}) = \dot{E}^2 - E\ddot{E}$ (the equation of the eigencone). Performing the partial differentiation at the point $E = E_o$, $\dot{E} = \dot{E}_o$, $\ddot{E} = \ddot{E}_o$ yields

$$-\ddot{E}_o (E - E_o) + 2\dot{E}_o (\dot{E} - \dot{E}_o) - E_o (\ddot{E} - \ddot{E}_o) = 0$$

Let $(E_o, \dot{E}_o, \ddot{E}_o) = \left(-\frac{K}{r_i}, K, -r_i K\right)$, any point on an eigenvector.

Thus

$$r_i K\left(E + \frac{K}{r_i}\right) + 2K(\dot{E} - K) + \frac{K}{r_i}(\ddot{E} + r_i K) = 0$$

$$r_i KE + K^2 + 2K\dot{E} - 2K^2 + \frac{K}{r_i}\ddot{E} + K^2 = 0$$

Combining terms and dividing through by K gives:

$$r_i E + 2\dot{E} + \frac{\ddot{E}}{r_i} = 0$$

or

$$\ddot{E} + 2r_i \dot{E} + r_i^2 E = 0$$

which is the equation of an eigenplane defined by any two repeated real roots, r_i.

A special case of tangency between eigenplane and eigencone exists for the case of three repeated real roots. Here, the line of tangency corresponds to a single eigenvector which is the only eigenvector of the system, and is the eigenvector for all three roots.

Extending this reasoning further helps explain the existance of the previously mentioned pyramid of real root eigenplanes. If a system gain is high enough so that the root locus consists of one real root and a complex pair, there will be one real root eigenvector and a complex eigenplane in error space. As the gain is lowered such that the complex roots just enter the axis of reals, the complex eigenplane is tangent to the eigencone at the eigenvector corresponding to the two repeated real roots. As the system gain is lowered further, the entering roots will diverge on the axis of reals and the complex eigenplane breaks into two real eigenplanes, now passing through the eigencone and intersecting it at the real root eigenvectors. These two real root eigenvectors now form the pyramid with the original real root eigenvector.

Method of Determining Roots to Locate an Eigenplane in a Desired Location

A method of fixing the eigenplane in error space has been developed whereby, given any two traces of the eigenplane on the coordinate planes, the required system roots can be readily determined. As has been previously shown, only the complex conjugate roots of the system are necessary to define the complex eigenplane, and the real root of the system can be of any magnitude. The real roots, taken two at a time, will define the eigenplanes of a system with three real roots.

The method will first be developed in general terms, and then a numerical example will be given. First, consider the differential equation of a third order system:

$$\dddot{E} + a\ddot{E} + b\dot{E} + cE = 0 \qquad \text{(III-3)}$$

where: $a = r_1 + r_2 + r_3$

$b = r_1r_2 + r_2r_3 + r_1r_3$

$c = r_1r_2r_3$

Let $r_1 = z$

$r_2 = x + jy$

$r_3 = r_2^* = x - jy$

Thus:

$r_2 + r_3 = 2x$ and $r_2 r_3 = x^2 + y^2$

The equation of a typical eigenplane is given by:

$$\mu_1 = \ddot{E} + (r_2 + r_3)\,\dot{E} + r_2 r_3\, E = 0$$

Substitution of the above expressions for $r_2 + r_3$ and $r_2 r_3$ into μ_1 yields:

$$\mu_1 = \ddot{E} + (2x)\,\dot{E} + (x^2 + y^2)\,E = 0$$

This expression will give the following traces of μ_1 in the three coordinate planes:

(In $E/\dot{E}$ plane) $\quad 2x\dot{E} + (x^2 + y^2)\,E = 0$ (III-4a)

(In $\dot{E}/\ddot{E}$ plane) $\quad \ddot{E} + 2x\dot{E} = 0$ (III-4b)

(In $E/\ddot{E}$ plane) $\quad \ddot{E} + (x^2 + y^2)\,E = 0$ (III-4c)

Rewriting the above trace equations in terms of the angle at the origin yields:

$$\frac{\dot{E}}{-E} = -\tan\alpha = \frac{x^2 + y^2}{2x} \qquad \text{(III-5a)}$$

$$\frac{\dot{E}}{-\ddot{E}} = -\tan\beta = \frac{1}{2x} \qquad \text{(III-5b)}$$

$$\frac{\ddot{E}}{-E} = -\tan\gamma = x^2 + y^2 \qquad \text{(III-5c)}$$

Where α, β, and γ are defined in Fig. 14

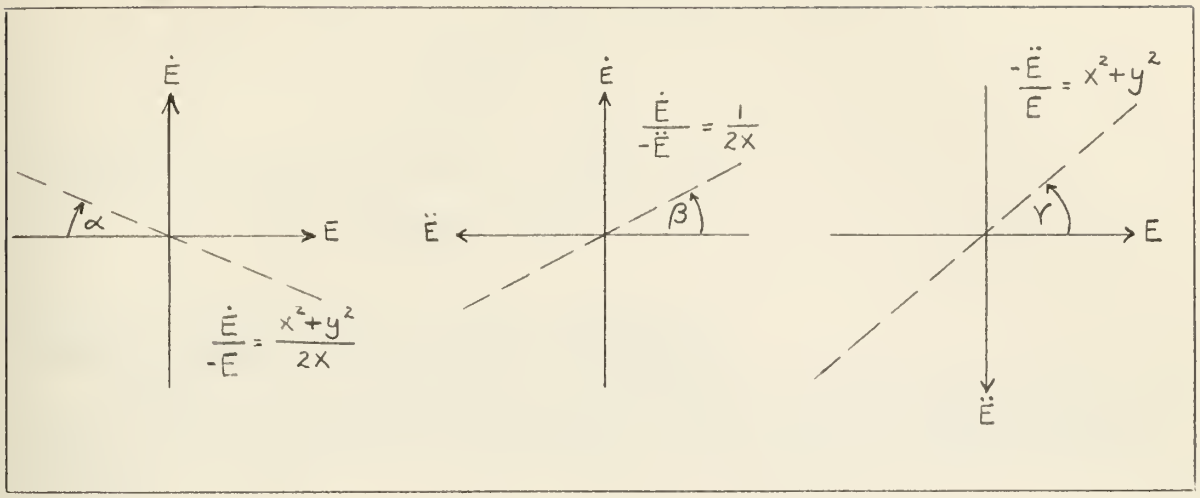

Fig. 14. Angles α, β, and γ on the coordinate planes.

By determining any two of the three angles, α, β, and γ, and substituting these angles into the corresponding tangent equations(III-5), a system of two equations in the two unknowns, x and y, are established. On solving for x and y, r_2 and r_3 are determined. If y is determined to be complex, substitution into the expression $r_{2,3} = x \pm jy$ yields r_2 and r_3 as real roots. If y is real, then r_2 and r_3 are complex conjugate roots.

Numerical Example for Complex Eigenplane

Assume that a complex eigenplane is required to be located such that its trace in the $E/\dot{E}$ plane is defined by $\alpha = 45^\circ$, and in the $\dot{E}/\ddot{E}$ plane by $\beta = 60^\circ$.

Substituting these into Equations (III-5a) and (III-5b) yields:

$$\tan 45^\circ = \frac{x^2+y^2}{2X} = 1 \qquad \text{(III-6a)}$$

$$\tan 60^\circ = \frac{1}{2X} = \sqrt{3} \qquad \text{(III-6b)}$$

Solution of (III-6b) directly determines x:

$$X = \frac{1}{2\sqrt{3}} = .288$$

and this, when substituted into (III-6a) yields:

$$(+.288)^2 + y^2 = +2\ (+.288)$$

$$y^2 = .576 - .0833 = .4927$$

or $$y = \sqrt{.4927} = .701$$

Therefore the required roots r_2 and r_3 are:

$$r_{2,3} = .288 \pm j\ .701$$

Numerical Example for Real Root Eigenplane

Assume that an eigenplane is required to be located such that its trace in the $E/\dot{E}$ plane is defined by $\alpha = 15^o$, and in the $\ddot{E}/E$ plane by $\gamma = 45^o$.

Substituting these values into Equations (III-5a) and (III-5c) yields:

$$\tan 15^\circ = \frac{X^2 + y^2}{2X} = .268$$

$$\tan 45^\circ = X^2 + y^2 = 1$$

Substitution into the upper equation yields x directly:

$$\frac{1}{2X} = .268$$

$$X = \frac{1}{2(.268)} = \frac{1}{.536} = 1.865$$

$$(1.865)^2 + y^2 = 1$$

$$y^2 = 1 - 3.475$$

$$y = \pm\sqrt{-2.475}$$

$$y = \pm j\ 1.573$$

$$r_2 = x + jy$$

$$= 1.865 + j(j1.573)$$

$$= .292$$

$$r_3 = 1.865 - j(j1.573)$$

$$= 3.439$$

Note that since r_2 and r_3 are complex conjugate roots, only one value of y, either positive or negative, need be substituted into $r_{2,3} = x \pm jy$.

Chapter IV

PHASE TRAJECTORIES OF THIRD ORDER LINEAR SYSTEMS

General

It is well known that the time solution to the differential equation of a linear third order feedback control system can be represented by a continuous curve in three-dimensional error space. If the differential equation of a third order system,

$$\dddot{E} + a\ddot{E} + b\dot{E} + cE = 0 \qquad \text{(IV-1)}$$

is solved by Laplace transform methods, the time solution obtained is:

$$E(t) = \frac{\ddot{E}_o + (r_2+r_3)\dot{E}_o + (r_2r_3)E_o}{(r_2-r_1)(r_3-r_1)}\epsilon^{-r_1t} + \frac{\ddot{E}_o + (r_1+r_3)\dot{E}_o + (r_1r_3)E_o}{(r_1-r_2)(r_3-r_2)}\epsilon^{-r_2t}$$

$$+ \frac{\ddot{E}_o + (r_1+r_2)\dot{E}_o + (r_1r_2)E_o}{(r_1-r_3)(r_2-r_3)}\epsilon^{-r_3t} \qquad \text{(IV-2)}$$

where E_o, $\dot{E}_o$, and $\ddot{E}_o$ are the initial conditions of error, error velocity, and error acceleration respectively. Successive differentiation of Equation (IV-2) with respect to time yields similar expressions for $\dot{E}(t)$ and $\ddot{E}(t)$.

Substituting the values of initial conditions E_o, $\dot{E}_o$, and $\ddot{E}_o$, system root values, and time into Equation (IV-2) and its derivatives yields the coordinates of points which describe the "state", i.e., the error, error velocity, and error acceleration of the system at that particular time. The locus of all these points is the phase trajectory of the system.

The calculation of trajectories by direct substitution into Equation (IV-2) and its derivatives would be a laborious process. This simple but time consuming method of solving for phase trajectories suggests solution by means of electronic computers.

In the initial stages of this investigation, solution of the differential equation (IV-1) was accomplished utilizing the Control Data Corporation 1604 high speed solid state general purpose digital computer. The digital computer program was written in FORTRAN language and is given in Appendix A along with its flow diagram. This FORTRAN program is based on the Runge-Kutta method of numerical integration. In order to obtain the desired accuracy of solution, state points were computed at intervals of 0.01 sec. but were printed out at intervals of 0.05 sec. A sample print out of the digital solution is also given in Appendix A. The program was allowed to run for a total problem time of 10.0 sec., and in practically all cases, at the end of this time, the values of E, $\dot{E}$, and $\ddot{E}$ were small enough to consider that the trajectory had reached the origin of error space. In the beginning of the investigation, it had been anticipated that a digital to x-y plotter would be used to obtain the trajectories in graphical form. However, this plotting equipment did not become available, and it was necessary to hand plot all phase trajectories.

In the latter stages of the investigation, in order to obtain trajectories more rapidly, a Donner 3100 analog computer was used in conjunction with an x-y servo plotter. The flow chart and scaling data for the analog computer solution are given in Appendix B.

In both the digital and analog solutions, plots of the trajectories in the three coordinate planes, $E/\dot{E}$, $E/\ddot{E}$, and $\dot{E}/\ddot{E}$ were made and then transferred to the corresponding planes of the plexiglass models. Using these projections, the three-dimensional models of the phase trajectories were constructed. Samples of the three projections of a typical phase trajectory of a three real root system, as obtained from the analog computer, are given in Figs. 15 through 17.

Effect of Root Location on Phase Trajectories

For a system defined by a given set of roots, the phase trajectories in response to various initial conditions are constrained by the eigenvectors and eigenplanes associated with the defining roots. Since it has been shown previously that eigenvector and eigenplane orientation are

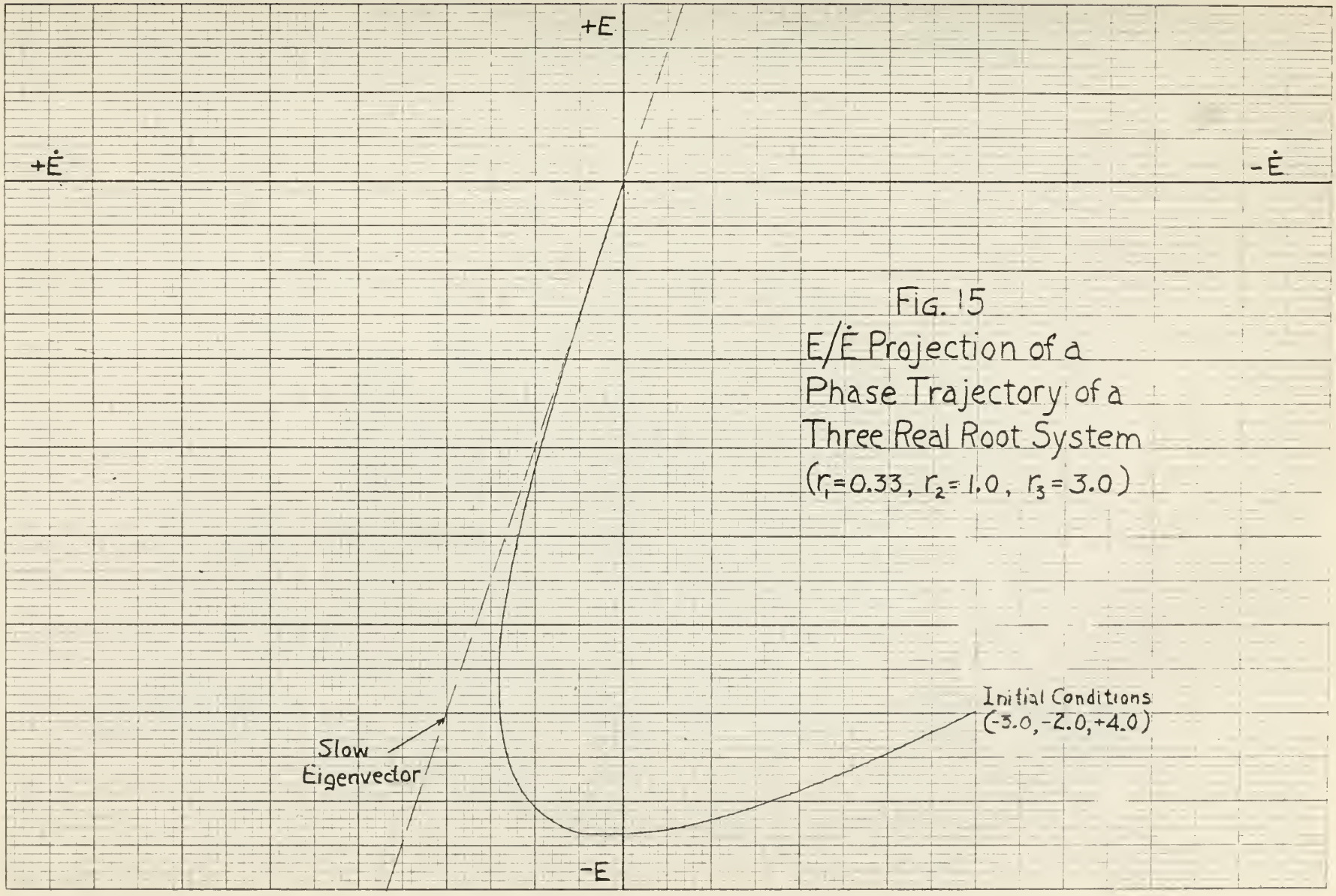

Fig. 15
E/Ė Projection of a
Phase Trajectory of a
Three Real Root System
($r_1 = 0.33$, $r_2 = 1.0$, $r_3 = 3.0$)

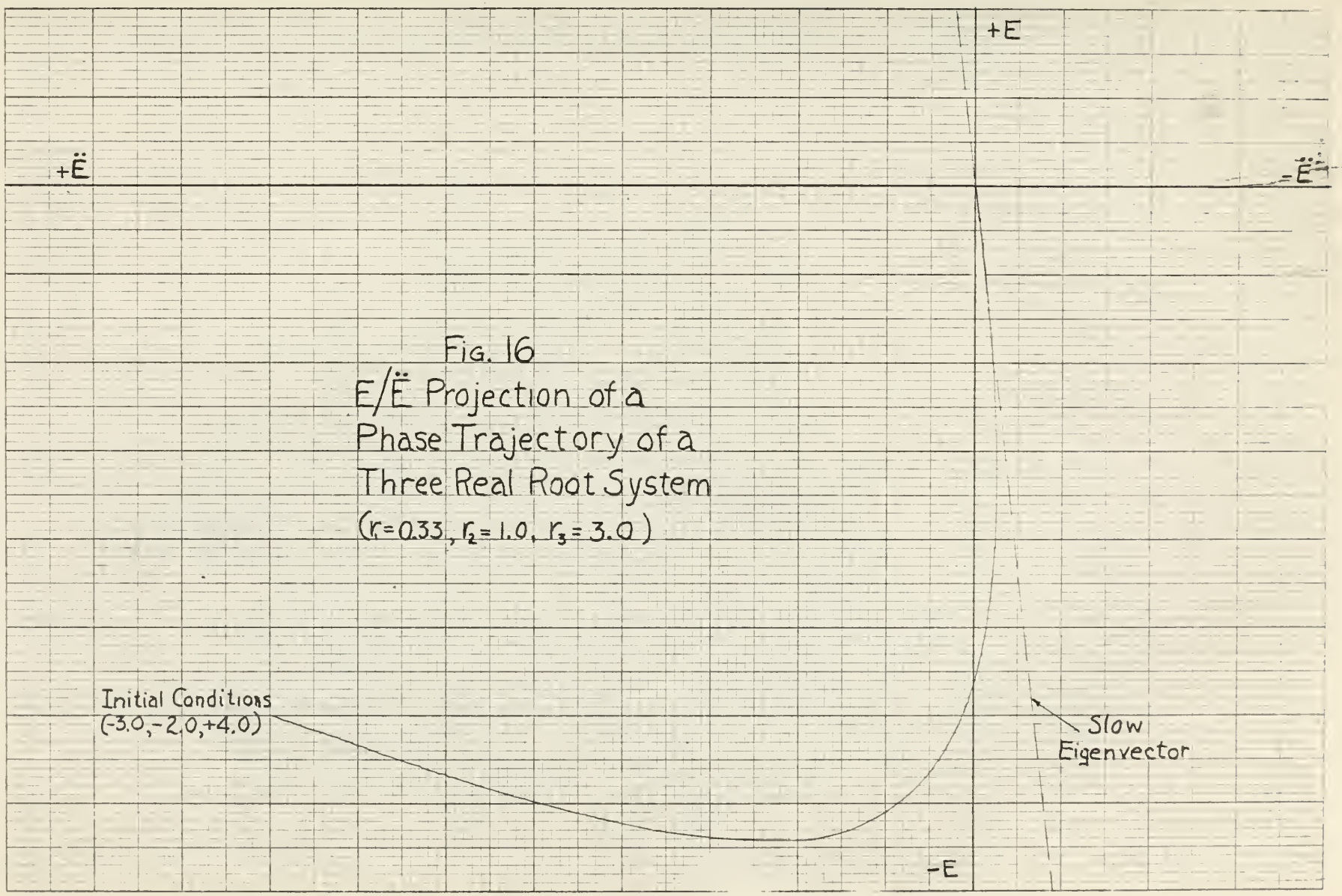

Fig. 16
E/Ë Projection of a
Phase Trajectory of a
Three Real Root System
(r_1=0.33, r_2=1.0, r_3=3.0)

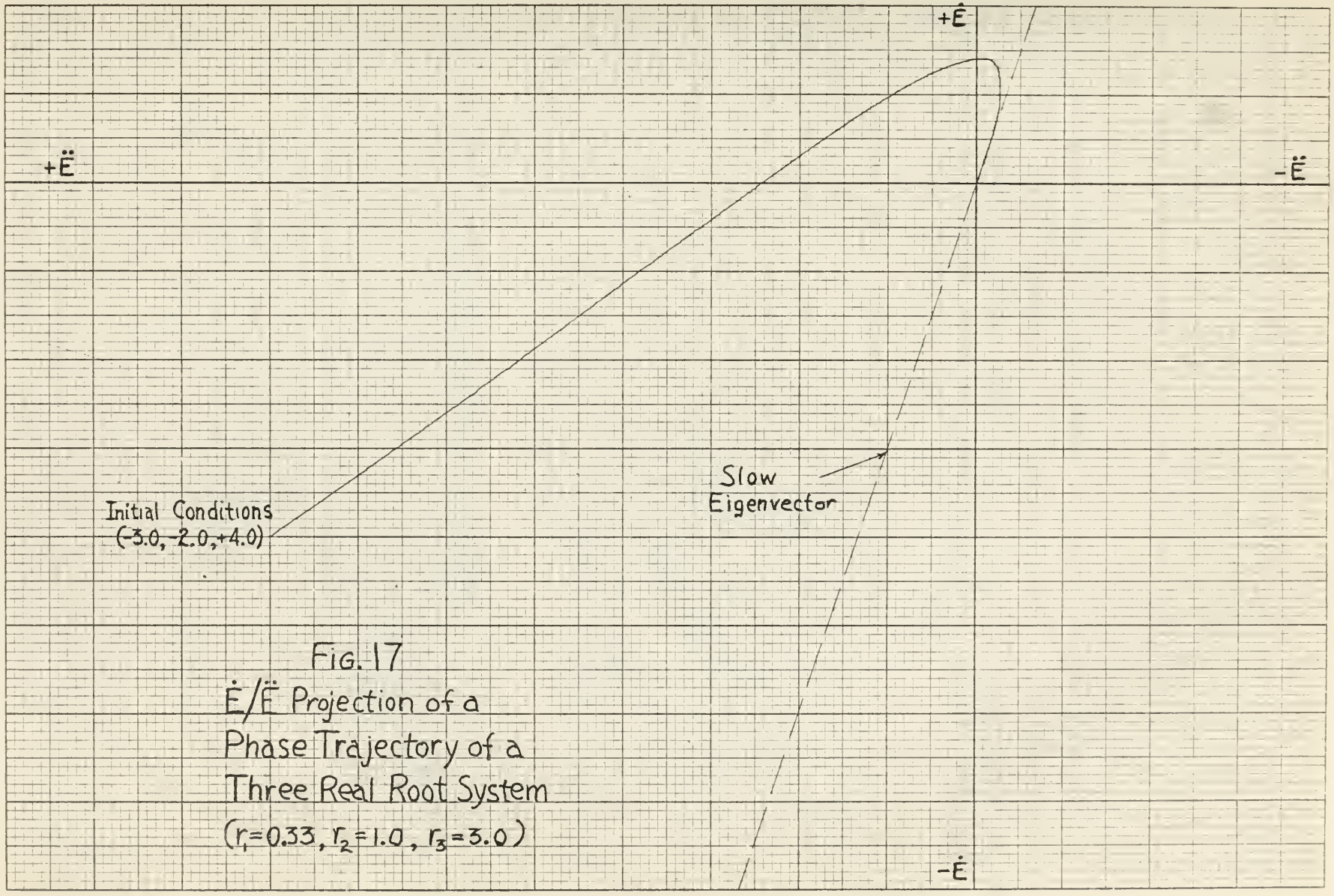

Fig. 17
Ė/Ë Projection of a
Phase Trajectory of a
Three Real Root System
(r_1=0.33, r_2=1.0, r_3=3.0)

dependent only on root location, any change in root location will cause a reorientation of eigenvectors and eigenplanes and so define a different system. The phase trajectories of this system will be altered from that of the original system in a manner dictated by the new orientation.

For a system defined by three real roots, it has been previously shown that any change in root location will effect the orientation and size of the pyramid bounded by the three eigenplanes. The phase trajectories will exhibit the same general characteristics in response to initial conditions as discussed in the following sections but will be dependent on the particular orientation and size of the pyramid.

As was previously indicated, a system defined by one real root and two complex conjugate roots has only one eigenvector and one eigenplane. Changing the location of the real root changes the time response of the system by moving the eigenvector along the surface of the eigencone towards either a slower or faster trajectory. When the complex roots are changed, the eigenplane is reoriented and the phase trajectories are changed with regard to their E, $\dot{E}$, and $\ddot{E}$ overshoots. In addition to eigenplane reorientation, if the complex roots are changed so as to produce a change in damping ratio, ζ, the general oscillatory nature of the trajectories is increased or decreased.

Effect of Initial Conditions on Phase Trajectories

One of the primary purposes of this investigation was to study the effect of varying initial conditions on the phase trajectories of third order linear systems. In particular, three general areas for the location of these initial conditions were selected:

1) Initial conditions on an eigenvector.
2) Initial conditions in an eigenplane.
3) Initial conditions not in an eigenplane.

Each of these will be discussed in the following paragraphs.

1. Initial Conditions on an Eigenvector.

If initial conditions corresponding to any point located on an eigenvector are substituted into Equation (IV-2), two of the three terms on the right side of the equation vanish. As an example, let:

$$E_o = \frac{K}{r_1}, \quad \dot{E}_o = -K, \quad \text{and} \quad \ddot{E}_o = Kr_1.$$

Substitution into Equation (IV-2) yields:

$$E(t) = K \frac{r_1 - r_2 - r_3 + \frac{r_2 r_3}{r_1}}{(r_2 - r_1)(r_3 - r_1)} \epsilon^{-r_1 t}$$

This further simplifies to

$$E(t) = \frac{K}{r_1} \epsilon^{-r_1 t}$$

From which

$$\dot{E}(t) = -K\epsilon^{-r_1 t} \quad \text{and} \quad \ddot{E}(t) = Kr_1 \epsilon^{-r_1 t}$$

Hence it can be seen that at any time, t, the state point of the system has the same coordinates, $\left(\frac{K}{r_1}, -K, Kr_1 \right)$, as any arbitrary point on an eigenvector and the trajectory is a straight line coinciding with the eigenvector. Figures 18 through 20 are typical analog solutions of a trajectory with initial conditions on a system eigenvector.

This statement that a phase trajectory having initial conditions on an eigenvector will remain on the eigenvector holds for both a system with three real roots, and a system with one real root and two complex conjugate roots. This is apparent from Equation (IV-2) which holds for both systems.

As an interesting sidelight to this property of phase trajectories with initial conditions on eigenvectors, an unstable system with complex roots in the right half plane and its real root in the left half plane was simulated on the analog computer. This system was given a set of initial conditions on an eigenvector, and as the solution was generated,

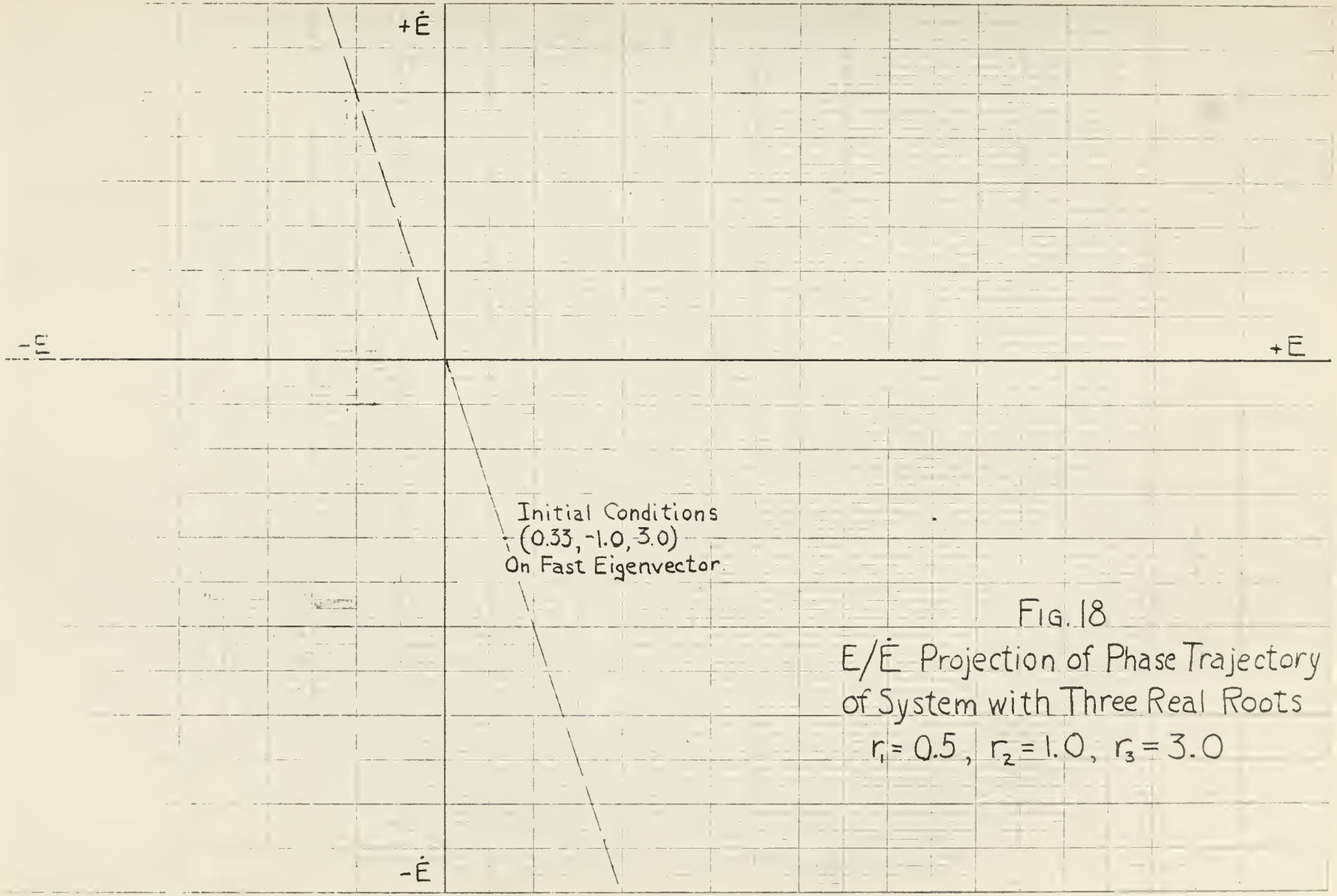

FIG. 18
E/Ė Projection of Phase Trajectory
of System with Three Real Roots
$r_1 = 0.5$, $r_2 = 1.0$, $r_3 = 3.0$

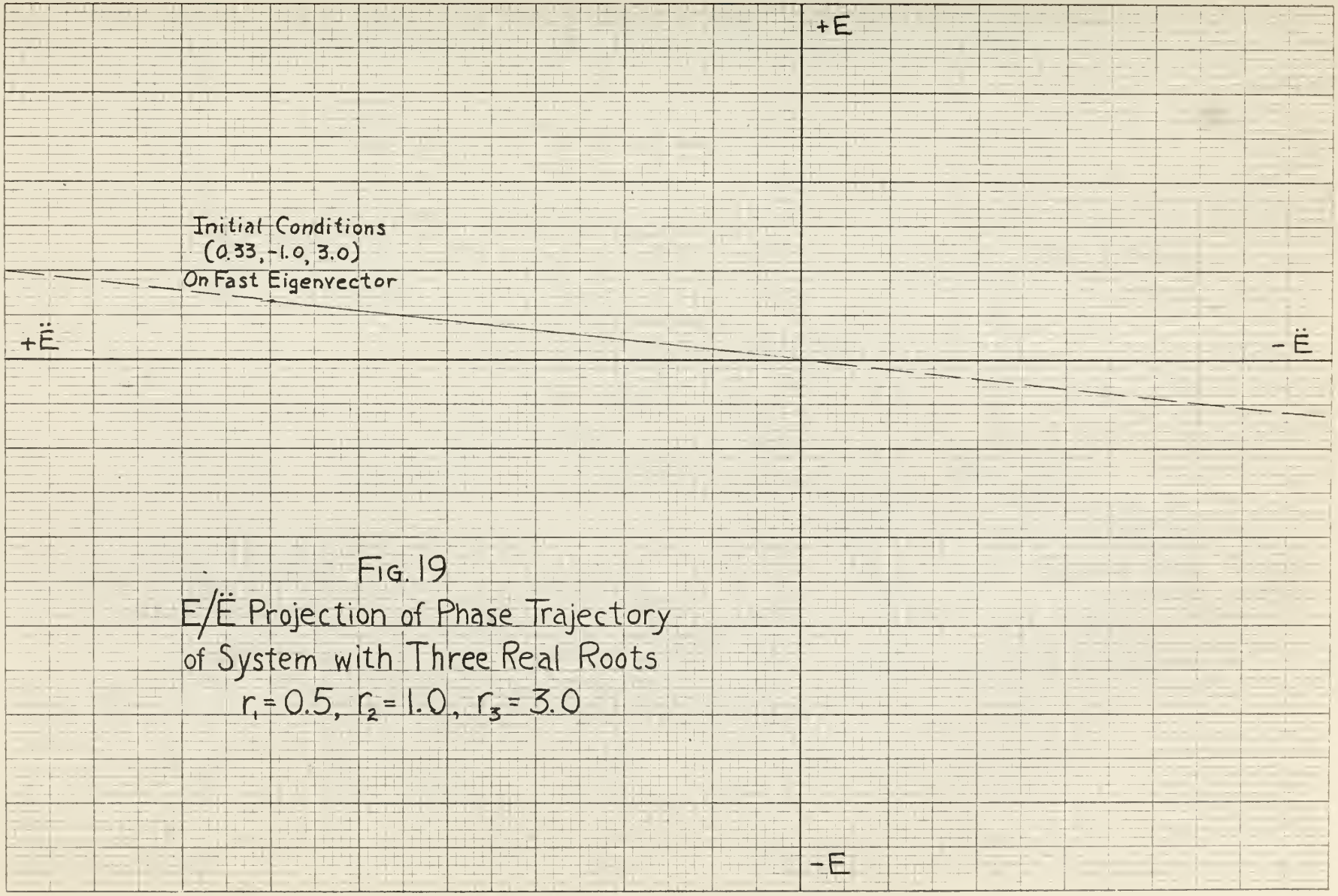

FIG. 19

E/Ë Projection of Phase Trajectory of System with Three Real Roots

$r_1 = 0.5,\ r_2 = 1.0,\ r_3 = 3.0$

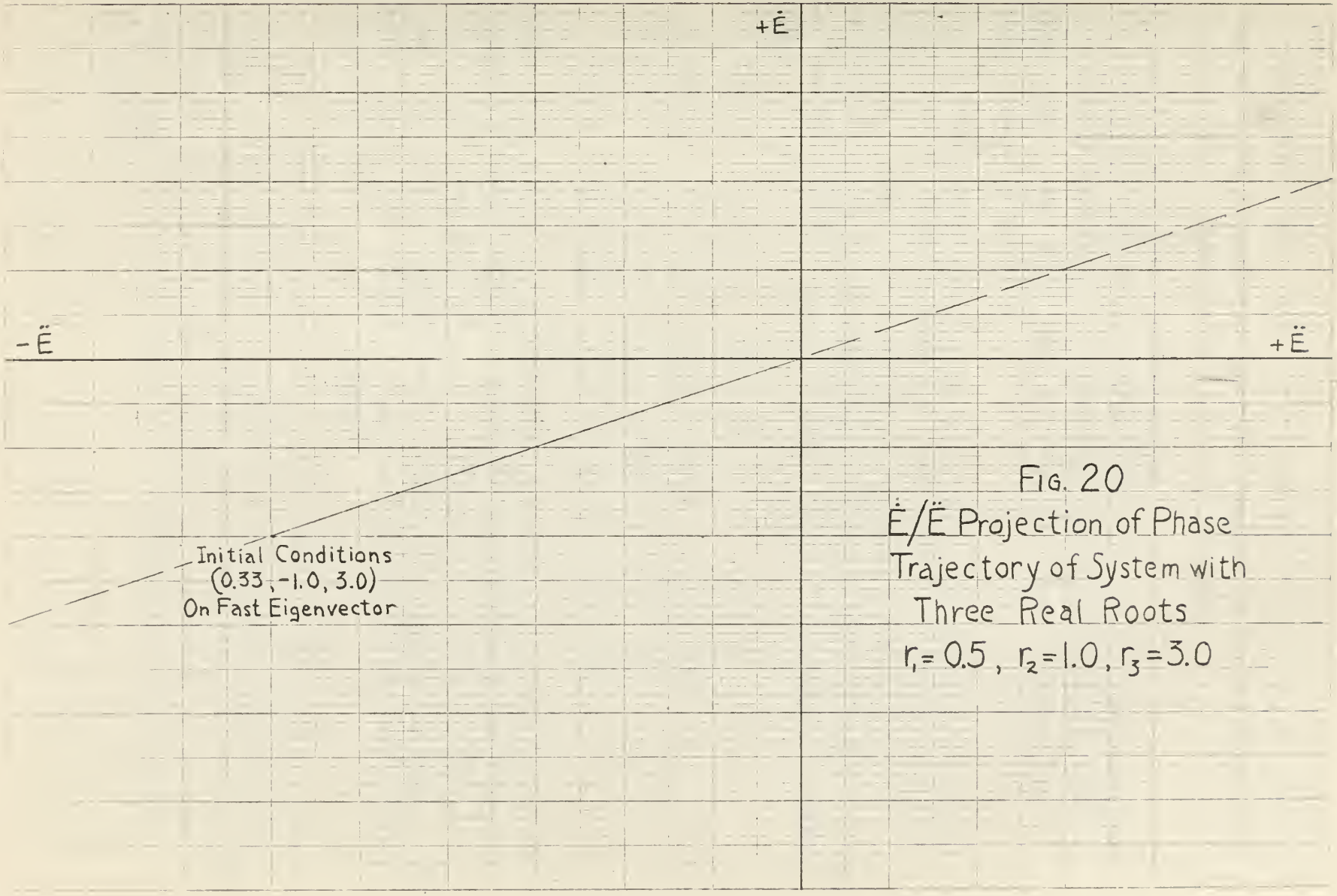

FIG. 20
Ė/Ë Projection of Phase Trajectory of System with Three Real Roots
$r_1 = 0.5$, $r_2 = 1.0$, $r_3 = 3.0$

the phase trajectory coincided with the eigenvector until just before it reached the origin. Here, the instability of the system caused the development of diverging oscillations about the origin. Figure 21 is the projection of this trajectory on the $E/\dot{E}$ plane.

2. Initial Conditions in an Eigenplane.

If initial conditions corresponding to any point in an eigenplane or a complex eigenplane are substituted into Equation (IV-2), Han has shown (Ref. 1, pp. 26-36) that the resulting phase trajectory will always remain in the plane.

A phase trajectory starting in a complex eigenplane will be an oscillatory curve that spirals into the origin of error space, always remaining in the complex eigenplane. Figure 22 shows the general oscillatory nature of the trajectories of four different systems having one real root and two complex conjugate roots. The systems illustrated are:

Case L	$r_1 \approx 0.5$	$r_{2,3} \approx 1 \pm j3$	($\zeta \approx .3$)
Case B	$r_1 \approx 3.0$	$r_{2,3} \approx 1 \pm j1$	($\zeta \approx .707$)
Case C	$r_1 \approx 3.0$	$r_{2,3} \approx 2 \pm j2$	($\zeta \approx .707$)
Case A	$r_1 \approx 3.0$	$r_{2,3} \approx .5 \pm j.5$	($\zeta \approx .707$)

Figure 23 is a view of the same model, but looking down the edge of the complex eigenplane of Case A. Figure 24 shows the phase trajectories of Case L only, looking into octant 1. Figure 25 is a view of the same model of Case L but looking down the edge of the complex eigenplane. The dashed line in Figs. 24 and 25 represents the eigenvector corresponding to the real root, $r_1 \approx 0.5$, of Case L.

In a system having three real and distinct roots the phase trajectories will also remain in an eigenplane if the initial conditions are located in this eigenplane. However, the trajectories will not have the oscillatory nature as in Figs. 22 through 25, but will be curves that become asymptotic to the slower of the two eigenvectors which define the eigenplane.

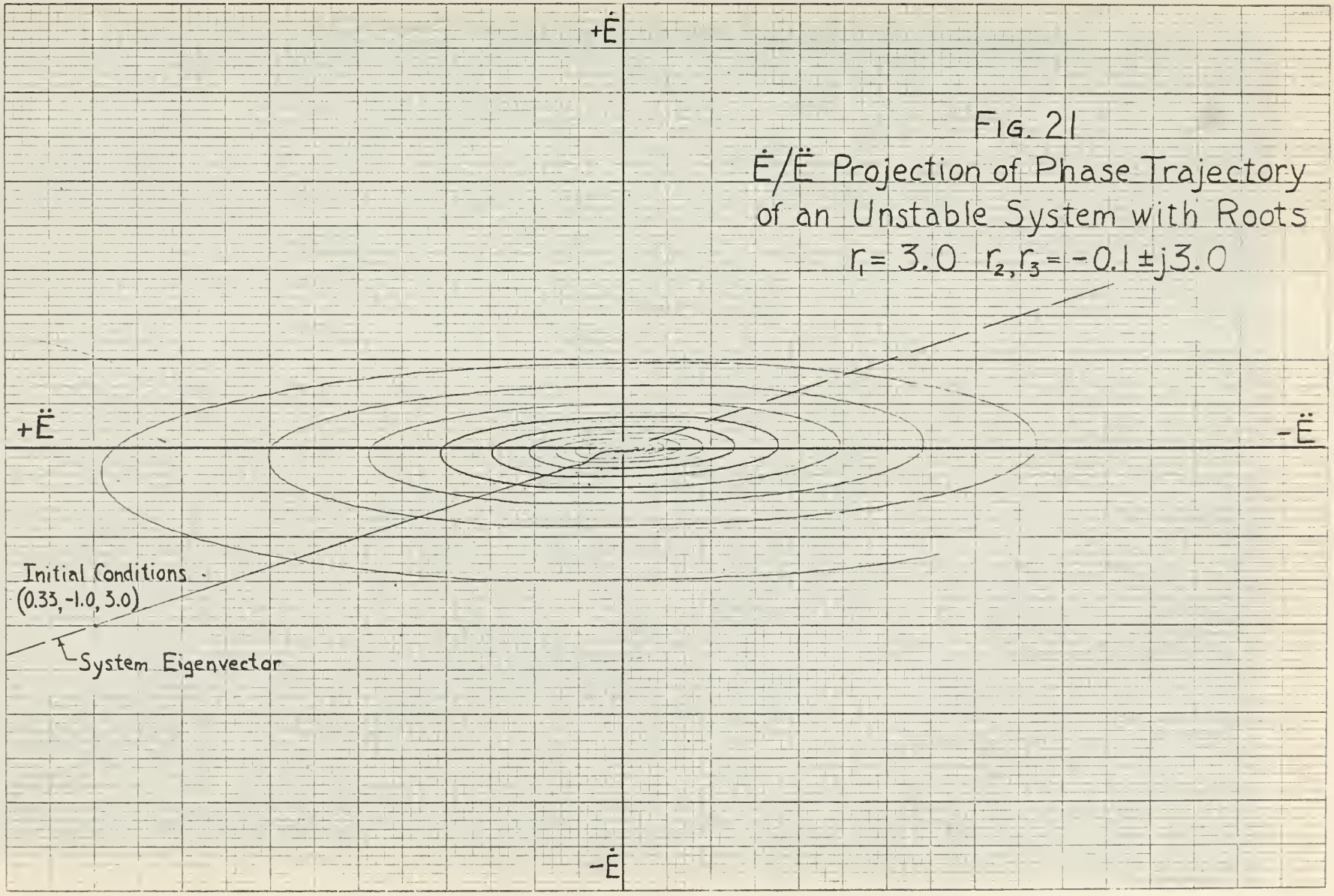

FIG. 21
Ė/Ë Projection of Phase Trajectory
of an Unstable System with Roots
$r_1 = 3.0 \quad r_2, r_3 = -0.1 \pm j3.0$

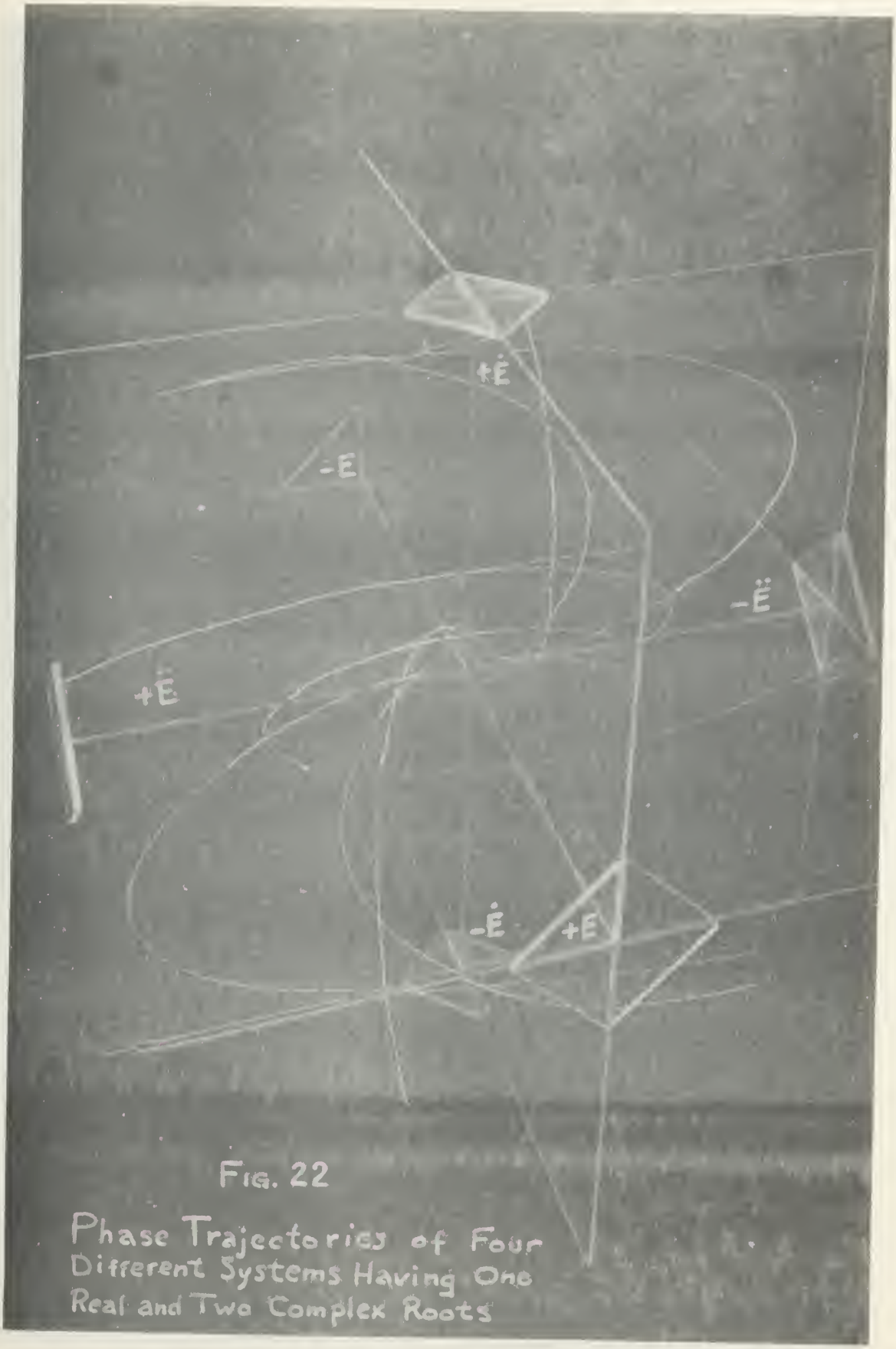

FIG. 22

Phase Trajectories of Four Different Systems Having One Real and Two Complex Roots

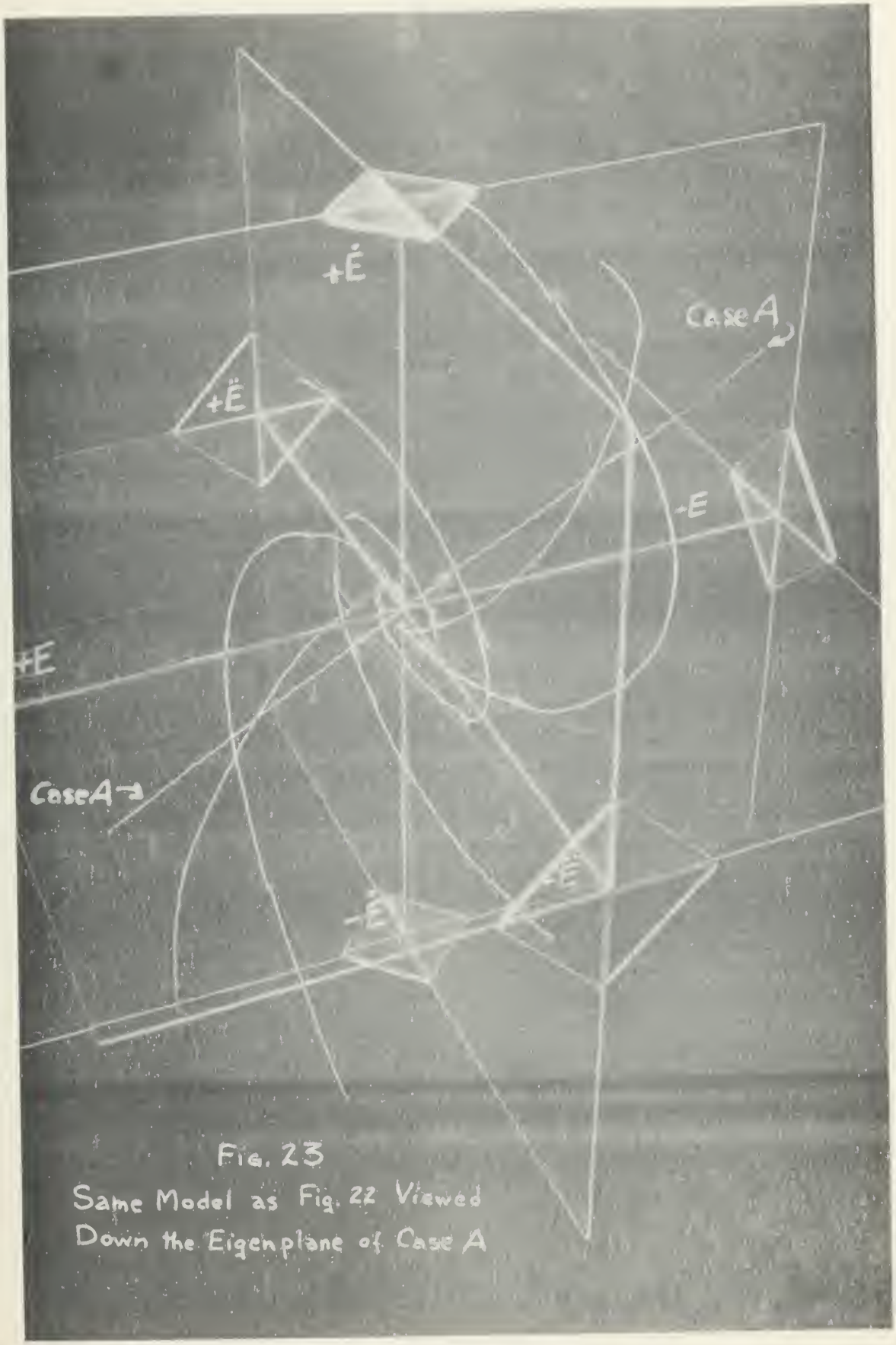

Fig. 23
Same Model as Fig. 22 Viewed
Down the Eigenplane of Case A

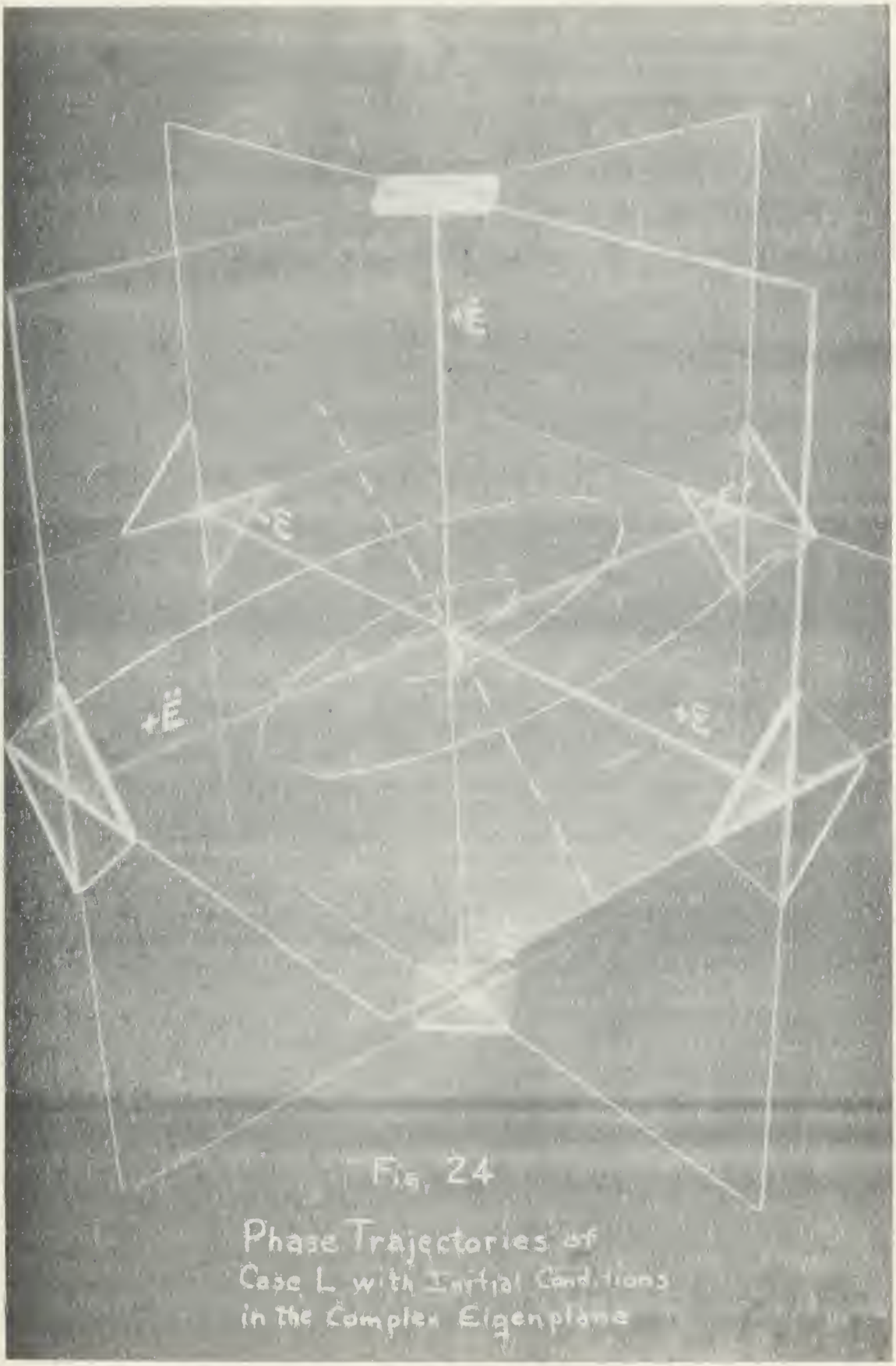

Fig. 24

Phase Trajectories of
Case L with Initial Conditions
in the Complex Eigenplane

Figure 26 shows a model constructed of a number of phase trajectories of a system with three real roots, $r_1 = 0.5$, $r_2 = 1.0$, $r_3 = 2.0$, all having initial conditions in the Third eigenplane, defined by the slow and intermediate eigenvectors. Note here that two of the phase trajectories, (A) and (B), are straight lines in octants 4 and 2', indicating that the initial conditions for these trajectories were chosen on the slow eigenvector. This figure readily illustrates the above statement that the phase trajectories become asymptotic to the slower of the two defining eigenvectors.

Figure 27 is another view of the same model but looking down the edge of the Third eigenplane, and showing that the phase trajectories all remain in the eigenplane.

Figure 28 shows phase trajectories of a system having three real roots, $r_1 = 0.333$, $r_2 = 1.0$, $r_3 = 3.0$. In this figure, Trajectory (A) has initial conditions in the First eigenplane and becomes asymptotic to the intermediate eigenvector, Trajectory (B) has initial conditions in the Second eigenplane and becomes asymptotic to the slow eigenvector, and Trajectory (C) has initial conditions in the Third eigenplane and also becomes asymptotic to the slow eigenvector.

3. Initial Conditions not in an Eigenplane.

Han and Thaler have stated (Ref. 3) that eigenplanes "subdivide the (error) space into regions so that no phase trajectories can pass out of one region and into another. Thus the (eigenplanes) act as boundaries which funnel the phase trajectories into the origin".

For a system having three real and distinct roots, this statement can be modified to read that "the pyramid of eigenplanes subdivides error space into regions so that phase trajectories starting inside the pyramid will remain inside and those phase trajectories originating outside the pyramid will never enter the pyramid of eigenplanes. Thus the pyramid acts as a boundary which funnels the phase trajectories into the origin".

It is important to note that not only does the pyramid funnel the phase trajectories into the origin, but it funnels them in asymptotic

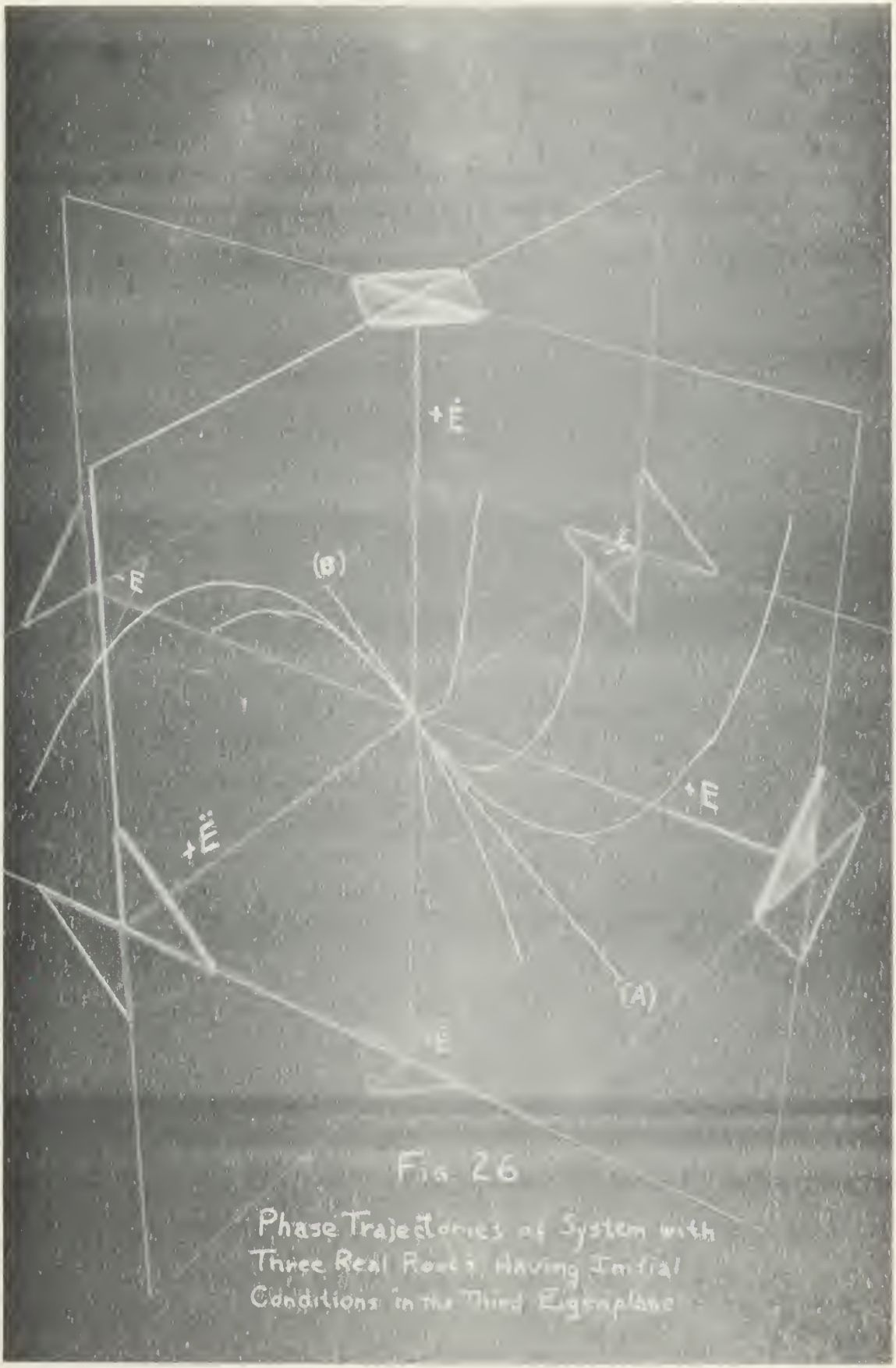

Fig. 26

Phase Trajectories of System with Three Real Roots Having Initial Conditions in the Third Eigenplane

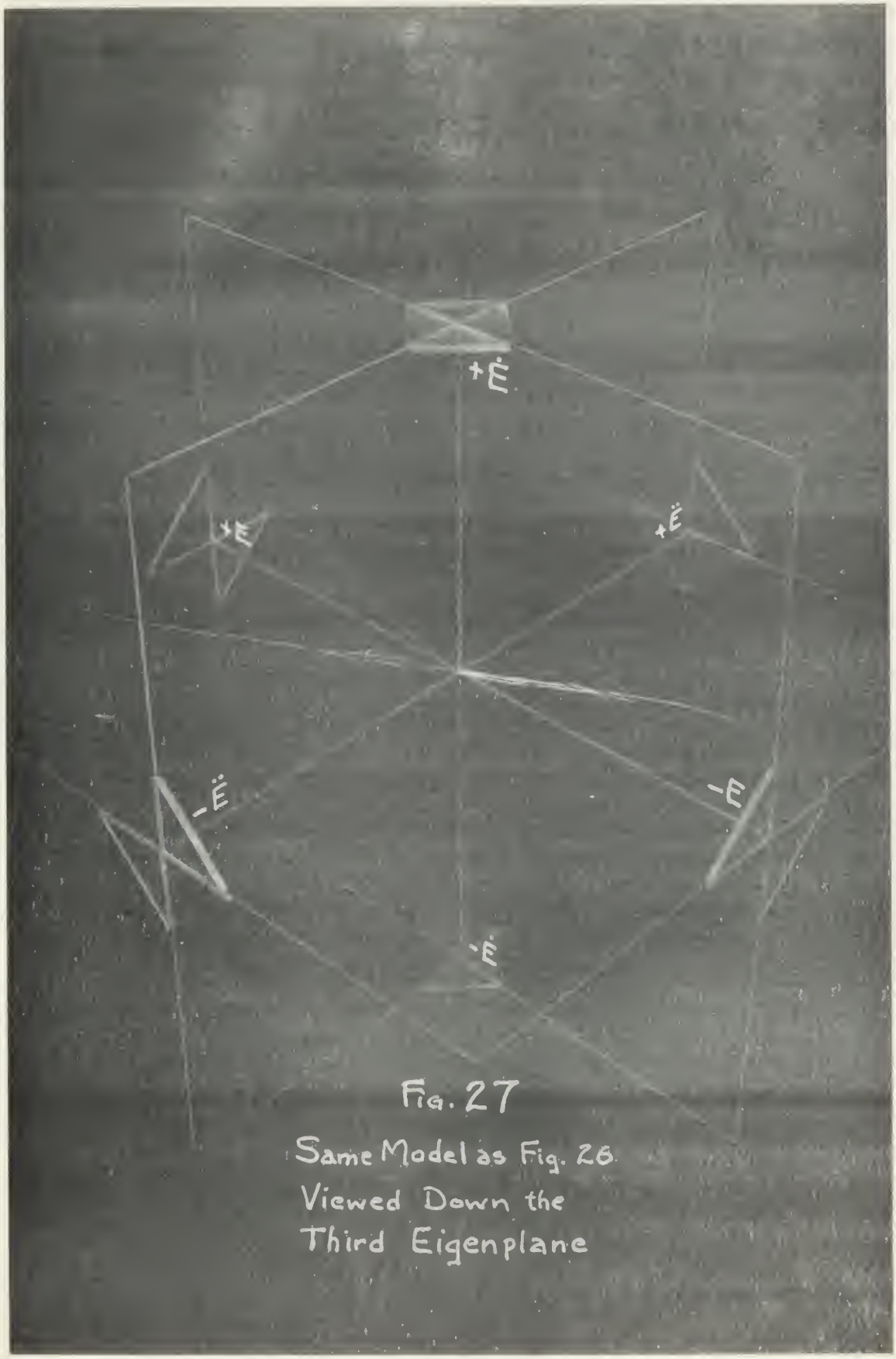

Fig. 27

Same Model as Fig. 26
Viewed Down the
Third Eigenplane

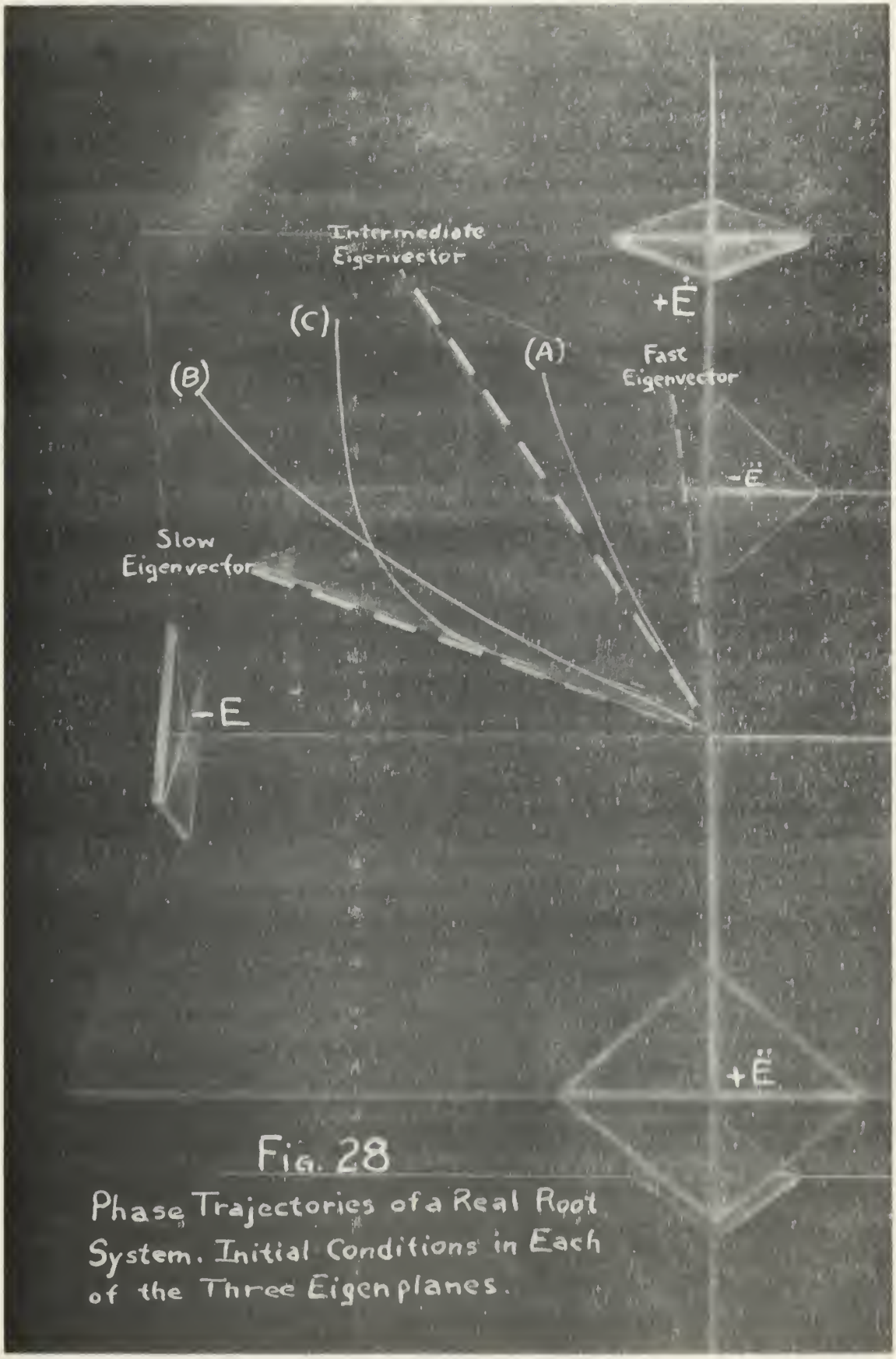

Fig. 28

Phase Trajectories of a Real Root System. Initial Conditions in Each of the Three Eigenplanes.

to the slow eigenvector, no matter how close the initial conditions might be to the fast or intermediate eigenvectors. Figure 29 shows two phase trajectories of a three real root system with roots: $r_1 = 0.333$, $r_2 = 1.0$, $r_3 = 3.0$, whose initial conditions are inside the pyramid of eigenplanes. It can readily be seen that both trajectories approach the slow eigenvector asymptotically even though (A) has its initial conditions near the intermediate eigenvector and (B) has its initial conditions approximately halfway between the intermediate and fast eigenvectors.

Figure 30 is an illustration of a number of phase trajectories whose initial conditions are all outside the pyramid of eigenplanes. Here again it can be seen that all phase trajectories originating outside the eigenplanes approach the origin of error space asymptotic to the slow eigenvector. Three of these trajectories exhibit interesting properties. Trajectory (A) originates in octant 4 near the fast eigenvector, but does not approach the origin along the slow eigenvector in the same octant. Instead it penetrates into octants 3 and 2, then finally approaches the origin asymptotic to the slow eigenvector in octant 2'. Trajectory (B) originates in octant 4', but instead of going to the slow eigenvector in the adjacent octant 4, it journeys through octants 4, 3, 2, and finally approaches the origin along the slow eigenvector in octant 2'. Trajectory (C) originates near the intermediate eigenvector in octant 4, approaches this intermediate eigenvector, parallels it for a short time, and then finally becomes asymptotic to the slow eigenvector very near the origin in octant 4.

These unusual excursions through error space of trajectories whose initial conditions are outside the pyramid of eigenplanes are results of the basic property of eigenplanes, i.e., eigenplanes act as boundaries on phase trajectories. When the initial conditions are between any two eigenplanes, the phase trajectories must always remain between them until the trajectories reach the slow eigenvector which exists between or on these bounding eigenplanes.

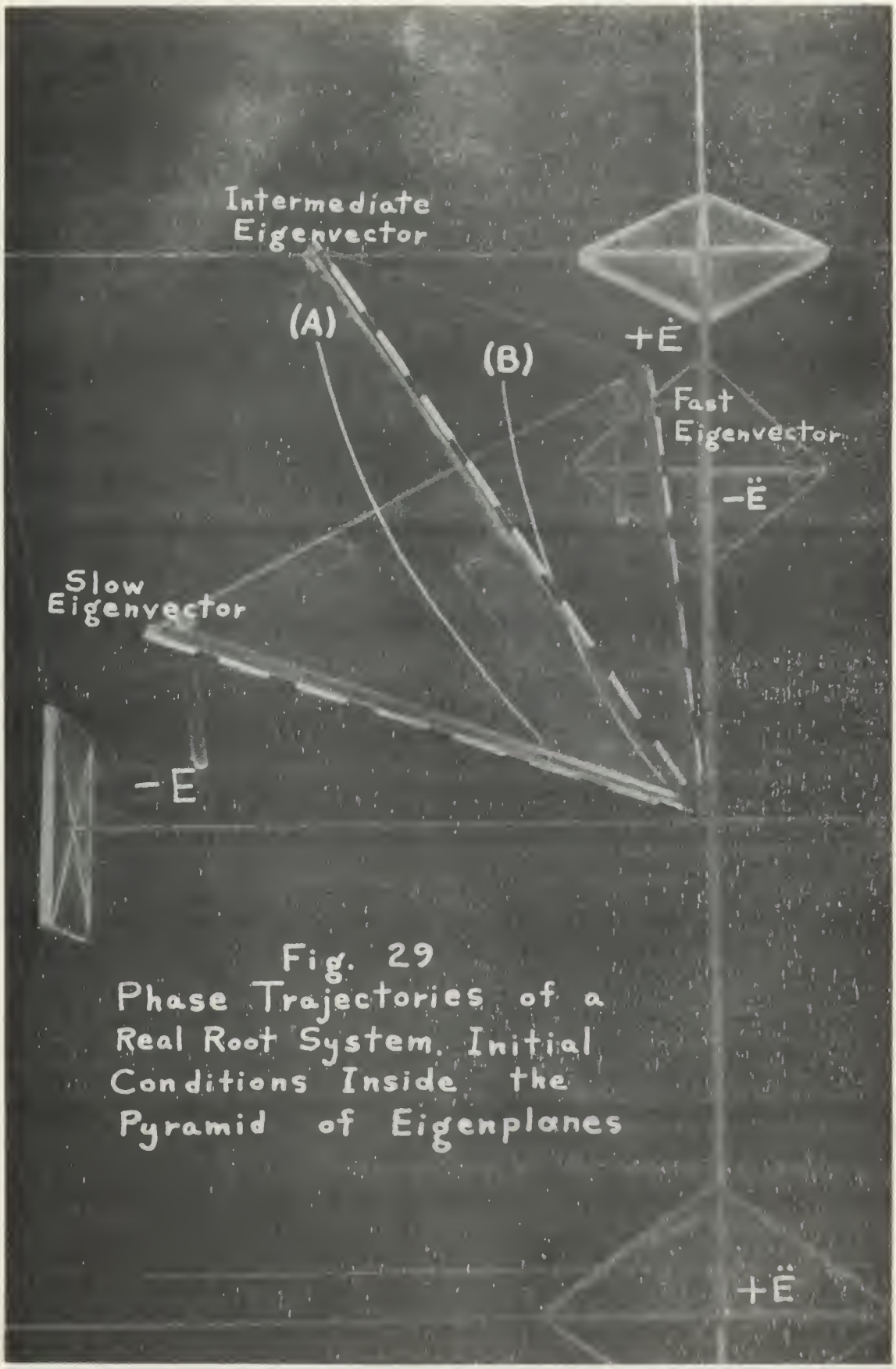

Fig. 29
Phase Trajectories of a Real Root System. Initial Conditions Inside the Pyramid of Eigenplanes

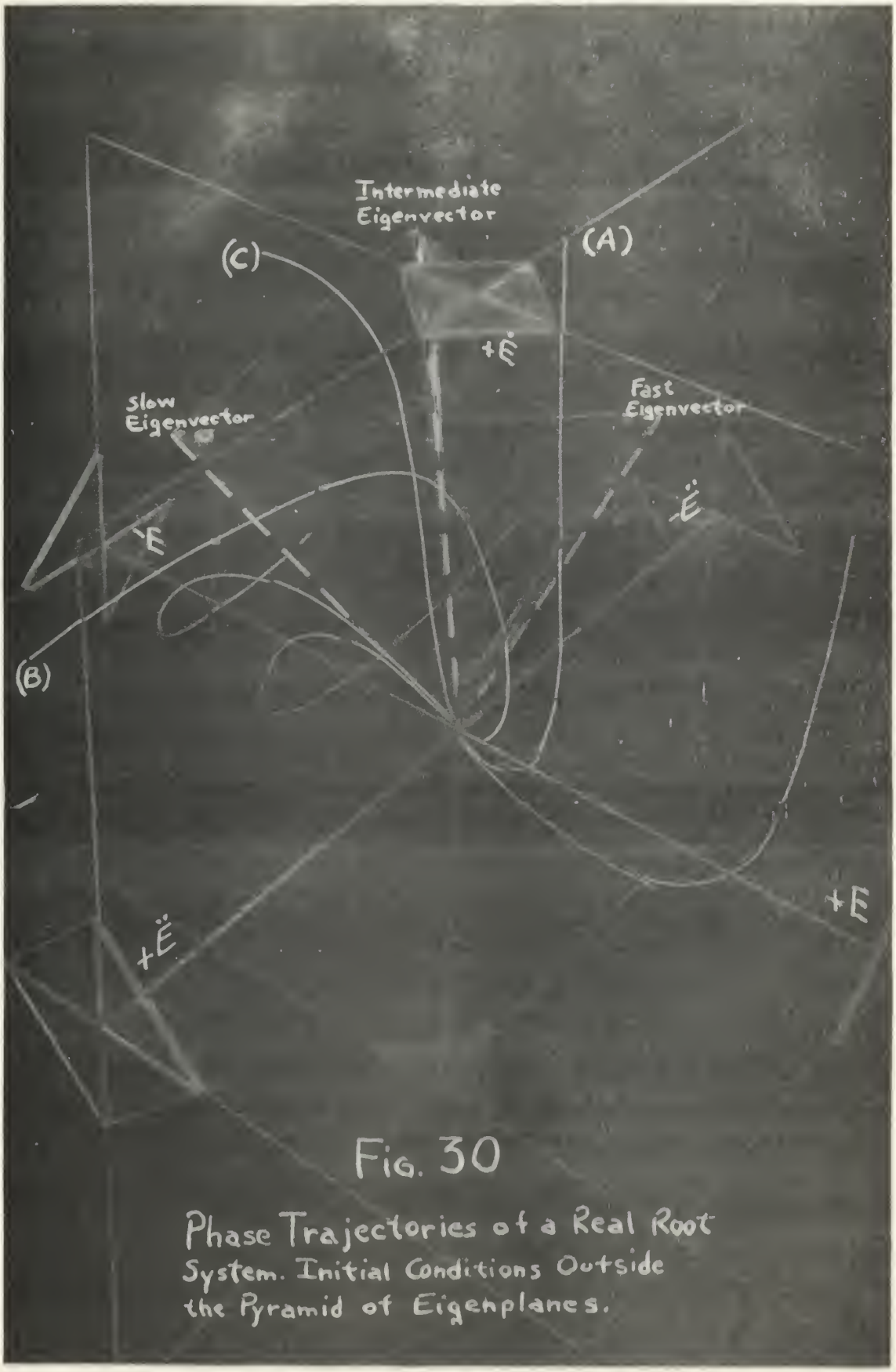

Fig. 30

Phase Trajectories of a Real Root System. Initial Conditions Outside the Pyramid of Eigenplanes.

In the investigation of the effect of initial conditions not in an eigenplane, more attention was focused on those systems having one real root and two complex conjugate roots. A number of interesting results were obtained.

The first complex root system which was studied had roots of: $r_1 = 3.0$, $r_{2,3} = .25 \pm j5.0$. This system was very lightly damped, having a value for ζ of 0.05. As might be expected, the phase trajectory was highly oscillatory. This can readily be seen in Fig. 31. In this particular three-dimensional model, the scaling of E, $\dot{E}$, and $\ddot{E}$ values of points on the phase trajectory were modified in order to obtain a model capable of analysis. Here, for one coordinate axis unit, $E = 2$, $\dot{E} = 4$, and $\ddot{E} = 1$. When a random initial condition, Point (A), not in the complex eigenplane, was applied to this system, the phase trajectory very quickly became asymptotic to the complex eigenplane. Figure 32, a view looking down the $\dot{E}$ axis, shows that the phase trajectory has become asymptotic to the complex eigenplane after less than one oscillation. Here it should be noted that this model pictured in Figs. 31 and 32 does not show the last five oscillations of the complete trajectory, and they would continue from Point (B) and eventually reach the origin of error space.

The next complex root system studied had roots at $r_1 = 0.5$, $r_{2,3} = 1.0 \pm j3.0$. The system was lightly damped, having $\zeta = 0.3$. The general nature of this system's oscillatory trajectories was seen previously in Fig. 24. In this investigation, a variety of initial conditions not in the complex eigenplane were applied and analyzed.

The first initial condition applied was a step input. In this instance, the step had a magnitude of 4.0 radians. Curve (A) of Fig. 33 is the resulting phase trajectory. Also shown in Fig. 33 is the real root eigenvector represented by the dashed line, and two trajectories having initial conditions in the complex eigenplane, Curves (B) and (B'). Figure 33 indicates that for this system, the phase trajectory starting outside the complex eigenplane does not approach the origin of error space asymptotic to the complex eigenplane,

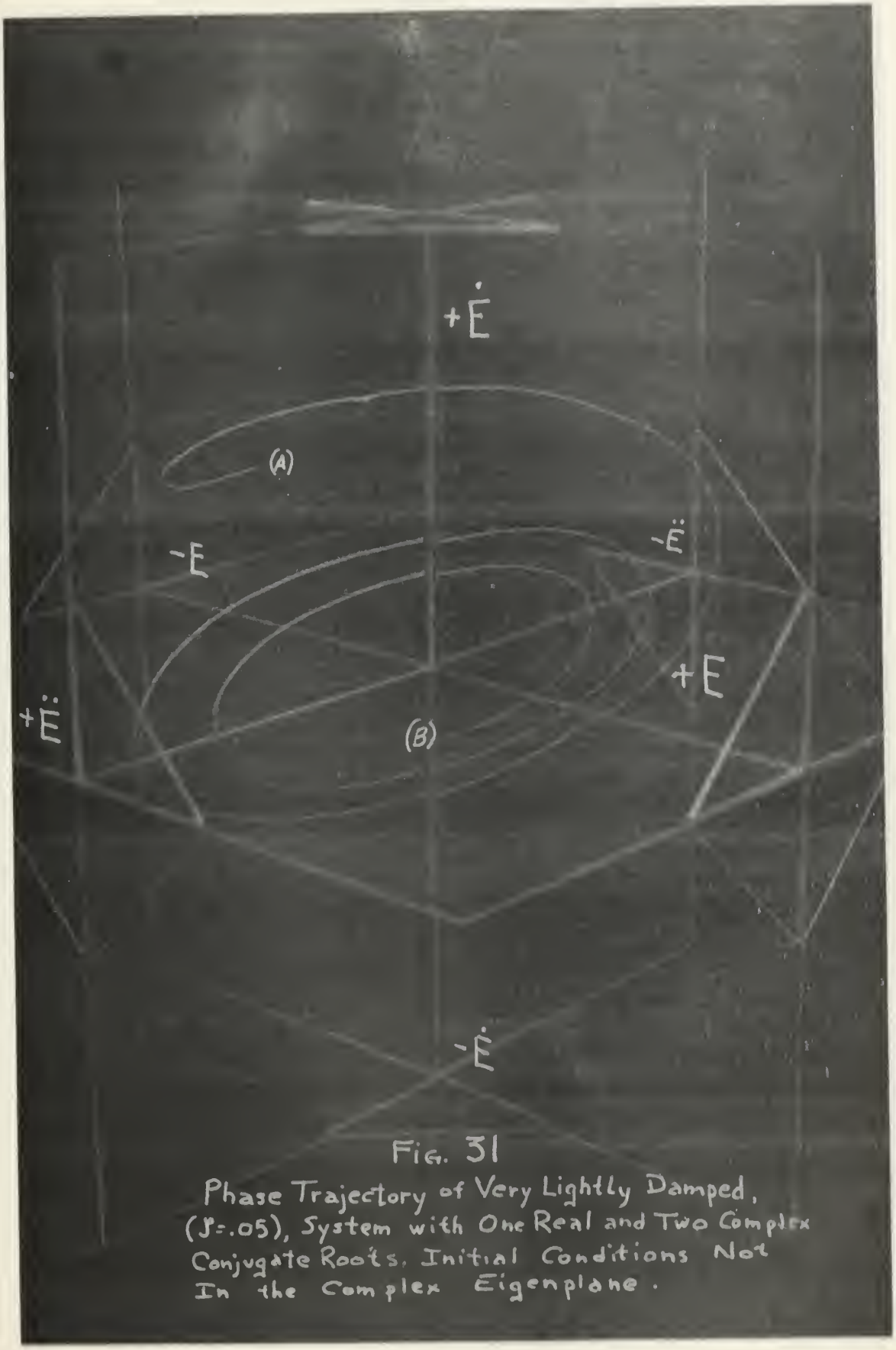

FIG. 31

Phase Trajectory of Very Lightly Damped, (J=.05), System with One Real and Two Complex Conjugate Roots. Initial Conditions Not In the Complex Eigenplane.

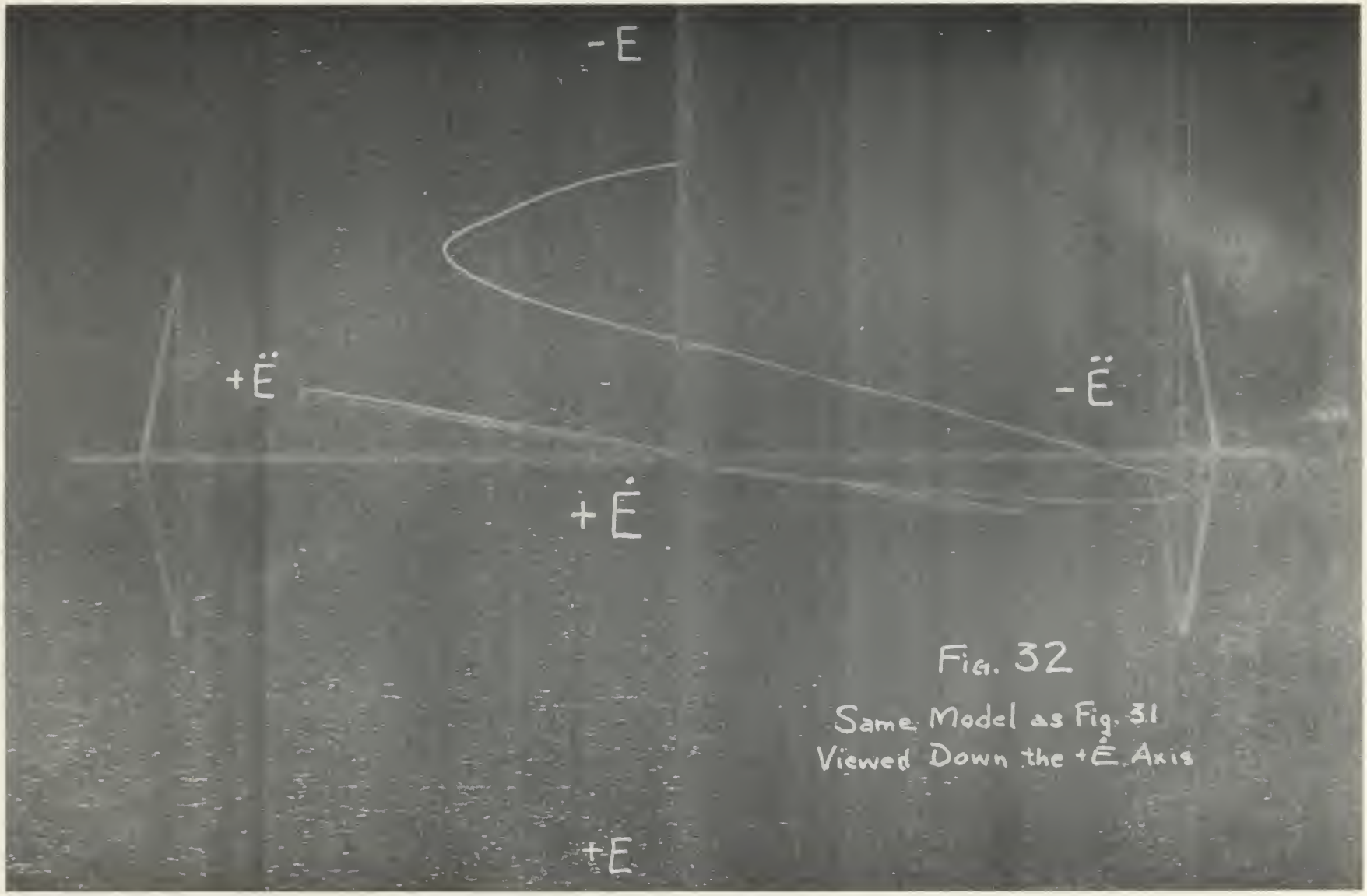

Fig. 32

Same Model as Fig. 31
Viewed Down the +Ė Axis

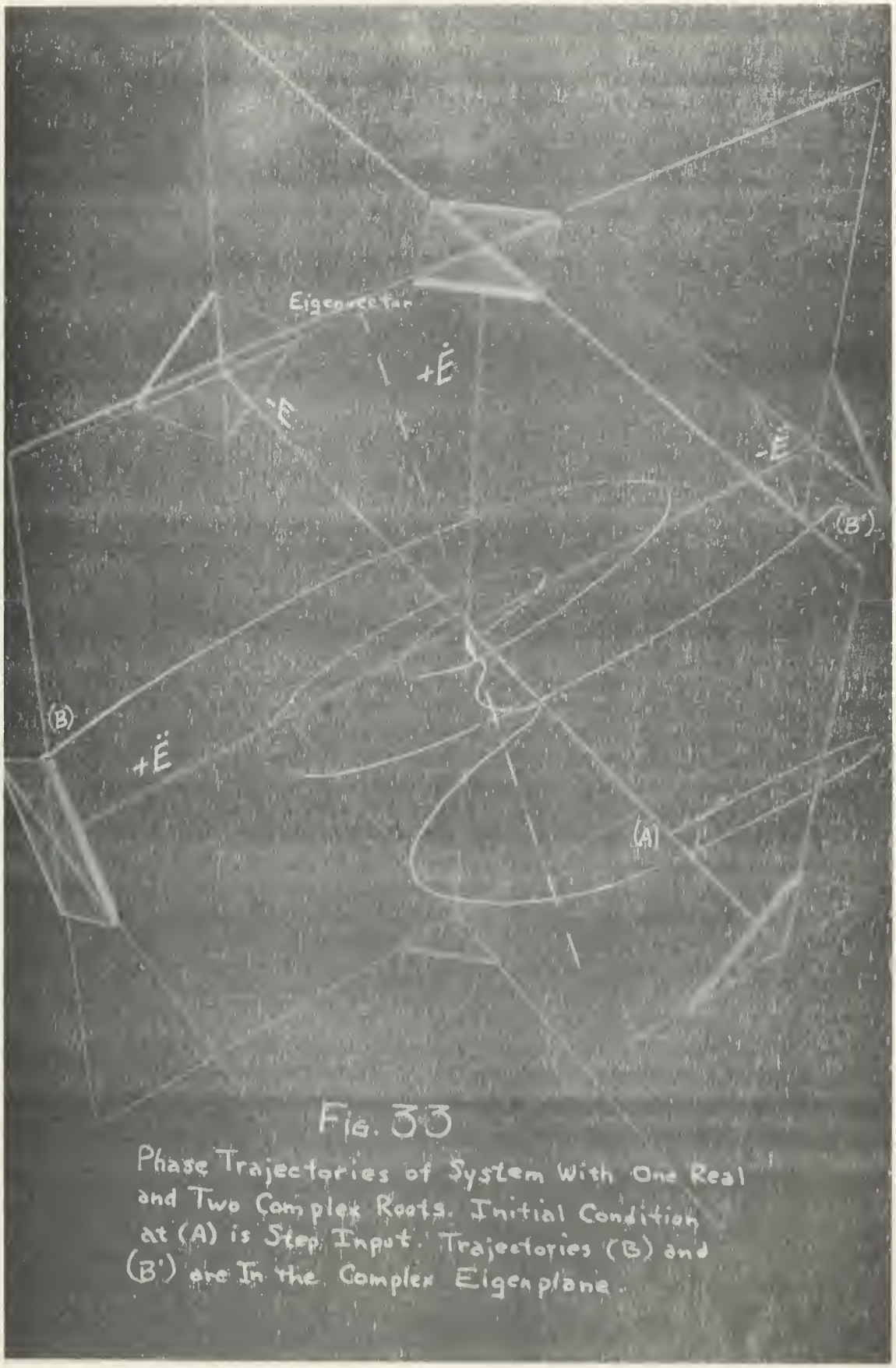

Fig. 33

Phase Trajectories of System With One Real and Two Complex Roots. Initial Condition at (A) is Step Input. Trajectories (B) and (B') are In the Complex Eigenplane.

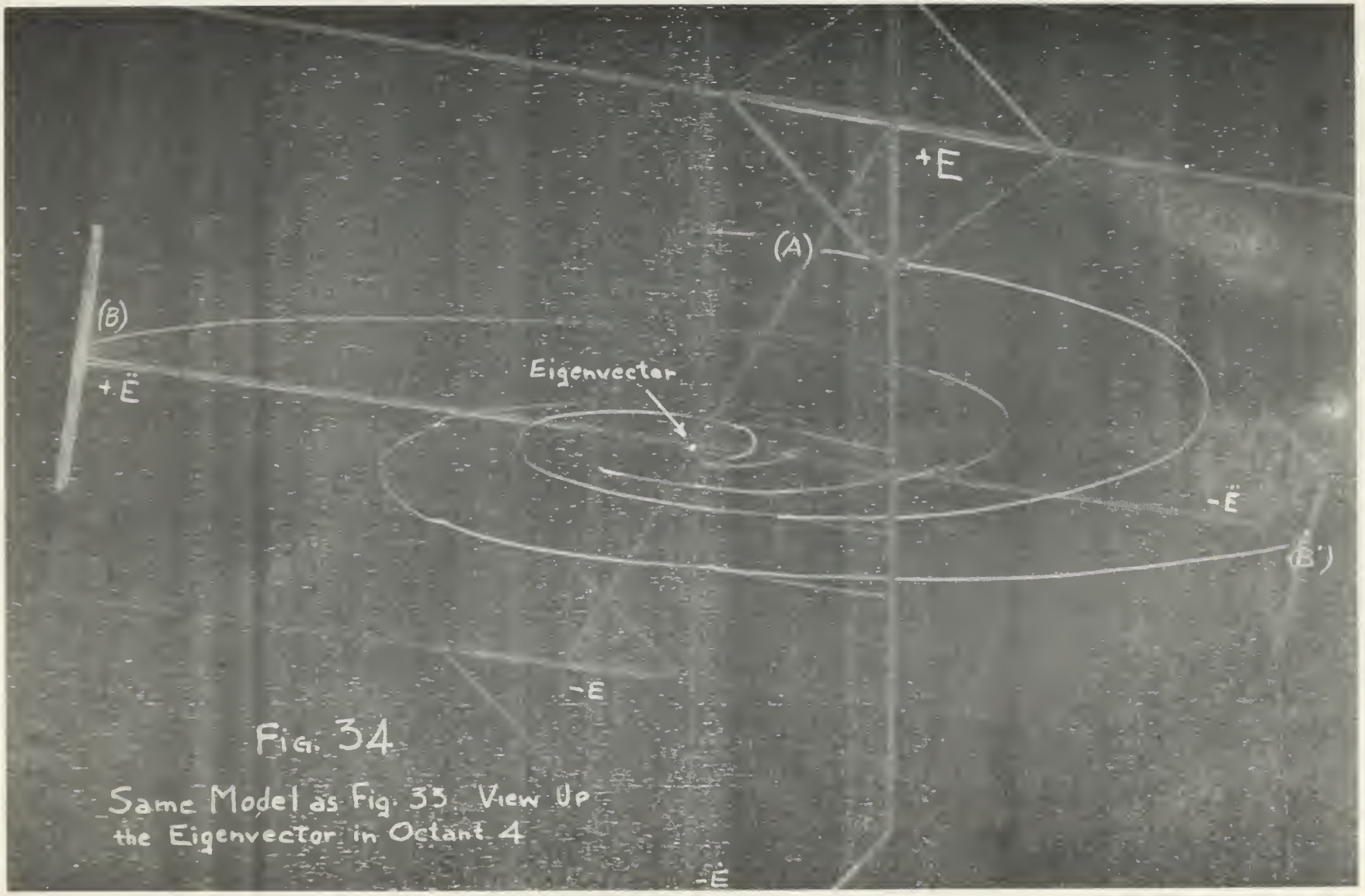

Fig. 34

Same Model as Fig. 33 View Up the Eigenvector in Octant 4

but instead appears to become asymptotic to the system eigenvector. Figure 34 is another view of the same model, but looking up the eigenvector in octant 4. Note here the similarity of the general shape of the phase trajectories having initial conditions in and out of the complex eigenplane.

The next initial conditions applied to this system was an initial velocity of magnitude 2.0 rad/sec . Curve (A) of Fig. 35 is the resulting phase trajectory. Also shown are the system eigenvector and the two trajectories in the complex eigenplane as before. Fig. 36 is a view of the same model looking down the edge of the complex eigenplane. Although it is difficult to tell from Fig. 36, the phase trajectory did not immediately become asymptotic to the complex eigenplane, as it did in the preceding system having $\zeta \approx 0.5$. Figure 37 is another view of the same model looking down the eigenvector in octant 2'. Note again the similar curvature of the phase trajectories having initial conditions in and out of the complex eigenplane.

Next, an initial condition very near the eigenvector was applied to the system. As can be seen from Fig. 38, the phase trajectory quickly became asymptotic to the eigenvector instead of to the complex eigenplane.

Finally an initial condition that was equidistant from the eigenvector and the complex eigenplane was applied to the system. Figure 39 shows the resulting phase trajectory as Curve (A) and the two trajectories in the eigenplane, curves (B) and (B') as well as the system eigenvector. As can be seen in Fig. 39, the phase trajectory again becomes asymptotic, not to the complex eigenplane, but to the eigenvector, developing the characteristic spiral around the eigenvector as was seen previously in Figs. 33 and 38. Figure 40 is a view of this model looking up the eigenvector in octant 4. The similarity of the phase trajectories with initial conditions in and out of the complex eigenplane noted here and in previously discussed views looking up the eigenvector indicated that there must be some relation between the phase trajectories and the eigenvector. This led to the next phase of the investigation.

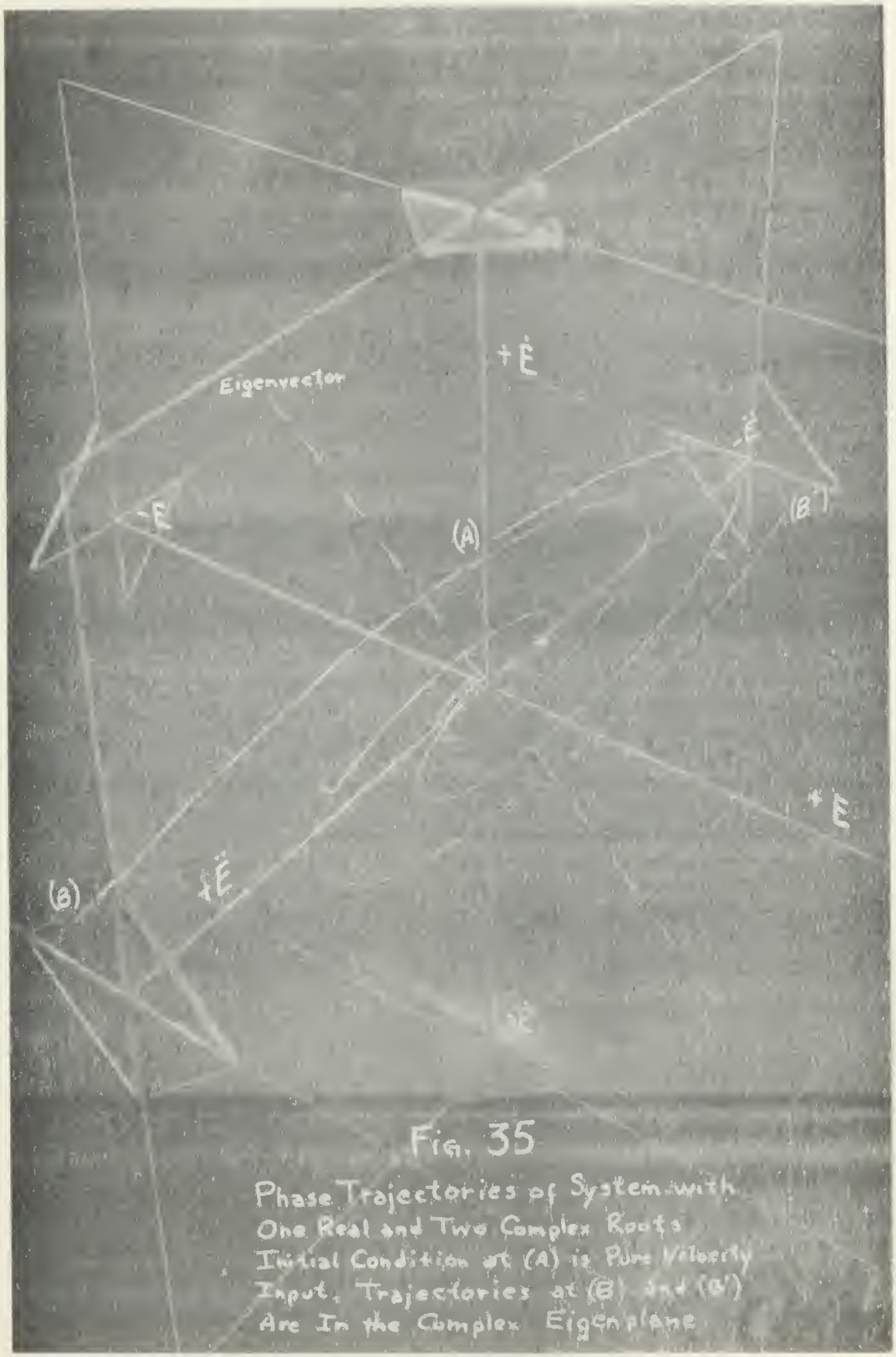

Fig. 35

Phase Trajectories of System with One Real and Two Complex Roots Initial Condition at (A) is Pure Velocity Input. Trajectories at (B) and (B') Are In the Complex Eigenplane

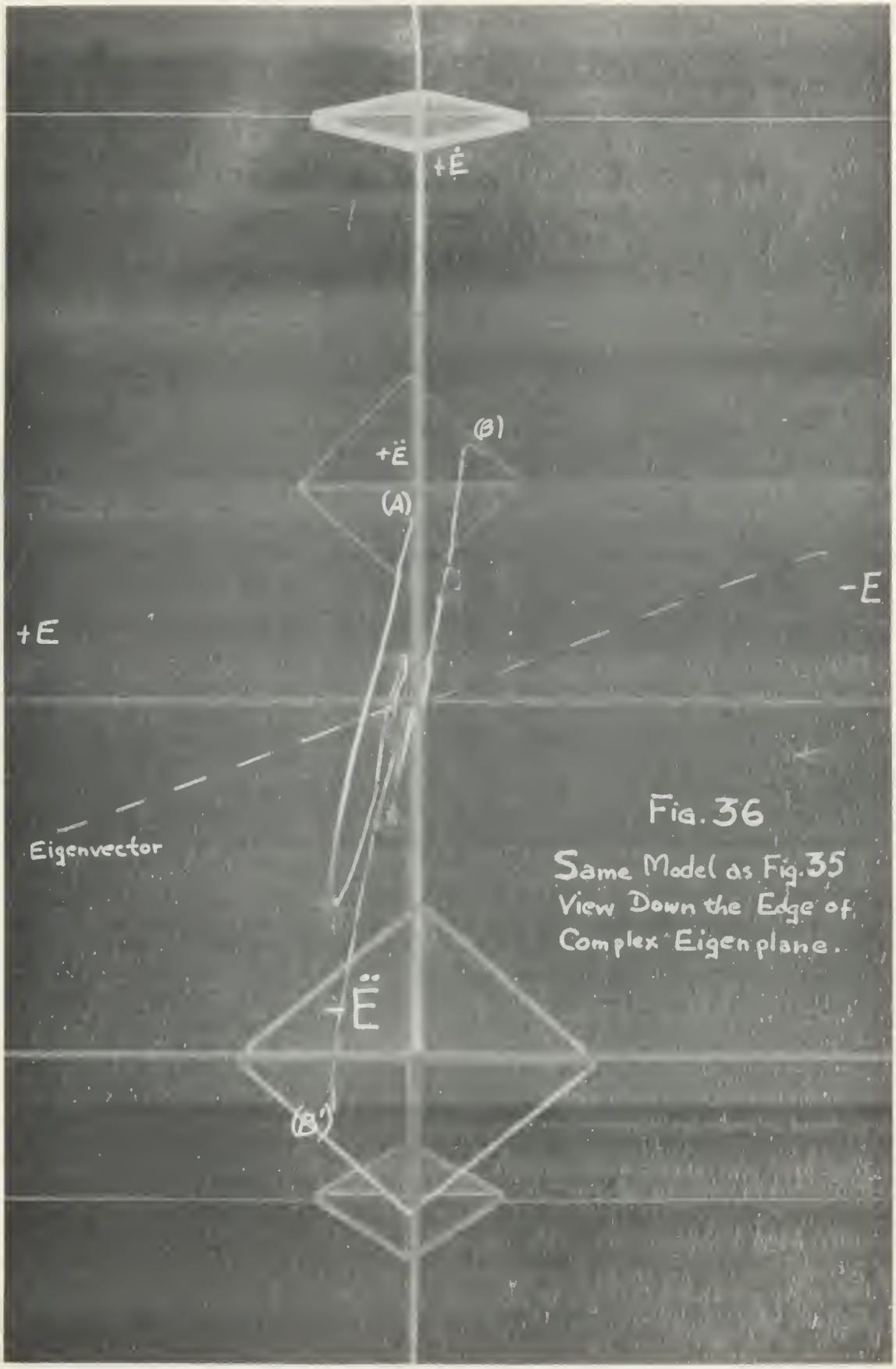

Fig. 36

Same Model as Fig. 35
View Down the Edge of
Complex Eigenplane.

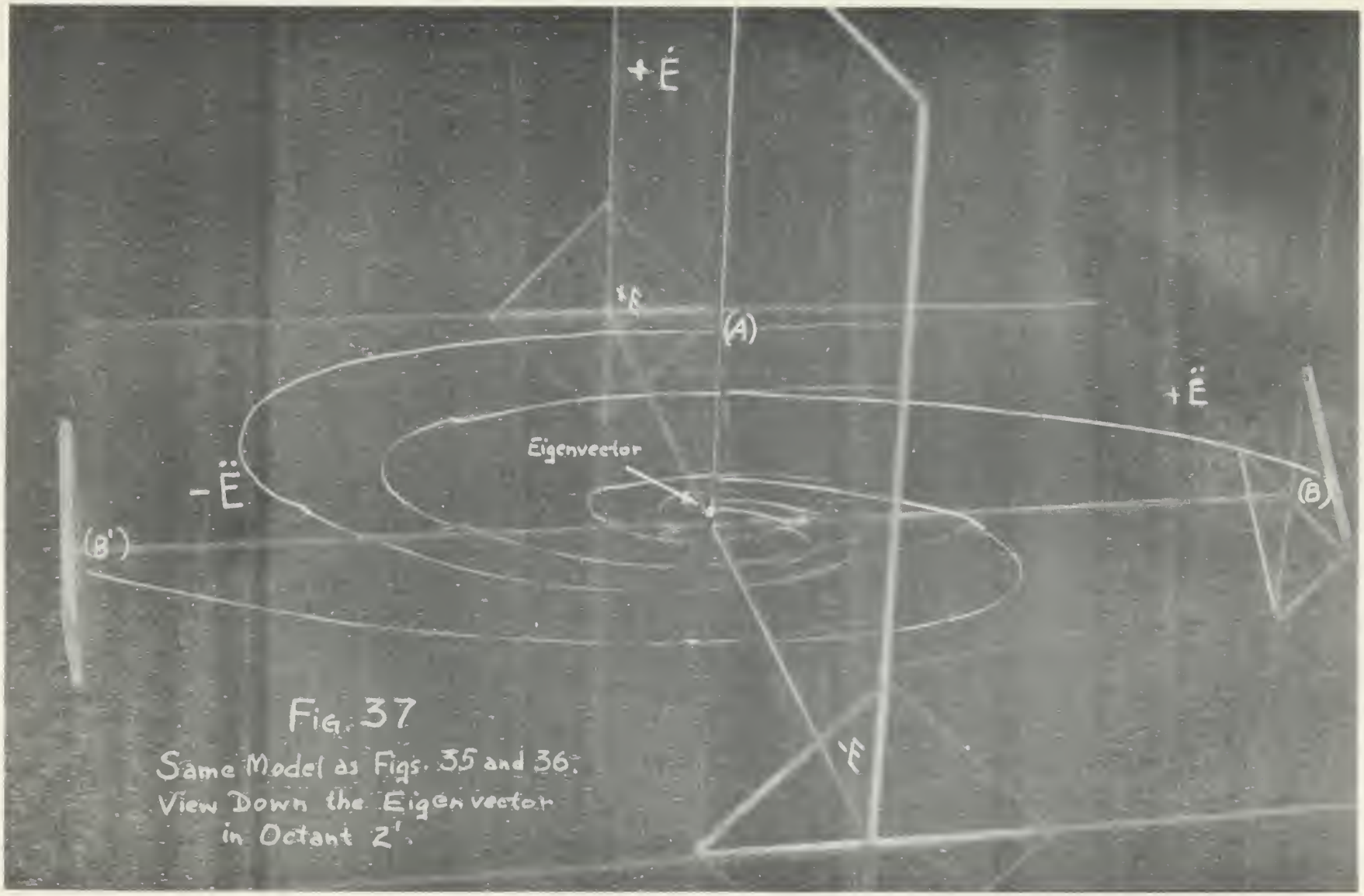

Fig. 37

Same Model as Figs. 35 and 36.
View Down the Eigenvector
in Octant 2'.

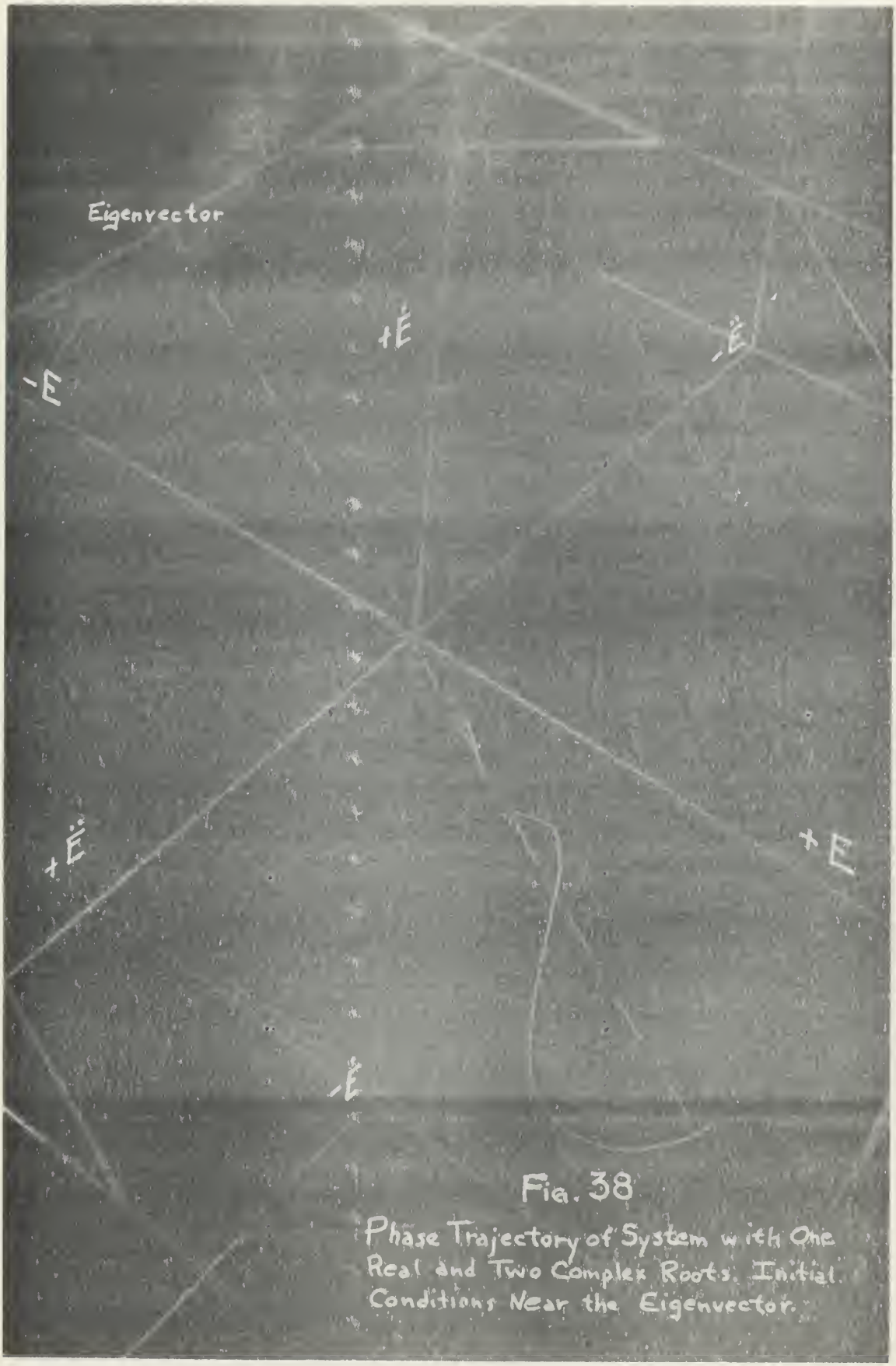

Fig. 38

Phase Trajectory of System with One Real and Two Complex Roots. Initial Conditions Near the Eigenvector.

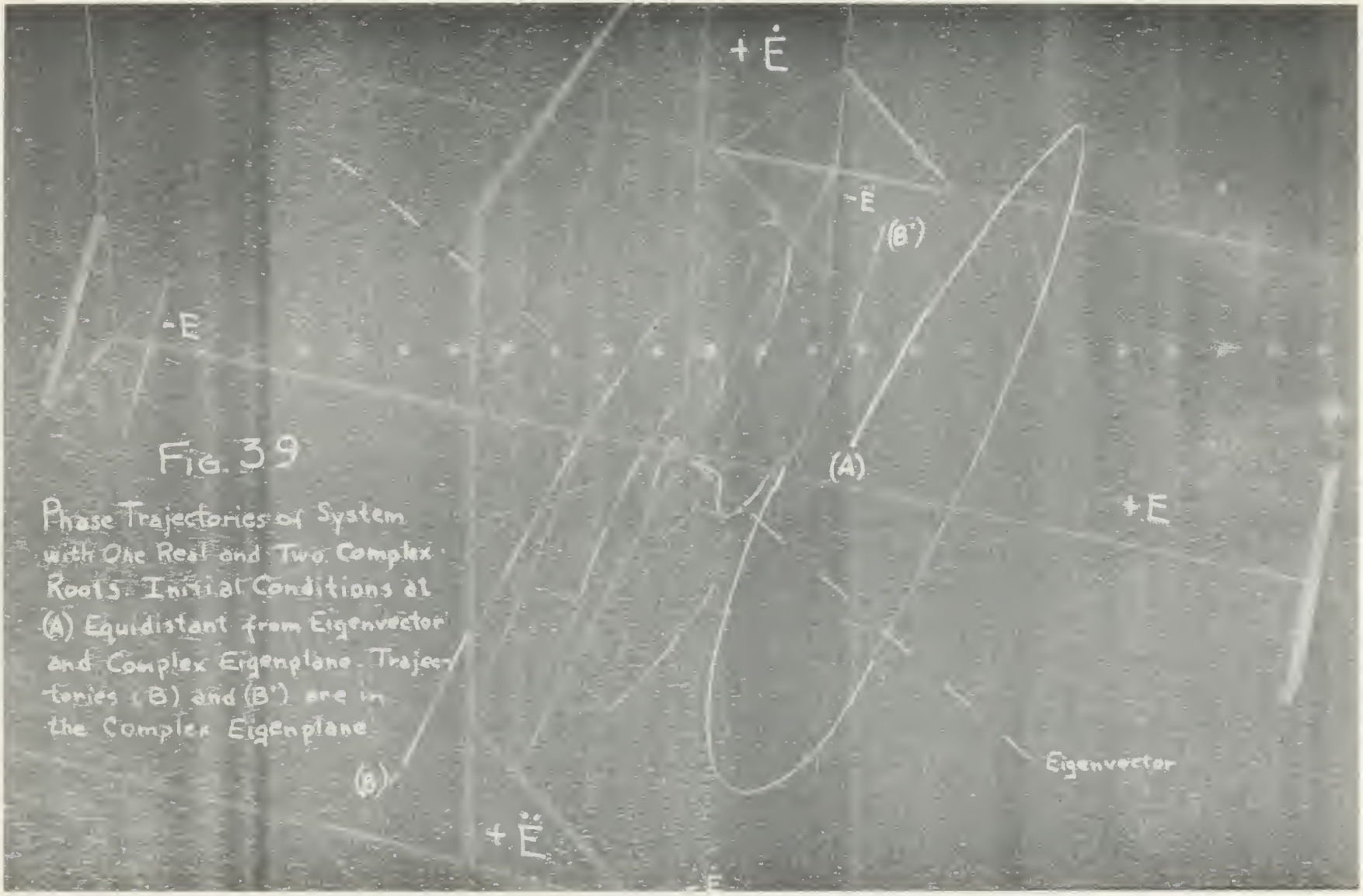

FIG. 39

Phase Trajectories of System with One Real and Two Complex Roots. Initial Conditions at (A) Equidistant from Eigenvector and Complex Eigenplane. Trajectories (B) and (B') are in the Complex Eigenplane

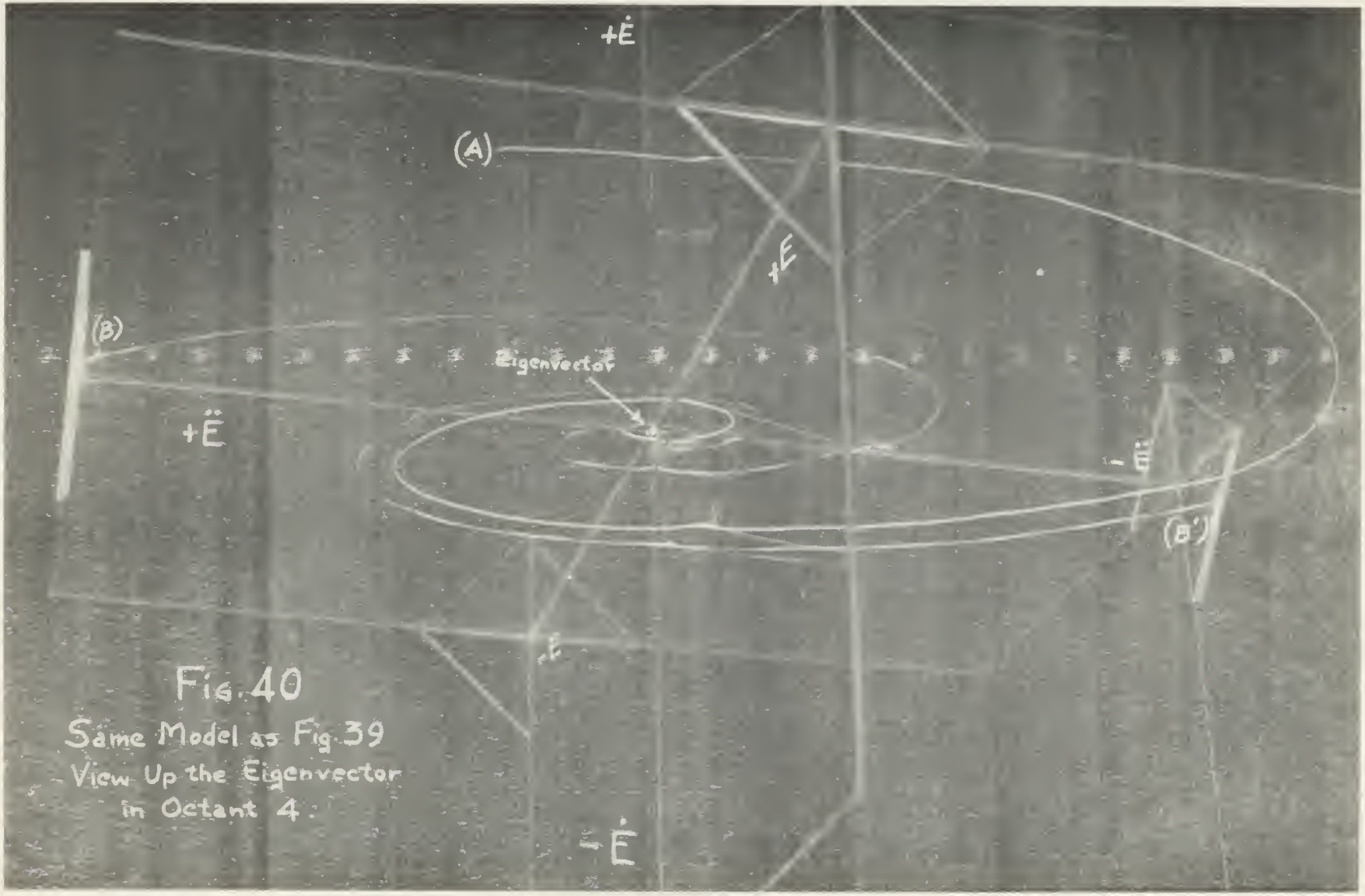

Fig. 40
Same Model as Fig. 39
View Up the Eigenvector
in Octant 4.

However, before proceeding further, the results of this phase of the investigation indicate that for systems having one real root and two complex roots, the phase trajectories of the systems that are very lightly damped tend to become asymptotic to the complex eigenplane. For systems with moderate to heavy damping, the trajectories become asymptotic to the system eigenvector as they approach the origin of error space.

Interrelation of Phase Trajectories, Eigenplanes, and Eigenvectors

In the study of phase trajectories of systems having one real and two complex conjugate roots, it was noted that a striking similarity existed between trajectories with initial conditions inside and outside the complex eigenplane when the trajectories were viewed looking along the system eigenvector, as in Fig. 40. Further investigation led to the following development of an interrelation among phase trajectories, eigenplanes, and eigenvectors.

It can be seen from the mathematics of Chapters II and III, and also in Figs. 24 and 25, that the system eigenvector pierces the complex eigenplane at the origin of error space. Mathematically, the complex eigenplane can be translated along the eigenvector, keeping the origin of the complex eigenplane coincident with the eigenvector, and keeping the complex eigenplane oriented parallel to its original position. A set of initial conditions can be applied to the system corresponding to the point on the eigenvector containing the origin of the translated eigenplane. If the complex eigenplane is then allowed to move along the eigenvector at the same velocity as the system state point, this state point will always coincide with the origin of the complex eigenplane as these points move toward the origin of error space. Extending this further, let the complex eigenplane be translated again along the eigenvector, and impose a set of initial conditions on the system such that the initial state point lies in the translated eigenplane some distance from the translated origin. If the complex eigenplane is allowed to move toward the origin along the eigenvector as before, the state point now traces the phase trajectory in three-dimensional error space. What has really happened is that the state point has never left

the translated complex eigenplane. The trace it has made in the complex eigenplane is exactly the same as the phase trajectory described by the state point had the initial conditions been applied in the original untranslated complex eigenplane at the same distance from the origin as the present initial conditions were from the eigenvector in the translated plane. Hence it can be seen that any phase trajectory is the result of the superposition of two separate sets of initial conditions, one set on the eigenvector and the other set in the complex eigenplane.

In a system with three real roots, the same results are obtained if an eigenplane is translated along the eigenvector not defining the eigenplane.

Hence, any phase trajectory in three-dimensional error space can be described as the superposition of the two trajectories resulting from initial conditions on an eigenvector, and initial conditions in either a complex or real root eigenplane.

This hypothesis was then checked using the analog computer set-up as given in Appendix C. In Fig. C-1, the upper system was given initial conditions corresponding to a point lying on the eigenvector. The lower, or "primed" system was given a set of initial conditions corresponding to a point offset from the eigenvector by a distance equivalent to the initial conditions in the complex eigenplane. The difference of the two systems was then plotted by x-y recorder and compared with the phase trajectory in the complex eigenplane.

Figure 41 is the $\dot{E}/\ddot{E}$ projection of the phase trajectory in the complex eigenplane and Fig. 42 is the $\dot{E}/\ddot{E}$ projection of the phase trajectory of the "difference" system. The validity of the above hypothesis can be seen by a comparison of the identical projections of the phase trajectories of Figs. 41 and 42.

Complex Root Phase Trajectories in Response to a Step Input

In Fig. 33, the phase trajectory of a system with one real root and a pair of complex conjugate roots is shown for a step input. By noting the tight spiral of the trajectory around the eigenvector, it must be concluded that for this particular case, the trajectory intersects the

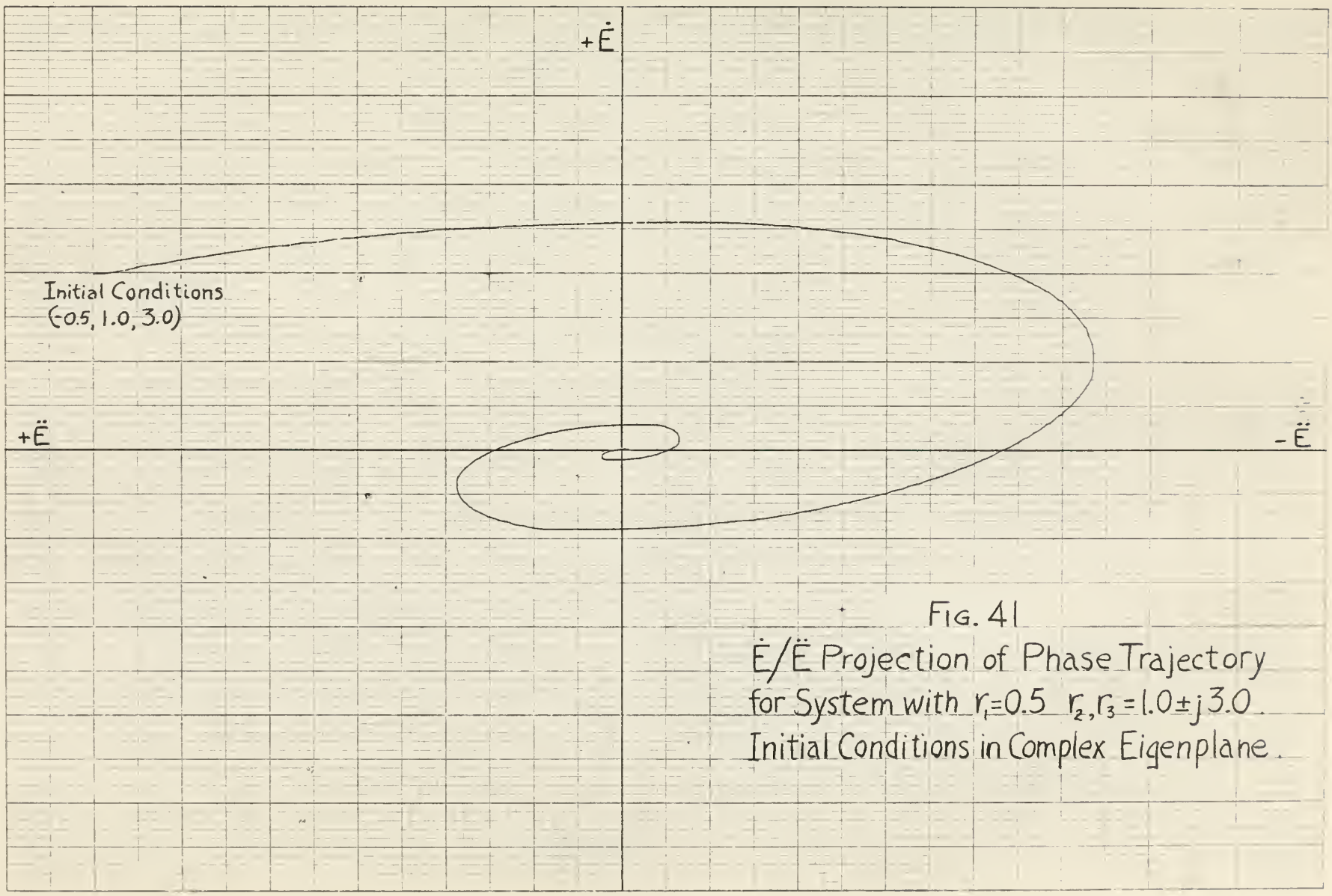

FIG. 41
Ė/Ë Projection of Phase Trajectory
for System with $r_1=0.5$ $r_2, r_3 = 1.0 \pm j3.0$.
Initial Conditions in Complex Eigenplane.

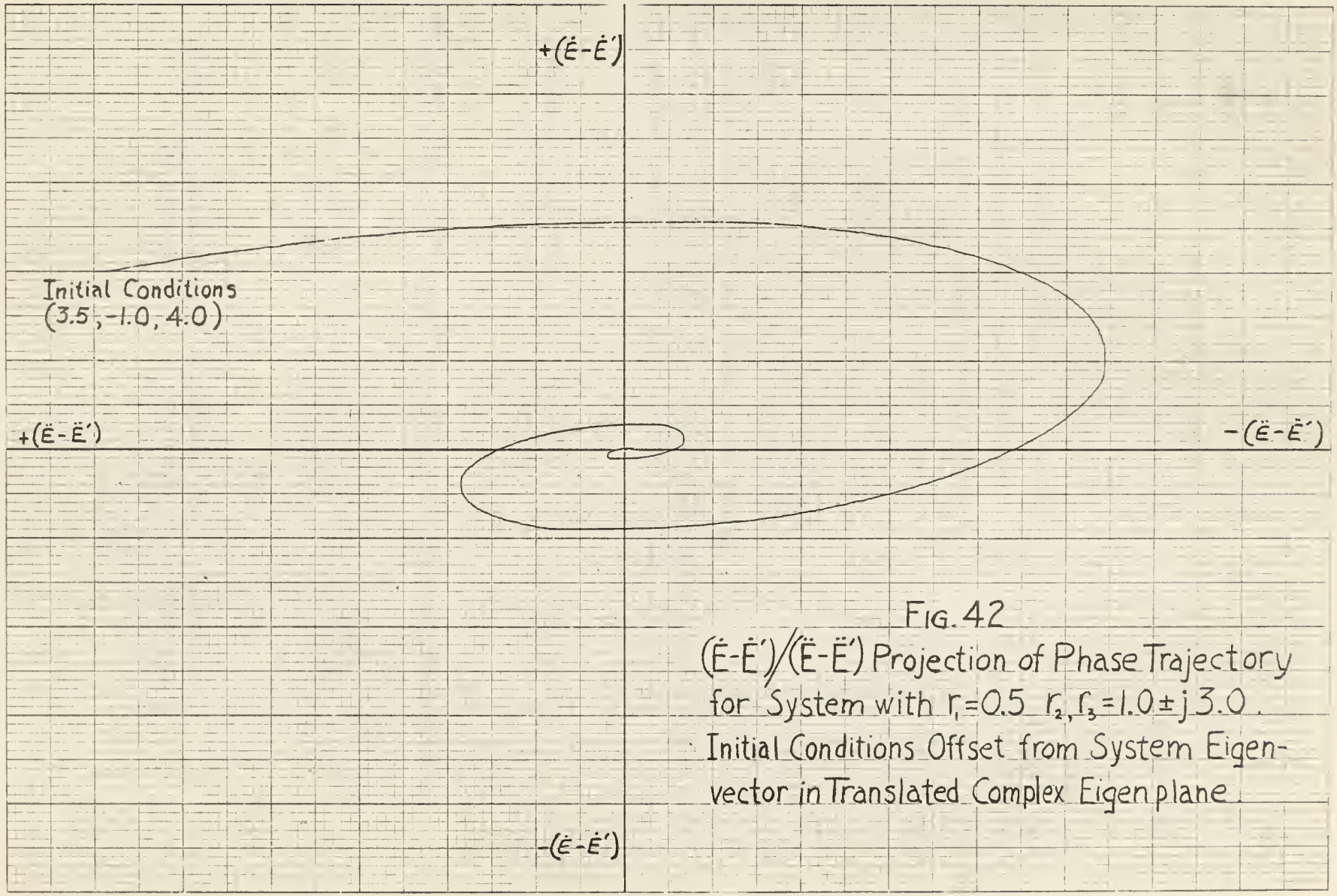

FIG. 42
$(\dot{E}-\dot{E}')/(\ddot{E}-\ddot{E}')$ Projection of Phase Trajectory for System with $r_1=0.5$ $r_2, r_3=1.0 \pm j\,3.0$. Initial Conditions Offset from System Eigenvector in Translated Complex Eigenplane.

eigencone. Since trajectories of this type could prove of great importance in switching applications, it was decided to investigate additional trajectories with step inputs to see if a definite pattern could be established as to if, where, and when the trajectories intersect the eigencone.

The three-dimensional models which had proved invaluable heretofore could not be constructed precisely enough to provide anything more than a general description of the trajectory. However, from the models it was established that all complex trajectories do not intersect the eigencone. A trajectory of this type is shown in Fig. 31. Also, a study of Figs. 5 and 33, indicates that if a trajectory does intersect the eigencone, it will occur at a faster eigenvector than that of the system

After having exhausted the possibilities of the three-dimensional models, an analytical approach was adopted. If the initial conditions of a phase trajectory are chosen such that $\dot{E}_o = \ddot{E}_o = 0$, the initial condition E_o is an initial step and can be considered as a step input. Introducing these initial conditions into Equation (IV-2):

$$E(t) = E_o \left[\frac{r_2 r_3}{(r_2 - r_1)(r_3 - r_1)} \epsilon^{-r_1 t} + \frac{r_1 r_3}{(r_1 - r_2)(r_3 - r_2)} \epsilon^{-r_2 t} + \frac{r_1 r_2}{(r_1 - r_3)(r_2 - r_3)} \epsilon^{-r_3 t} \right] \qquad \text{(IV-3)}$$

Taking the first and second derivatives of the above expression:

$$\dot{E}(t) = E_o \left[-\frac{r_1 r_2 r_3}{(r_2 - r_1)(r_3 - r_1)} \epsilon^{-r_1 t} - \frac{r_1 r_2 r_3}{(r_1 - r_2)(r_3 - r_2)} \epsilon^{-r_2 t} - \frac{r_1 r_2 r_3}{(r_1 - r_3)(r_2 - r_3)} \epsilon^{-r_3 t} \right] \qquad \text{(IV-4)}$$

$$\ddot{E}(t) = E_o \left[\frac{r_1^2 r_2 r_3}{(r_2 - r_1)(r_3 - r_1)} \epsilon^{-r_1 t} + \frac{r_1 r_2^2 r_3}{(r_1 - r_2)(r_3 - r_2)} \epsilon^{-r_2 t} + \frac{r_1 r_2 r_3^2}{(r_1 - r_3)(r_2 - r_3)} \epsilon^{-r_3 t} \right] \qquad \text{(IV-5)}$$

Substituting the above expressions for $E(t)$, $\dot{E}(t)$, and $\ddot{E}(t)$ into Equation (II-14), the equation of the eigencone:

$$\frac{r_3}{(r_3-r_1)(r_3-r_2)}\epsilon^{-(r_1+r_2)t} + \frac{r_2}{(r_2-r_1)(r_2-r_3)}\epsilon^{-(r_1+r_3)t} + \frac{r_1}{(r_1-r_2)(r_1-r_3)}\epsilon^{-(r_2+r_3)t} = 0 \qquad \text{(IV-6)}$$

This equation satisfies the conditions that exist when and if the phase trajectory in response to a step input intersects the eigencone. It can be seen from this equation that if an intersection occurs, the time of intersection is independent of the size of the step input. Furthermore, on obtaining a time of intersection, the equation becomes linear and indicates that all points of intersection are along a straight line on the surface of the eigencone. This line, by definition, must be along the same eigenvector.

In order to obtain a solution to Equation (IV-6), the equation is simplified as shown in Appendix D to obtain the transcendental equation:

$$\text{Cos } \beta t + \sigma \text{ Sin } \beta t = \epsilon^{(a-\alpha)t} \qquad \text{(IV-7)}$$

where: a = real root

α = real part of complex root

β = imaginary part of complex root

$$\sigma = \frac{\alpha a - \alpha^2 - \beta^2}{\beta a}$$

If a time of intersection exists other than the trivial case of $t = 0$, it can be obtained from a graphical solution of the above equation. If a solution exists, in all except special cases, it is possible to obtain more than one solution if the plot is continued beyond the first intersection. Figure 33 is a trajectory which would produce multiple intersections as noted by the tight spiral around the eigenvector.

In order to avoid plotting Equation (IV-7) for systems with no intersections, R. L. Ashford (Ref. 6) has devised a criteria whereby it is possible to determine whether or not a solution exists. In essence, it amounts to expanding both sides of Equation (IV-7) in a Maclaurin series and taking the coefficient of the first power term in order to determine the slope of each curve. The slope of the curve for the left side of the equation is given by $\sigma\beta$ while that of the right is $(a-\alpha)$. Ashford states that when $(a-\alpha)$ is less than zero, there will always be an infinite number of solutions, and when $(a-\alpha)$ is greater than zero, a non-trivial solution will exist provided $\sigma\beta$ is greater than $(a-\alpha)$. Ashford's criteria, then, states that a phase trajectory in response to a step input will intersect the eigencone whenever:

1. $(a-\alpha) < 0$
2. $(a-\alpha) \geq 0$ and $\sigma\beta > (a-\alpha)$

If, through Ashford's criteria, an intersection is indicated, a graphical solution of Equation (IV-7) will determine the time of intersection. By substituting this value of time into Equations (IV-3), (IV-4), and (IV-5), the point of intersection of the trajectory with the eigencone is determined and hence, the eigenvector.

Chapter V

CONCLUSIONS

From the results of this investigation, the following conclusions can be made regarding the eigenvector geometry and phase trajectories of third order linear feedback control systems:

1) The orientation of system eigenvectors in third order error space if a function of the location of the roots of the system on the complex s-plane.

2) The locus of all eigenvectors associated with a third order system is a conic surface describing two right elliptical cones located in octants 1, 2, 3' and 4' with apexes at the origin of error space.

3) An eigenplane can be fixed at a desired orientation in error space by proper choice of system roots.

4) The orientation of the complex eigenplane in error space is completely independent of the real root of the system and depends only on the location of the complex conjugate roots on the complex s-plane.

5) The complex eigenplane never intersects the eigencone except at the origin, however, it can become tangent, and its point of tangency is along the eigenvector associated with a pair of repeated real roots.

6) The three eigenplanes of a system having three real and distinct roots form a pyramid interior to the eigencone. This pyramid serves to funnel phase trajectories into the origin of error space.

7) Phase trajectories of systems with three real roots having initial conditions in an eigenplane will remain in this plane and will approach the origin of error space asymptotic to the slowest of the two defining eigenvectors.

8) Phase trajectories of systems with one real and two complex conjugate roots having initial conditions in the complex eigenplane will remain in the complex eigenplane.

9) Phase trajectories of moderate and heavily damped complex root systems, having initial conditions not in the complex eigenplane, spiral into the origin of error space asymptotic to the system eigenvector.

10) Phase trajectories of very lightly damped complex root systems, having initial conditions not in the complex eigenplane, will spiral toward the origin asymptotic to the complex eigenplane.

11) Phase trajectories of a system with three real roots whose initial conditions are not in an eigenplane cannot penetrate an eigenplane and will approach the origin of error space asymptotic to the slow eigenvector.

12) Any third order phase trajectory in response to any initial conditions can be described by the superposition of the two phase trajectories resulting from initial conditions on an eigenvector and initial conditions in either a complex or real root eigenplane. (See Chapter IV, pp. 67 , 68)

13) If the phase trajectory of a system with one real and a pair of complex conjugate roots intersects the eigencone in response to a step input, the time of intersection is independent of the size of step and the intersection will occur along a faster eigenvector than the original system eigenvector.

Chapter VI

RECOMMENDATIONS

From the results of this thesis it can be seen that there are certain areas of interest which warrant further investigation. A logical extension of this thesis would be an attempt to project the results obtained herein for third order systems into the more general case of Nth order systems. The existence of hypersurfaces in N-dimensional error space corresponding to the three-dimensional eigenplanes has been well established in the literature. While not yet proven, it seems reasonable to assume that there must also exist in N-dimensions a hypersurface which corresponds to the eigencone. Thus it should be possible to describe the characteristics of phase trajectories of Nth order systems in terms of the various hypersurfaces defined by the N-dimensional eigenvectors.

The results of this thesis could also have applications in the design of discontinuous control systems. The literature contains a great deal of information on various schemes which utilize hypersurfaces as switching surfaces, but none of these hypersurfaces are comparable to the eigencone. However, in the N-dimensional case, it would have to be proven mathematically that under certain conditions the phase trajectories intersect an N-dimensional eigencone and that eigencone switching could be effected.

The effect of non-linearities on the phase trajectories of third order and higher systems is another field of investigation to which the results of this thesis can also be extended. The regions of three-dimensional error space in which a system is linear can be defined by various planes which establish the boundaries of the linear region. For example, in the case of velocity saturation, the linear region is defined by the planes $\dot{E} = \pm K$, where K is a constant. Similarly, the linear region in the case of torque saturation is established by the planes $\ddot{E} = \pm K$. In N-dimensions it seems reasonable to assume that corresponding hypersurfaces exist which also establish the boundaries of these linear regions, and their effect on phase trajectories has not been adequately described.

REFERENCES

1. Han, K. W., "Phase Space Methods for the Analysis and Design of Discontinuous Systems", Unpublished Doctoral Dissertation, United States Naval Postgraduate School, 1961.

2. Bogner, I., "An Investigation of the Switching Criteria for Higher Order Contactor Servomechanisms", Interim Progress Report Number PR 16-9, Contract Number AF 33(038)-21673 E. O. Number 460-42-5, Cook Research Laboratories, 1953.

3. Han, K. W., and Thaler, G. J., "Phase Space Analysis and Design of Linear Discontinuously Damped Feedback Control Systems", Trans. AIEE (Applications and Industry), September 1961.

4. Ostrovskii, G. M., "Increasing the Speed of Response of Certain Automatic Control Systems By Means of Non-linear and Computer Devices", Avtomatika Telemekhanika, 19:209-16, Number 3, March 1958.

5. Fuller, A. T., "Phase Space in the Theory of Optimum Control", Journal of Electronics and Control, Vol. VIII, Number 5, May 1960.

6. Ashford, R. L., "Third Order Phase Trajectories and Their Design Applications", Unpublished paper presented at AIEE District Student Paper Contest, United States Naval Postgraduate School, April 1962.

APPENDIX A

DIGITAL COMPUTER FLOW DIAGRAM, PROGRAM, AND SAMPLE PRINT OUT OF THIRD ORDER DIFFERENTIAL EQUATION SOLUTION

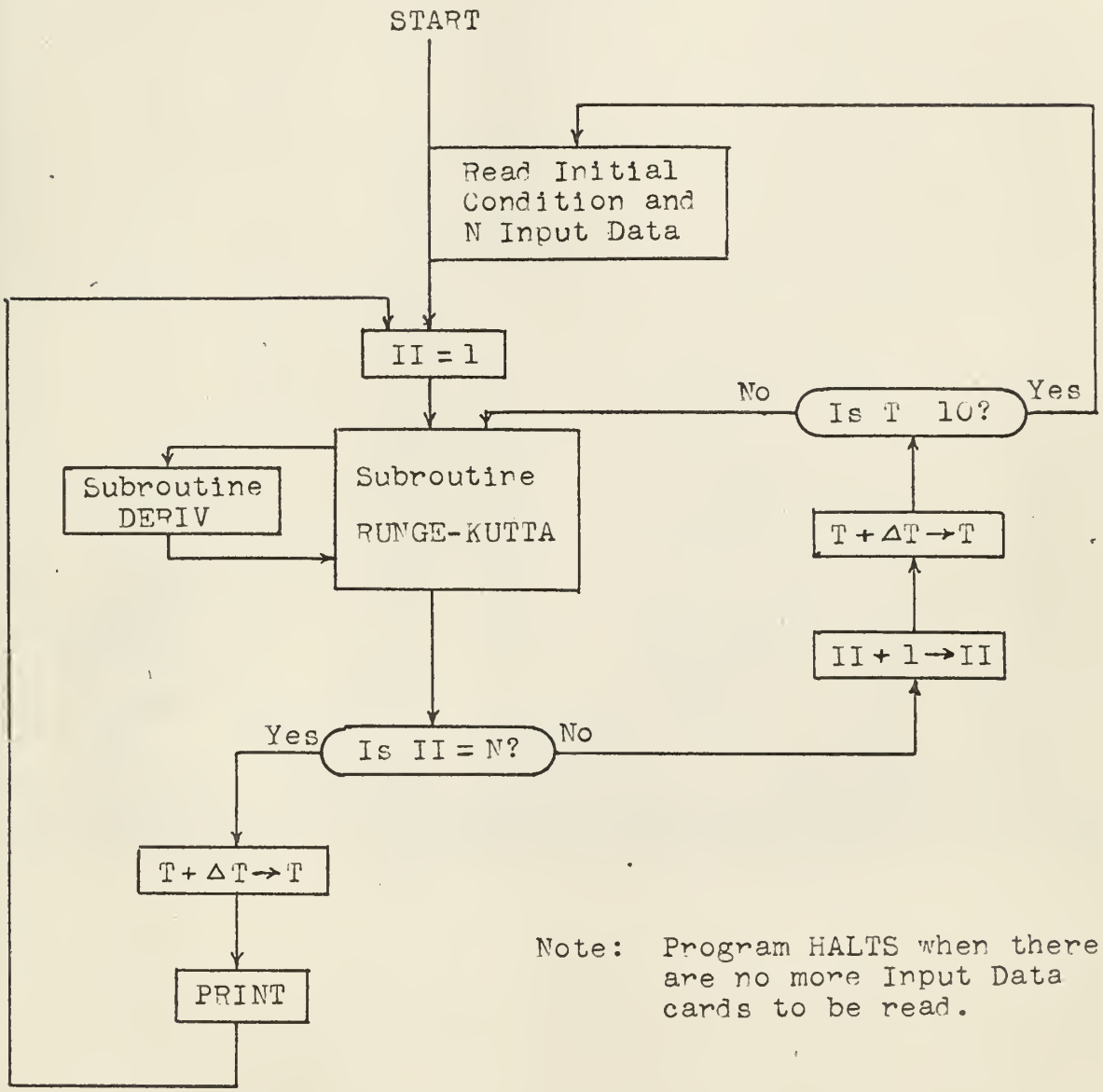

Fig. A-1 Flow Diagram of Digital Computer Program

FORTRAN PROGRAM FOR DIGITAL COMPUTER SOLUTION OF THIRD ORDER DIFFERENTIAL EQUATION

```
      PROGRAM PHATRAJ
C     DIETZ-WESTBROOK THESIS          COMPLEX        CASE F
      DIMENSION Y(3)
      READ 6, DELTAT,N
    6 FORMAT (F5.2, 5X, I3)
   13 READ 4, T, (Y(I), I=1,3)
    4 FORMAT (F7.3, 3(5X,F8.4))
    9 II=1
   11 CALL RKUTTA (3, T, Y, DELTAT)
      IF (II-N) 7, 8, 8
    7 II=II+1
      T=T+DELTAT
      IF (T-10.0) 11, 11, 13
    8 T=T+DELTAT
      WRITE OUTPUT TAPE 8, 5, T, (Y(I), I=1,3)
    5 FORMAT (3HT= F7.3,4X,3HE= F8.4,4X,4HE1= F8.4,4X,4HE2= F8.4)
      GO TO 9
      END
      SUBROUTINE  RKUTTA(NUMBER,XVAR,YVARS,STEP)
      DIMENSION YVARS(30),AK(4,30),DY(30),YC(30),C(4)
      C(1)=0.0
      C(2)=0.5
      C(3)=0.5
      C(4)=1.0
      DO 1 I=1,4
      XC=XVAR + C(I)*STEP
      DO 2 J=1,NUMBER
    2 YC(J) =YVARS(J) + C(I)*AK(I-1,J)
      CALL DERIV(XC,YC,DY)
      DO 1 J=1,NUMBER
    1 AK(I,J) = STEP * DY(J)
      DO 3 J = 1,NUMBER
    3 YVARS(J) =YVARS(J)+(AK(1,J)+2.*AK(2,J)+2.*AK(3,J)+AK(4,J))/6.
      RETURN
      END
      SUBROUTINE DERIV (T, Y, DY)
      DIMENSION Y(3), DY(3)
      A=4.0
      B=3.5
      C=1.5
      DY(1)=Y(2)
      DY(2)=Y(3)
      DY(3)=-C*Y(1)-B*Y(2)-A*Y(3)
      RETURN
      END
      END
```

Sample Digital Print Out - PROGRAM PHATRAJ

Initial Conditions : on Eigenvector

T=	.000	E=	-.6667	E1=	2.0000	E2=	-6.0000
T=	.050	E=	-.5738	E1=	1.7214	E2=	-5.1642
T=	.100	E=	-.4939	E1=	1.4816	E2=	-4.4449
T=	.150	E=	-.4251	E1=	1.2753	E2=	-3.8258
T=	.200	E=	-.3659	E1=	1.0976	E2=	-3.2929
T=	.250	E=	-.3149	E1=	.9447	E2=	-2.8342
T=	.300	E=	-.2711	E1=	.8131	E2=	-2.4394
T=	.350	E=	-.2333	E1=	.6999	E2=	-2.0996
T=	.400	E=	-.2008	E1=	.6024	E2=	-1.8072
T=	.450	E=	-.1729	E1=	.5185	E2=	-1.5554
T=	.500	E=	-.1488	E1=	.4463	E2=	-1.3388
T=	.550	E=	-.1281	E1=	.3841	E2=	-1.1523
T=	.600	E=	-.1102	E1=	.3306	E2=	-.9918
T=	.650	E=	-.0949	E1=	.2846	E2=	-.8536
T=	.700	E=	-.0817	E1=	.2449	E2=	-.7347
T=	.750	E=	-.0703	E1=	.2108	E2=	-.6324
T=	.800	E=	-.0605	E1=	.1814	E2=	-.5443
T=	.850	E=	-.0521	E1=	.1562	E2=	-.4685
T=	.900	E=	-.0448	E1=	.1344	E2=	-.4032
T=	.950	E=	-.0386	E1=	.1157	E2=	-.3471
T=	1.000	E=	-.0332	E1=	.0996	E2=	-.2987
T=	1.050	E=	-.0286	E1=	.0857	E2=	-.2571
T=	1.100	E=	-.0246	E1=	.0738	E2=	-.2213
T=	1.150	E=	-.0212	E1=	.0635	E2=	-.1905
T=	1.200	E=	-.0182	E1=	.0547	E2=	-.1639
T=	1.250	E=	-.0157	E1=	.0470	E2=	-.1411
T=	1.300	E=	-.0135	E1=	.0405	E2=	-.1214
T=	1.350	E=	-.0116	E1=	.0349	E2=	-.1045
T=	1.400	E=	-.0100	E1=	.0300	E2=	-.0900
T=	1.450	E=	-.0086	E1=	.0258	E2=	-.0774
T=	1.500	E=	-.0074	E1=	.0222	E2=	-.0667
T=	1.550	E=	-.0064	E1=	.0191	E2=	-.0574
T=	1.600	E=	-.0055	E1=	.0165	E2=	-.0494
T=	1.650	E=	-.0047	E1=	.0142	E2=	-.0425
T=	1.700	E=	-.0041	E1=	.0122	E2=	-.0366
T=	1.750	E=	-.0035	E1=	.0105	E2=	-.0315
T=	1.800	E=	-.0030	E1=	.0090	E2=	-.0271
T=	1.850	E=	-.0026	E1=	.0078	E2=	-.0233
T=	1.900	E=	-.0023	E1=	.0067	E2=	-.0201
T=	1.950	E=	-.0019	E1=	.0058	E2=	-.0173
T=	2.000	E=	-.0017	E1=	.0050	E2=	-.0149
T=	2.050	E=	-.0014	E1=	.0043	E2=	-.0128
T=	2.100	E=	-.0012	E1=	.0037	E2=	-.0110
T=	2.150	E=	-.0011	E1=	.0032	E2=	-.0095
T=	2.200	E=	-.0009	E1=	.0027	E2=	-.0082
T=	2.250	E=	-.0008	E1=	.0024	E2=	-.0070
T=	2.300	E=	-.0007	E1=	.0020	E2=	-.0060
T=	2.350	E=	-.0006	E1=	.0017	E2=	-.0052
T=	2.400	E=	-.0005	E1=	.0015	E2=	-.0045
T=	2.450	E=	-.0004	E1=	.0013	E2=	-.0039
T=	2.500	E=	-.0004	E1=	.0011	E2=	-.0033
T=	2.550	E=	-.0003	E1=	.0010	E2=	-.0029
T=	2.600	E=	-.0003	E1=	.0008	E2=	-.0025
T=	2.650	E=	-.0002	E1=	.0007	E2=	-.0021
T=	2.700	E=	-.0002	E1=	.0006	E2=	-.0018
T=	2.750	E=	-.0002	E1=	.0005	E2=	-.0016
T=	2.800	E=	-.0002	E1=	.0005	E2=	-.0014
T=	2.850	E=	-.0001	E1=	.0004	E2=	-.0012
T=	2.900	E=	-.0001	E1=	.0003	E2=	-.0010
T=	2.950	E=	-.0001	E1=	.0003	E2=	-.0009
T=	3.000	E=	-.0001	E1=	.0003	E2=	-.0007
T=	3.050	E=	-.0001	E1=	.0002	E2=	-.0006
T=	3.100	E=	-.0001	E1=	.0002	E2=	-.0006
T=	3.150	E=	-.0001	E1=	.0002	E2=	-.0005
T=	3.200	E=	-.0001	E1=	.0001	E2=	-.0004
T=	3.250	E=	-.0000	E1=	.0001	E2=	-.0004
T=	3.300	E=	-.0000	E1=	.0001	E2=	-.0003

Appendix B

ANALOG COMPUTER SOLUTION OF THIRD ORDER DIFFERENTIAL EQUATION

General third order equation:

$$\dddot{E} + a\ddot{E} + b\dot{E} + cE = 0$$

$$a = r_1 + r_2 + r_3$$
$$b = r_1 r_2 + r_1 r_3 + r_2 r_3$$
$$c = r_1 r_2 r_3$$

Scaling factors:

$$\alpha_t = 10$$

$$\alpha_{\ddot{E}} = \alpha_{\dot{E}} = \alpha_E = 0.1$$

Basic equation for an integrator:

$$e_o = -\int_o^{t_p} \left(\frac{a_i \alpha_t}{R_i C_f} e_i + \dots \right) dt_p$$

Scaling of amplifier stages:

1. Amplifier 1

$$\ddot{E} = -\int_o^t (a\ddot{E} + b\dot{E} + cE)\,dt$$

$$\overline{\ddot{E}} = -\int_o^{t_p} \left(a\frac{\alpha_{\ddot{E}}}{\alpha_{\ddot{E}}}\ddot{E} + b\frac{\alpha_{\dot{E}}}{\alpha_{\ddot{E}}}\dot{E} + c\frac{\alpha_E}{\alpha_{\ddot{E}}}E \right) dt_p = -\int_o^{t_p} (a\ddot{E} + b\dot{E} + cE)\,dt_p$$

$$a = \frac{a_{11}\alpha_t}{R_1 C_{f_1}} \qquad a_{11} = \frac{a R_1 C_{f_1}}{\alpha_t}$$

$$b = \frac{a_{12}\alpha_t}{R_2 C_{f_1}} \qquad a_{12} = \frac{b R_2 C_{f_1}}{\alpha_t}$$

$$c = \frac{a_{13}\alpha_t}{R_3 C_{f_1}} \qquad a_{13} = \frac{c R_3 C_{f_1}}{\alpha_t}$$

2. Amplifier 3

$$\dot{E} = \int_0^t \ddot{E}\, dt$$

$$\overline{\dot{E}} = -\int_0^{t_p} \frac{\alpha_{\ddot{E}}}{\alpha_{\dot{E}}} \ddot{E}\, dt_p = -\int_0^{t_p} \ddot{E}\, dt_p$$

$$1 = \frac{a_{14}\alpha_t}{R_4 C_{f2}} \qquad a_{14} = \frac{R_4 C_{f2}}{\alpha_t}$$

3. Amplifier 5

$$E = \int_0^t \dot{E}\, dt$$

$$\overline{E} = -\int_0^{t_p} \frac{\alpha_{\dot{E}}}{\alpha_E} \dot{E}\, dt_p = -\int_0^{t_p} \dot{E}\, dt_p$$

$$1 = \frac{a_{15}\alpha_t}{R_5 C_{f3}} \qquad a_{15} = \frac{R_5 C_{f3}}{\alpha_t}$$

4. Amplifiers 21, 22, 23

No scaling required since these amplifiers are used only as sign changers.

The analog computer schematic for the general solution is shown in Fig. B-1.

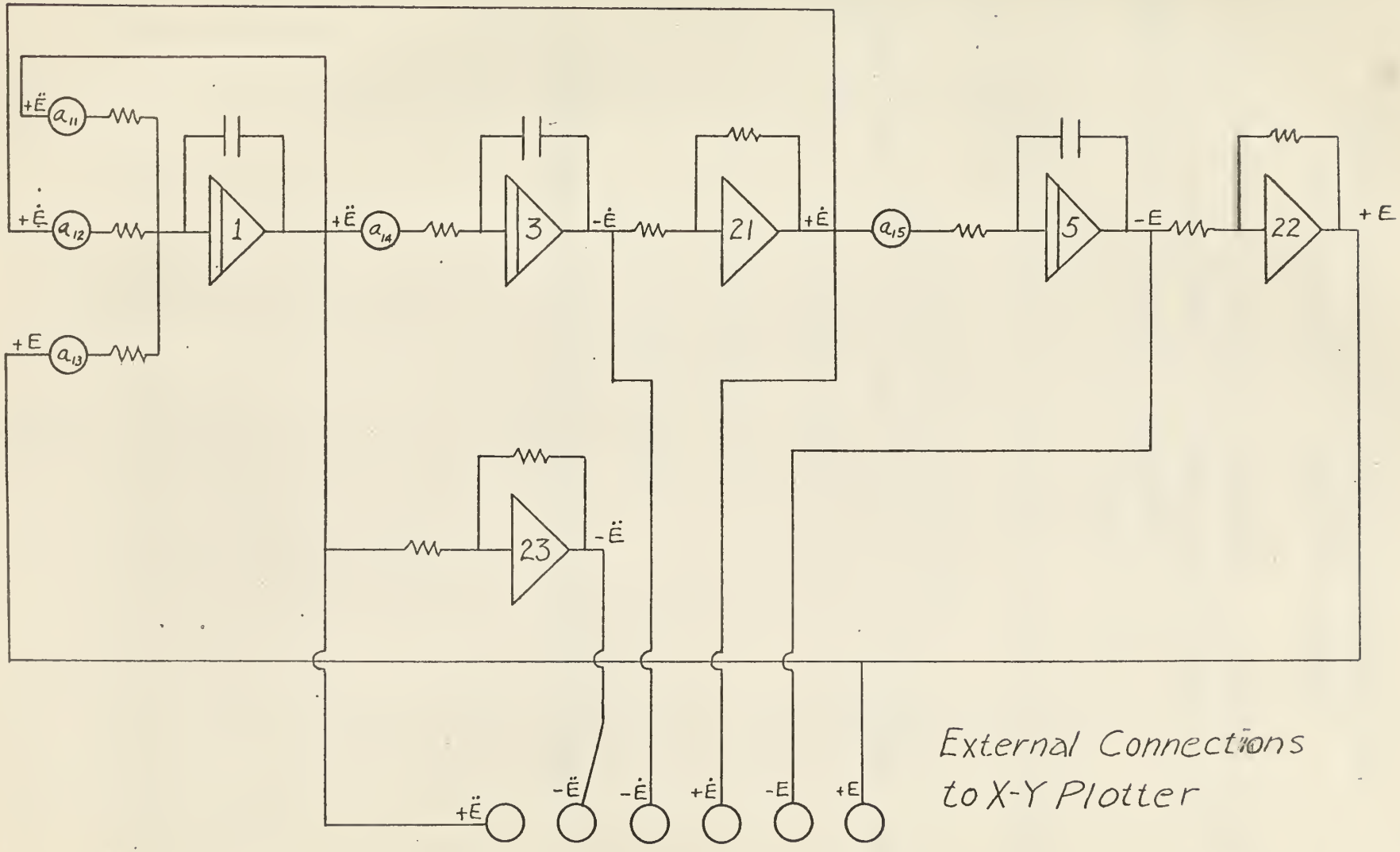

Fig. B-1 Analog Computer Set-up for Third Order Phase Trajectories

Appendix C

COMPUTER SET-UP AND INITIAL CONDITION DERIVATION FOR PHASE TRAJECTORIES IN TRANSLATING EIGENPLANE

The computer set-up as used on the Donner 3100 is given in Fig. C-1.

The initial conditions for the phase trajectory shown in Fig. 41 were for a point in the complex eigenplane and were:

$$E_o = -0.5,\ \dot{E}_o = +1.0,\ \ddot{E}_o = +3\ 0$$

The complex eigenplane was translated to a point on the eigenvector corresponding to:

$$E = +4.0,\ \dot{E} = -2.0,\ \ddot{E} = 1.0$$

Therefore the initial conditions of the point in the translated eigenplane were:

$$E_o' = E + E_o = +3.5$$

$$\dot{E}_o' = \dot{E} + \dot{E}_o = -1.0$$

$$\ddot{E}_o' = \ddot{E} + \ddot{E}_o = +4.0$$

These initial conditions gave the phase trajectory of Fig. 42.

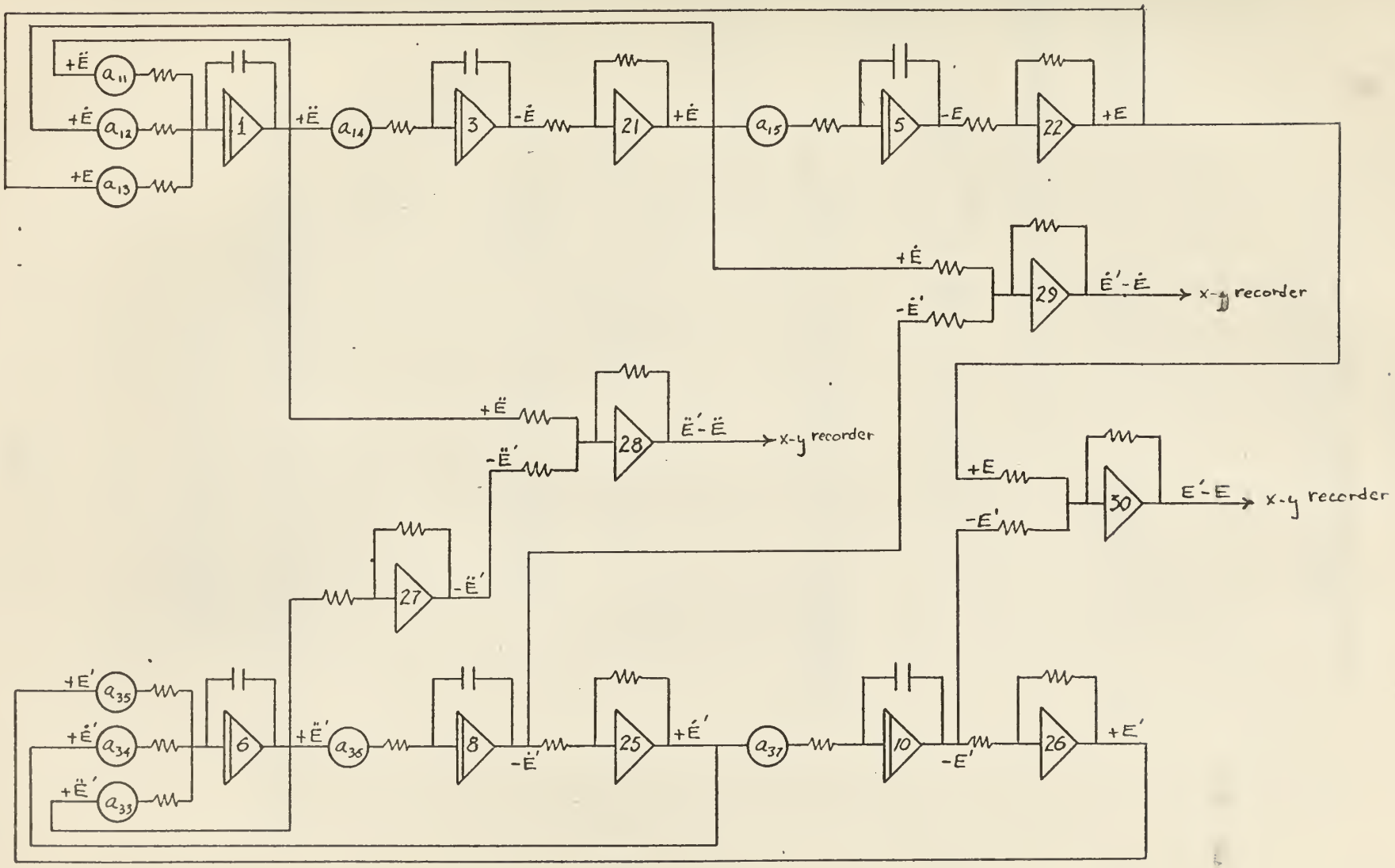

Fig. C-1 Analog Computer Set-up Used to Obtain Phase Trajectory of Fig. 42

Appendix D

DERIVATION OF THE TRANCENDENTAL EQUATION
$\cos \beta t + \sigma \sin \beta t = \epsilon^{(a-\alpha)t}$

$$\frac{r_3 \epsilon^{-(r_1+r_2)t}}{(r_3-r_1)(r_3-r_2)} + \frac{r_2 \epsilon^{-(r_1+r_3)t}}{(r_2-r_1)(r_2-r_3)} + \frac{r_1 \epsilon^{-(r_2+r_3)t}}{(r_1-r_2)(r_1-r_3)} = 0 \qquad \text{(D-1)}$$

This expression may be rewritten as

$$A\epsilon^{-(r_1+r_2)t} + B\epsilon^{-(r_1+r_3)t} = C\epsilon^{-(r_2+r_3)t} \qquad \text{(D-2)}$$

where

$$A = \frac{r_3}{(r_3-r_1)(r_3-r_2)} \quad B = \frac{r_2}{(r_2-r_1)(r_2-r_3)} \quad C = \frac{-r_1}{(r_1-r_2)(r_1-r_3)}$$

Dividing through by C,

$$\frac{A}{C}\epsilon^{-(r_1+r_2)t} + \frac{B}{C}\epsilon^{(r_1+r_3)t} = \epsilon^{-(r_2+r_3)t} \qquad \text{(D-3)}$$

Here, $\frac{A}{C} = \frac{r_3(r_1-r_2)}{r_1(r_3-r_2)}$ and $\frac{B}{C} = \frac{r_2(r_1-r_3)}{r_1(r_2-r_3)}$

Let $r_1 = a$

$r_2 = \alpha + j\beta$

$r_3 = \alpha - j\beta$

Then $\frac{A}{C} = \frac{a\alpha - \alpha^2 - ja\beta - \beta^2}{-2ja\beta} = \frac{1}{2} + \frac{a\alpha - \alpha^2 - \beta^2}{-2ja\beta} = \frac{1}{2} - \frac{\sigma}{2j}$

where $\sigma = \frac{a\alpha - \alpha^2 - \beta^2}{a\beta}$

Similarly, $\frac{B}{C} = \frac{1}{2} + \frac{\sigma}{2j}$

Multiplying (D-3) by $\epsilon^{\left(r_1 + \frac{r_2}{2} + \frac{r_3}{2}\right)t}$,

$$\frac{A}{C}\epsilon^{\left(\frac{r_3 - r_2}{2}\right)t} + \frac{B}{C}\epsilon^{\left(\frac{r_2 - r_3}{2}\right)t} = \epsilon^{\left(r_1 - \frac{r_2}{2} - \frac{r_3}{2}\right)t} \qquad \text{(D-4)}$$

Substituting for r_1, r_2, r_3, $\frac{A}{B}$ and $\frac{B}{C}$ in (D-4),

$$\left(\frac{1}{2} - \frac{\sigma}{2j}\right)\epsilon^{-j\beta t} + \left(\frac{1}{2} + \frac{\sigma}{2j}\right)\epsilon^{j\beta t} = \epsilon^{(a-\alpha)t}$$

$$\frac{1}{2}\left(\epsilon^{j\beta t} + \epsilon^{-j\beta t}\right) + \frac{\sigma}{2j}\left(\epsilon^{j\beta t} - \epsilon^{-j\beta t}\right) = \epsilon^{(a-\alpha)t}$$

$$\cos \beta t + \sigma \sin \beta t = \epsilon^{(a-\alpha)t}$$